Publications of the Astronomical Society of Australia (2021), **38**, e035, 39 pages
doi:10.1017/pasa.2021.18

CAMBRIDGE UNIVERSITY PRESS

Dawes Review

The Dawes Review 9: The role of cold gas stripping on the star formation quenching of satellite galaxies

L. Cortese[1,2], B. Catinella[1,2] and R. Smith[3]

[1]International Centre for Radio Astronomy Research, The University of Western Australia, 35 Stirling Hw, 6009 Crawley, Australia, [2]ARC Centre of Excellence for All Sky Astrophysics in 3 Dimensions (ASTRO 3D), Australia and [3]Korea Astronomy and Space Science Institute (KASI), 776 Daedeokdae-ro, Yuseong-gu, Daejeon 34055, Republic of Korea

Abstract

One of the key open questions in extragalactic astronomy is what stops star formation in galaxies. While it is clear that the cold gas reservoir, which fuels the formation of new stars, must be affected first, how this happens and what are the dominant physical mechanisms involved is still a matter of debate. At least for satellite galaxies, it is generally accepted that internal processes alone cannot be responsible for fully quenching their star formation, but that environment should play an important, if not dominant, role. In nearby clusters, we see examples of cold gas being removed from the star-forming discs of galaxies moving through the intracluster medium, but whether active stripping is widespread and/or necessary to halt star formation in satellites, or quenching is just a consequence of the inability of these galaxies to replenish their cold gas reservoirs, remains unclear. In this work, we review the current status of environmental studies of cold gas in star-forming satellites in the local Universe from an observational perspective, focusing on the evidence for a physical link between cold gas stripping and quenching of the star formation. We find that stripping of cold gas is ubiquitous in satellite galaxies in both group and cluster environments. While hydrodynamical mechanisms such as ram pressure are important, the emerging picture across the full range of dark matter halos and stellar masses is a complex one, where different physical mechanisms may act simultaneously and cannot always be easily separated. Most importantly, we show that stripping does not always lead to full quenching, as only a fraction of the cold gas reservoir might be affected at the first pericentre passage. We argue that this is a key point to reconcile apparent tensions between statistical and detailed analyses of satellite galaxies, as well as disagreements between various estimates of quenching timescales. We conclude by highlighting several outstanding questions where we expect to see substantial progress in the coming decades, thanks to the advent of the Square Kilometre Array and its precursors, as well as the next-generation optical and millimeter facilities.

Keywords: galaxies: evolution – galaxies: clusters – galaxies: groups – galaxies: disc galaxies – interstellar medium: galaxies

(Received 3 December 2020; revised 1 April 2021; accepted 3 April 2021)

1. Introduction

In our current paradigm of galaxy formation and evolution, galaxies are no longer thought of as isolated entities, but as self-regulated systems whose life is governed by the balance between gas replenishment (via inflows from the intergalactic medium), consumption (via star formation), and ejection (outflows)—the so-called 'gas-regulator' model (e.g., Oort 1970; Larson 1972; Rees & Ostriker 1977; White & Frenk 1991; Kereš et al. 2005; Bouché et al. 2010; Lilly et al. 2013). In star-forming galaxies, gas is converted into stars at a relatively steady rate, maintaining objects on a well-defined relation known as 'star-forming main sequence' (e.g., Brinchmann et al. 2004; Noeske et al. 2007; Whitaker et al. 2012). If this equilibrium is somehow broken, star formation is directly affected and galaxies experience either starbursts or quenching phases. While the starburst phase is generally short-lived ($\sim 10^8$ yr or less, e.g., Larson & Tinsley 1978; Rieke et al. 1980; Heckman, Armus, & Miley 1990), quenching appears to be a critical stage in the life cycle of galaxies. Very few systems seem able to recover from it and resume a star formation activity typical of the main sequence. Indeed, understanding what makes galaxies passive (e.g., reduce their star formation by a factor $\sim$4 or more, roughly $\gtrsim 2\sigma$ below the main sequence) is one of the main open questions in galaxy evolution.

A number of physical processes have been invoked to explain how star formation is quenched in galaxies. Even though this question remains unanswered, two key facts have become clear. First, a basic requirement to halt star formation is to affect the galaxy's cold gas reservoir by either removing it, consuming it, or keeping it stable against fragmentation. Second, the way that galaxies quench is very different depending on whether they are satellites of a bigger galaxy within their host halo or are centrals.

In the case of central galaxies—the most massive galaxies within a halo and usually those sitting at (or near) the centre of the

Author for correspondence: L. Cortese, E-mail: luca.cortese@uwa.edu.au

Cite this article: Cortese L, Catinella B and Smith R. (2021) The Dawes Review 9: The role of cold gas stripping on the star formation quenching of satellite galaxies. *Publications of the Astronomical Society of Australia* **38**, e035, 1–39. https://doi.org/10.1017/pasa.2021.18

The Dawes Reviews are substantial reviews of topical areas in astronomy, published by authors of international standing at the invitation of the PASA Editorial Board. The reviews recognise William Dawes (1762–1836), second lieutenant in the Royal Marines and the astronomer on the First Fleet. Dawes was not only an accomplished astronomer, but also spoke five languages, had a keen interest in botany, mineralogy, engineering, cartography, and music, compiled the first Aboriginal-English dictionary, and was an outspoken opponent of slavery.

This review is dedicated to the Arecibo 305m radio telescope in Puerto Rico, tragically collapsed on 2020 December 1, in recognition to its outstanding contribution to the field of research discussed in this work.

© The Author(s), 2021. Published by Cambridge University Press on behalf of the Astronomical Society of Australia.

dark matter potential well—, ‘internal’ processes such as feedback from star formation and/or accreting super-massive black holes are currently the most popular culprits to explain quenching in the local galaxy population (e.g., Croton et al. 2006). Conversely, the fate of satellite galaxies appears to be directly shaped by the external physical processes influencing them while orbiting around the central system in their host dark matter halo (e.g., Gunn & Gott 1972; van den Bosch et al. 2008; Weinmann et al. 2009; Wetzel, Tinker, & Conroy 2012; Bluck et al. 2020).

How is the gas cycle in satellites affected such that star formation is quenched? In this review, we focus on the physical mechanisms that halt star formation in satellite galaxies in the local Universe, with particular emphasis on the importance of active stripping of their cold gas reservoirs. By ‘cold gas’, we refer to both atomic and molecular hydrogen (H I and H_2, with typical temperatures $T < 10^4$ K and $T < 50$ K, respectively) in the interstellar medium (ISM) of galaxies, which fuel star formation. We aim to review the progress made in this field in the past few decades and summarise the status of our knowledge before the next-generation H I surveys with the Square Kilometre Array (SKA; Dewdney et al. 2009) and its pathfinders open a new era for studies of gas in galaxies. While doing so, we endeavour to clarify common misconceptions, as well as perceived tensions between theoretical and observational approaches attempting to identify the physical process driving galaxies outside the star-forming main sequence.

To set the background, we begin by reviewing the quenching mechanisms usually invoked to break the gas-star formation cycle in satellite galaxies (Section 2). Next, we summarise and contrast the various definitions of *gas poorness* or *deficiency* adopted in the literature, as this is a key property to quantify environmental effects on the cold gas reservoirs of galaxies that has led to substantial confusion in the field (Section 3). At this point, we are well equipped to critically examine the observational evidence for cold gas stripping, its effect on star formation and the important, related question of quenching timescales for satellite galaxies in nearby clusters (Section 4) and groups (Section 5), as well as the potential role of pre-processing and large-scale structure in gas stripping and quenching (Section 6). This will allow us to build a comprehensive picture of how environment affects the cold gas and star formation of satellites (Section 7). While this is mostly an observational review, we link our discussion to predictions of theoretical models throughout, and towards the end provide a high-level view of what can be learned on this topic from state-of-the-art semi-analytic and hydrodynamical simulations of galaxy formation and evolution (Section 8). We conclude by looking ahead and highlighting future prospects and challenges for this field (Section 9).

2. Quenching mechanisms in satellite galaxies

When it comes to studying the effect of nurture on galaxy evolution, it has been common practice to conceptually categorise complex physical processes into separate boxes and to force either observations or models to fit into the single box able to better reproduce the observed properties of galaxies. This has led not only to debates focused on perceived dichotomies (e.g., ram pressure vs starvation, hydrodynamical vs tidal interactions, stripping vs evaporation, etc.), but also to the use of the same word (e.g., starvation, see below) to refer to different physical processes, creating some confusion among the community.

As today’s passive satellites have typically spent at least a few billion years in their host halos (e.g., McGee et al. 2009; Han et al. 2018), during such a long time it is inevitable that most of the primary quenching mechanisms invoked in the literature must have played a role in shaping their properties. Thus, the question of *which* physical process affects satellite galaxies can be re-framed in terms of *how*, *when*, and *for how long (i.e., on which timescale)* each process contributes to halt the gas-star formation cycle.

It is indeed now clear that in most cases, multiple processes are at play simultaneously, and that it may not always be possible to isolate a dominant one, at least observationally, especially when we consider the population of passive satellites in the local Universe rather than individual objects. Instead, a more pragmatic approach is to first identify which step(s) of the star formation cycle has(have) been broken, causing star formation to halt, and then assess the role and impact of the various physical processes that might have led to it. As shown schematically in Figure 1, there are several mechanisms that could decrease or even halt star formation, by stopping the supply of gas that replenishes the ISM or by removing cold gas from the star-forming disc (either via external processes or internal ones, such as heating/ejection by nuclear activity and stellar feedback). Cold gas could also simply be consumed by star formation or stabilised against fragmentation and thus unable to form new stars. We briefly review these scenarios below.

2.1. Starvation—halting gas accretion

At least for galaxies with stellar masses greater than $\sim 10^9$ $M_\odot$, the typical timescale for cold gas depletion (i.e., the ratio of gas mass to star formation rate, $\tau_{\rm dep} \equiv M_{\rm gas}/{\rm SFR}$) is a few billion years for both molecular and atomic phases, assuming a constant SFR (Kennicutt 1983b; Boselli et al. 2001; Saintonge et al. 2017). This is generally used to argue that, in order to keep forming stars at a constant rate, the cold reservoir of galaxies in star-forming discs needs to be continuously replenished. Support to this picture also comes from the fact that, at least for molecular hydrogen, depletion times appear to have been even shorter at higher redshift (Schinnerer et al. 2016; Scoville et al. 2016).

While how gas gets into galaxies is still unclear, cosmological simulations suggest that, in the last few billion years, cold accretion via filaments and/or smooth accretion from the intergalactic medium (IGM) have gradually become inefficient (Dekel et al. 2009; Anglés-Alcázar et al. 2017; Grand et al. 2019), as cold streams no longer reach the galactic disc. Instead, either accretion of gas-rich companions (i.e., minor or major mergers) or wind recycling (e.g., direct cooling of the hot circumgalactic medium (CGM) via galactic fountain; Fraternali & Binney 2008; Marinacci et al. 2010) appear to be the most likely accretion channels to keep local star-forming galaxies active. Regardless of which physical mechanism(s) is(are) responsible for quenching star formation in the first place, further accretion of cold gas needs to be prevented in order to avoid that quenched galaxies restart their star formation. Indeed, while rare, rejuvenation cases are both observed in the local Universe (Cortese & Hughes 2009; Thilker et al. 2010) and predicted by numerical simulations (Birnboim, Dekel, & Neistein 2007; Nelson et al. 2018). Thus, in general, a galaxy that no longer has access to a source of gas will eventually run out of fuel and stop forming stars (Figure 1, top row).

In the literature, the lack of replenishment of cold gas in the ISM is generally referred to as *starvation*. This general idea was originally proposed by Larson, Tinsley, & Caldwell (1980) to explain the existence of passive disc galaxies outside clusters, where stripping of the ISM could not be effective. In this case,

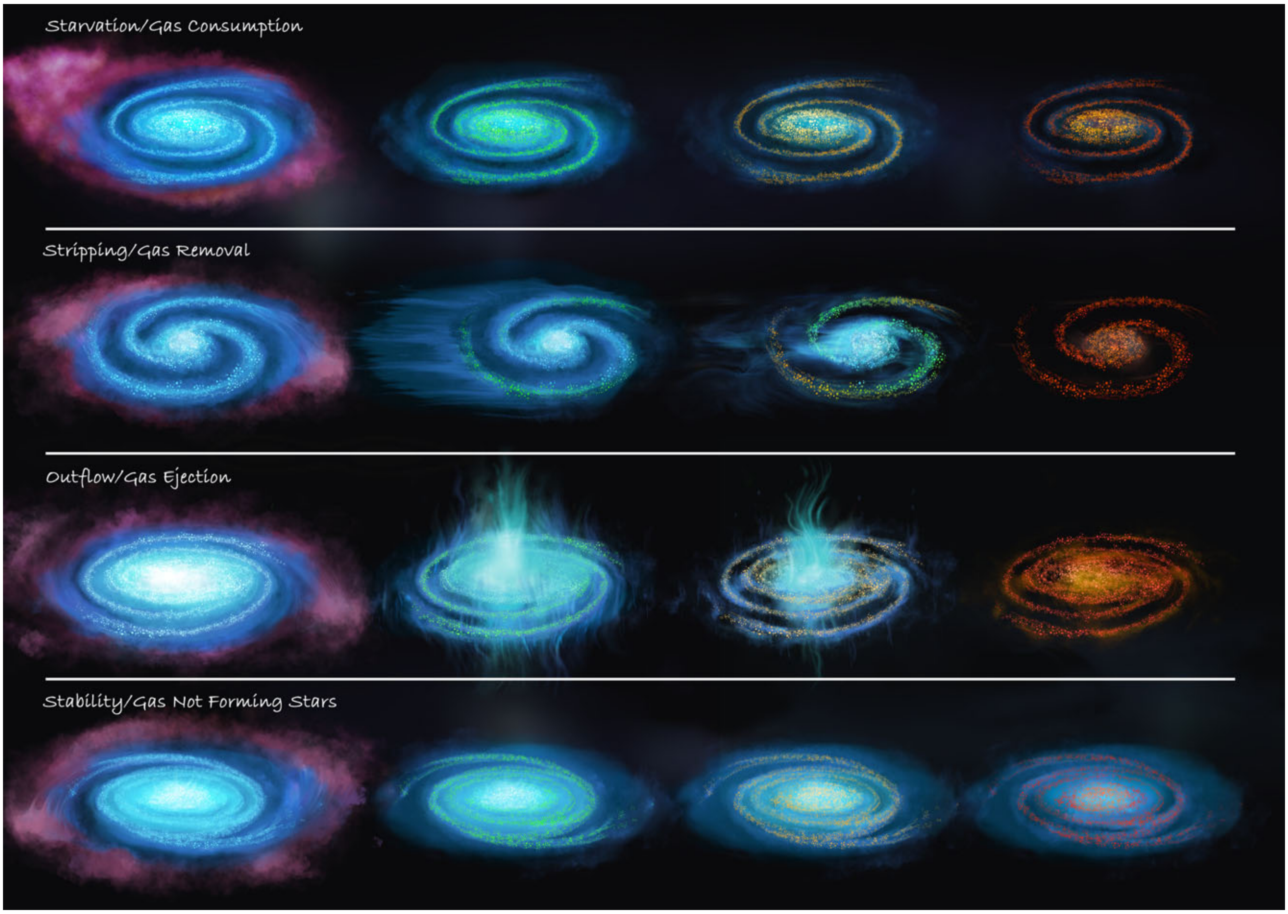

Figure 1. Illustration showing the various quenching pathways discussed in Section 2, with particular emphasis on what happens to the cold gas component of the ISM (diffuse blue). Each 'quenching sequence' starts with the galaxy losing its ability to accrete gas from the surrounding CGM/IGM (pink). The colour of the stars (from blue/young to red/old) indicates the stage of quenching.

accretion was thought to take place via either minor mergers or infall of clouds of cold gas (i.e., primarily atomic hydrogen), and galaxies with no access to such a supply would simply run out of gas. With the advent of semi-analytic cosmological models, this picture has significantly evolved into the removal of the hot gas component (only) in the halo of the galaxy (i.e., the primary reservoir of gas directly available to the galaxy to support star formation; Cole et al. 2000). This also corresponds to the introduction of the term *strangulation* (Balogh & Morris 2000), and now both *starvation* and *strangulation* are interchangeably used to refer to the cessation of accretion from both IGM and CGM.

Regardless of how exactly gas infall is halted, it is obvious that this is the necessary condition to turn a star-forming galaxy into a quiescent system and keep it passive for the rest of its life. *Thus, we assume that gas accretion is prevented and focus on the ISM.* Here, the challenge is to determine whether gas already in the disc is simply consumed by star formation, or other physical processes directly affect its ability to feed star formation.

2.2. Stripping—removing cold gas from the disc

A more dramatic way to deprive a galaxy of its fuel for star formation is to directly remove the cold ISM already in its disc (Figure 1, second row). For satellite galaxies, the interaction with the environment of their host halo provides several channels to remove star-forming gas. Broadly, these can be divided into two general classes.

(1) Hydrodynamical mechanisms. These involve the direct interaction between the ISM and the intra-group, or intracluster medium (ICM), and include *ram pressure stripping* (i.e., the removal of the ISM due to the pressure exerted by the ICM while a satellite is moving through its host halo; Gunn & Gott 1972), viscous stripping (i.e., the removal of the outer layer of the ISM due to the viscosity momentum transfer with the ICM; Nulsen 1982) and thermal evaporation (increase of temperature, and subsequent evaporation of the cold ISM at the interface with the hot ICM; Cowie & Songaila 1977). While the vast majority of past work has focused on ram pressure, we have observational evidence (as well as theoretical predictions) that both viscous stripping and thermal evaporation can play a role (e.g., Bureau & Carignan 2002; Roediger & Hensler 2005; Boselli & Gavazzi 2006; Randall et al. 2008). Unfortunately, it is extremely challenging to separate these three physical processes observationally, and it is expected that all three—if present—affect simultaneously the cold ISM of galaxies. It is also important to remember that, technically,

starvation (i.e., the cessation of gas infall) is a hydrodynamical mechanism. It is, in practice, a mild ram pressure that is able to affect the gas in the halo but not that in the disc. This is primarily why starvation and ram pressure have been considered in the literature as two separate mechanisms, despite the physical process being most likely the same.

(2) Gravitational mechanisms. The ISM can also be removed from the disc by the gravitational pull affecting satellites while orbiting in groups and clusters (Boselli & Gavazzi 2006). The key element here is the variation (temporal and/or spatial) of the external gravitational potentials that baryons in the disc are subjected to (Binney & Tremaine 1987). This could be caused by fly-bys of companion satellites and/or interaction with the central galaxy (generally divided between low- and high-speed interactions depending on how the relative speed of the two galaxies compares to their rotational velocity), or by the interaction with the whole gravitational potential of groups and clusters (often referred to as the galaxy–cluster interaction; e.g., Byrd & Valtonen 1990). The combined effect of multiple high-speed galaxy–galaxy interactions over long timescales (i.e., longer than a typical crossing time, a mechanism generally referred to as *harassment*) has also been invoked to explain the properties of satellite galaxies in clusters (Moore et al. 1996; Smith, Davies, & Nelson 2010a).

As discussed later, discriminating between hydrodynamical and gravitational processes on the ISM is not always straightforward, as both can perturb the cold ISM in the disc of galaxies in a similar way. Arguments based on geometry of disturbed features, on the comparison between gas and stellar distribution/kinematics, timescale of the interaction and distribution of star-forming regions can definitely help in the process but, as we will see, there is circumstantial evidence that both processes may sometime act simultaneously in galaxies and that *direct stripping* of the ISM from the disc is a fundamental step in the pathways of satellite galaxies towards quiescence.

2.3. Cold gas removal/heating by internal feedback mechanisms

Another way to remove cold ISM from galaxies is via internal feedback related to the star formation process (e.g., supernova feedback, stellar winds) or to the presence of an active galactic nucleus (AGN) at the centre of galaxies. In both cases, cold gas could be ejected from the disc and/or heated up, becoming unavailable for star formation (Figure 1, third row).

From a theoretical point of view, internal feedback is arguably the most popular mechanism invoked to explain the existence of passive central galaxies and to reproduce key statistical properties such as the SFR–stellar mass relation and the stellar mass function of galaxies (e.g., Croton et al. 2006; De Lucia et al. 2006; Hopkins et al. 2008). However, the fact that satellite galaxies appear to have lower cold gas content (e.g., Brown et al. 2017), less star formation, and a higher passive fraction at fixed stellar mass with respect to centrals (e.g., van den Bosch et al. 2008; Davies et al. 2019) has led to the conclusion that feedback may not always be the primary mechanism driving satellites into quiescence. Interestingly, it is certainly possible that feedback could *still play a role* by increasing the efficiency of other gas removal processes (see e.g., Sections 4.1 and 8), as also suggested by cosmological models (Zoldan et al. 2017; De Lucia, Hirschmann, & Fontanot 2019; Stevens 2019a). While neglected in the past due to a lack of observations, this is a scenario that may turn out to be more common than originally thought, thanks to the improvement of ground- and space-based facilities making it easier to identify gas outflows (e.g., via narrow-band imaging or integral field spectroscopy).

2.4. Stability of the cold gas against fragmentation and star formation

The processes discussed so far are related to the very first step of the star-formation cycle in galaxies (i.e., the availability of cold gas), based on the notion that, in order to stop forming stars, a galaxy must somehow run out of its atomic and molecular gas reservoirs. A different pathway to quenching is to affect the next steps of the cycle, that is, either the HI-to-H_2 conversion or the collapse of H_2 into stars. Although the formation of molecular gas might not be strictly required to form stars (it could just be a by-product of the gravitational collapse of atomic gas on its way to star formation; Glover & Clark 2012), this phase traces remarkably well the physical conditions under which new stars are formed (Krumholz, Leroy, & McKee 2011). In this sense, star formation could be halted by preventing the atomic gas reservoir from condensing into molecules and/or collapsing to form stars (Figure 1, bottom row). More specifically, atomic hydrogen could be kept stable on a rotating disc below the typical column density threshold for H_2 formation, thus halting star formation (e.g., Blitz & Rosolowsky 2006; Bigiel et al. 2008; Leroy et al. 2008). Additional factors regulating the rate of condensation of atoms into molecules could be the metallicity of the ISM and the intensity of the interstellar radiation field (e.g., Krumholz, McKee, & Tumlinson 2009; Gnedin & Kravtsov 2011). Typical examples of cases in which atomic hydrogen does not appear to be efficiently converted into molecular phase include the outer parts of star-forming discs (Bigiel et al. 2010a), low surface brightness galaxies (Wyder et al. 2009), early-type galaxies with significant HI reservoirs (e.g., Knapp, Turner, & Cunniffe 1985; Serra et al. 2012), and the even more extreme case of the so-called *HI-excess* systems (galaxies with unexpectedly large HI reservoirs based on their SFR and morphological structure; Geréb et al. 2016, 2018).

Alternatively, even if molecular clouds can be formed, these could remain stable against collapse due to adverse local conditions (e.g., high gas turbulence and/or high stellar velocity dispersion), significantly reducing the efficiency of star formation. Examples of this scenario are the inner parts of the Milky Way (Longmore et al. 2013) and of nearby, bulge-dominated systems (Martig et al. 2009), where turbulence is driven by gravitationally induced pressure from the bulge. In other words, the stability of the gas disc is enhanced by the presence of a dispersion-supported bulge component. However, as we will see, observations seem to exclude this path as an important one for satellite galaxies in groups and clusters. This is also because the reduction in star formation efficiency is generally not large enough to fully quench galaxies (e.g., Davis et al. 2014).

Of course, as mentioned at the beginning of this section, in order to be efficient in fully quenching star formation, gas stripping, gas ejection, and stability must be accompanied by a halt in gas replenishment onto the star-forming disc.

In what follows, we discuss the observational evidence in support or against these quenching scenarios and show that, after nearly half a century of observational work, we are in a position to build a coherent picture of the physical processes affecting the gas reservoir and star formation quenching in satellite galaxies at $z \sim 0$. As a necessary step to quantify environmental effects on cold gas content, we begin by reviewing the various definitions of gas deficiency and their implications.

3. Quantifying gas poorness—The concept of gas deficiency

Quantifying the degree of cold gas poorness, or *deficiency*, of galaxies located in group and cluster environments, compared to similar systems in the field, has been critically important to develop our understanding of quenching mechanisms. Interestingly, several techniques have been adopted to quantify gas deficiency, with often different implicit assumptions on the physics affecting the cold gas reservoirs of galaxies—sometimes leading to conflicting conclusions. Indeed, as discussed below, galaxies can simultaneously be gas-poor and gas-rich, depending on which definition is used.

Historically, most of the work in this area has focused on atomic hydrogen deficiency, mainly due to the lack of large statistical surveys of molecular hydrogen in galaxies. However, the arguments presented below are applicable also to molecular hydrogen.

3.1. Definitions based on optical diameter

Early studies of cluster galaxies started quantifying gas deficiency by comparing total HI mass-to-luminosity ratios (distance-independent quantities) of cluster and field systems at fixed luminosity and/or morphology (Robinson & Koehler 1965; Davies & Lewis 1973; Huchtmeier et al. 1976). However, it soon became clear that a more robust approach was to control galaxies by their morphological type and optical diameter (Chamaraux, Balkowski, & Gerard 1980). Indeed, the optical size versus HI mass relation turned out to be the tightest scaling relation (among those investigated at that time) linking HI mass to optical galaxy properties. While Chamaraux et al. (1980) were among the first to introduce the concept of HI deficiency, the first statistical definition of the concept of HI normalcy and HI deficiency (and arguably the foundation of this entire field) was presented by Haynes & Giovanelli (1984, hereafter HG84), in a study of a sample of 324 isolated galaxies extracted from the Karachentseva (1973) Catalog of Isolated galaxies and the Uppsala General Catalog (Nilson 1973) and observed with the Arecibo 305-m radio telescope. They showed that, at fixed morphological type, the optical property most strongly correlated with global HI mass is the galaxy isophotal optical diameter. This relation for isolated galaxies defines 'HI normalcy' and can be used to predict the total HI mass within $\sim$0.2–0.3 dex. Thus, HI deficiency is defined as:

$$DEF_{\rm HI} = \log(M_{\rm HI}^{\rm pred}[T, D_{\rm opt}]) - \log(M_{\rm HI}^{\rm obs}), \quad (1)$$

where $M_{\rm HI}^{\rm pred}[T, D_{\rm opt}]$ is the HI mass expected for an isolated galaxy with the same morphological type (T) and optical diameter ($D_{\rm opt}$) as the observed galaxy, that is,

$$\log(h^2 M_{\rm HI}^{\rm pred}[T, D_{\rm opt}]) = a_T + b_T \log(hD_{\rm opt})^2, \quad (2)$$

where $h = {\rm H}_0/100$, ${\rm H}_0$ is the Hubble constant, and a_T and b_T are the best-fitting coefficients tabulated as a function of morphological type.

In the past few decades, several independent works have presented revised versions of this calibration, primarily motivated by improvements in data quality, number statistics, morphological spread, and/or definition of isolated galaxy (e.g., Solanes, Giovanelli, & Haynes 1996; Boselli & Gavazzi 2009; Toribio et al. 2011; Dénes, Kilborn, & Koribalski 2014; Jones et al. 2018). Remarkably, the most recent re-calibration of the optical diameter-based HI deficiency presented by Jones et al. (2018)—based on the Analysis of the interstellar Medium in Isolated GAlaxies (AMIGA; Verdes-Montenegro et al. 2005) project—has shown that the original coefficients presented by HG84 are still very much consistent with those based on modern datasets. An additional variant of the HG84 definition is to ignore the morphological dependence and assume that all galaxies have the same average HI surface density (Chung et al. 2009). While qualitatively consistent with the original calibration, this implementation is less robust as the typical HI surface density of galaxies is not constant (Bigiel & Blitz 2012), but admittedly it has the advantage of not relying on morphological classification and all potential biases associated with this.

The fact that the isophotal diameter turned out to be more strongly correlated with total HI mass than other optical properties (such as luminosity) should not come as a surprise. Firstly, for a self-gravitating disc, it is easy to show that the gas mass of the disc is more tightly connected to the specific angular momentum than the luminosity of a system (or even its stellar mass, see also Sections 3.3 and 3.4). Indeed, at fixed total mass, the scatter in cold gas mass is primarily driven by the spread of spin parameter[a] (Mo, Mao, & White 1998; Boissier & Prantzos 2000; Huang et al. 2012; Maddox et al. 2015; Obreschkow et al. 2016) and, observationally, sizes are more directly linked to spin than optical luminosities. Secondly, for disc galaxies, scaling relations involving isophotal radii are always tighter than those based on scale lengths and/or effective radii (e.g., Saintonge & Spekkens 2011; Cortese et al. 2012b; Sánchez Almeida 2020; see also Section 4.3), as they better trace the outer parts, and thus the full extent, of the disc component of galaxies.[b]

A key point to note is that, *by defining HI deficiency at fixed morphology and optical diameter, we implicitly make strong assumptions on the type of physical processes that this indicator is sensitive to.* Namely, we indirectly imply that the mechanism(s) removing the HI: (a) does not change the morphology of the galaxy and (b) does not affect the extent of the stellar disc. Or, at the very least, the implication is that any morphological and/or size transformations take place on timescales significantly longer than those needed to make the galaxy HI-deficient. Thus, while ideal to trace most hydrodynamical mechanisms (including outflows and starvation), this definition may not always be suited to identify stripping events where gas and stars are affected simultaneously (e.g., tidal stripping) or to follow the long-term evolution if the stellar distribution or morphology do change with time.

3.2. Definitions based on colour and structural properties

Despite its popularity over the past few decades, the HG84 definition of HI deficiency has turned out not to be the ideal approach for an application to large datasets and comparison with cosmological simulations. With the advent of the Sloan Digital Sky

---

[a] The spin parameter, λ, is a dimensionless quantity used to parameterise the deviation from centrifugal equilibrium (or in other words the amount of rotation) of a dark matter halo.

[b] See also Stevens et al. (2019b) for an extensive discussion on the origin of the small observed scatter of the HI mass versus HI size relation.

Survey (SDSS, York et al. 2000) in the early 2000s, isophotal radii have gradually become 'less popular' than effective radii, and reliable estimates have been rarely available for large datasets overlapping with HI observations. At the same time, accurate determination of morphological types (e.g., the ability to discriminate between Sa, Sb, and Sc) for large statistical samples became more challenging already at distances beyond those of the Coma cluster ($\sim$100 Mpc, $z\sim$0.023), potentially boosting the uncertainty in the estimate of deficiency. Moreover, morphological types based on visual classification are also not a standard and/or consistent output of numerical simulations, which parameterise galaxy morphology using more quantitative indicators. These issues prompted the community to develop new HI deficiency estimators (and related definitions of HI *normalcy*) which, in many instances, have also been used as basis to predict HI masses for large samples of galaxies without 21-cm observations available.

One of such modern versions of HI deficiency is the so-called HI *gas fraction plane* introduced by Catinella et al. (2010). By taking advantage of data from the GALEX Arecibo SDSS Survey (GASS), they show that the best predictor of HI-to-stellar mass ratio is a linear combination of the observed (i.e., not corrected for internal dust attenuation) near-ultraviolet minus r-band colour (NUV-r) and stellar mass surface density ($\mu_* \equiv M_*/(2\pi\ \mathrm{R}^2_{50,z})$, where M_* is the total stellar mass and $R_{50,z}$ is the radius containing 50% of the galaxy light in the z-band), with a typical scatter of $\sim$0.3 dex (see also Catinella et al. 2013):

$$\log\left(M_{\rm HI}/M_*\right) = a_1(NUV - r) + a_2\mu_* + a_3, \tag{3}$$

where a_i are the coefficients of the best fit. The potential advantage of this definition is that it does not require a morphological classification and is based on quantities that are now readily available for hundreds of thousands of nearby galaxies.

Interestingly, so far this technique has primarily been used to identify HI-excess systems (see Section 2.4) and only Cortese et al. (2011) have tested it as a potential indicator for HI deficiency. They show that, while the deviations from the gas fraction plane and the HG84 HI deficiency are correlated, the scatter can be significant ($\sim$0.4 dex), with important systematic offsets. While this is partially due to the sample used to calibrate the scaling relations (e.g., isolated galaxies vs field objects vs centrals), there is a fundamental physical reason why these two techniques do not always agree. The position of a galaxy in the gas fraction plane is primarily driven by its NUV-r colour (i.e., a proxy for its unobscured SFR, traced by the NUV emission, per unit stellar mass, traced by emission in r-band), with a secondary dependence on optical size (via μ_*). Indeed, it has been shown by several works that HI is much more directly correlated with the star formation traced by the ultraviolet than with the bulk of (mostly obscured) star formation in galaxies (e.g., Bigiel et al. 2010b; Catinella et al. 2018). Thus, contrary to the HG84 definition, *the underlying assumption in this case is that HI is affected but star formation is not (at least within the timescale traced by the NUV-r colour, i.e.,* $\sim 10^8$ *yr)*. This implies that this parametrisation is sensitive only to processes that either: (a) remove cold gas from galaxies on a significantly shorter timescale than that needed to affect the star formation, or (b) act only on the part of the atomic gas reservoir that is not directly fuelling star formation (e.g., the outer discs of galaxies).

3.3. Definitions based on broad-band luminosity or stellar mass

Another approach to quantify gas deficiency is via correlations between gas mass and broad-band optical/near-infrared luminosities (or even stellar masses; Chamaraux et al. 1980). This technique has recently regained some popularity thanks to Dénes et al. (2014), who estimated scaling relations between HI mass and luminosities in B, r, K, H, and J bands for galaxies detected by the HI Parkes All Sky Survey (HIPASS; Barnes et al. 2001). Within the HIPASS sample, these relations have a typical scatter of $\sim$0.3 dex, comparable to that of other HI deficiency proxies, and are used by the authors to identify HI-excess and HI-deficient galaxies.

While this approach has the advantage of requiring only a single band luminosity, recent works have highlighted its significant limitations (see also Bottinelli & Gouguenheim 1974 and HG84 for early discussions on why this approach may not be ideal). We now know that the optical luminosity/stellar mass versus HI mass relation is primarily driven by the fact that there are increasing numbers of star-forming (gas-rich) galaxies compared to passive (gas-poor) systems as we shift to considering lower stellar masses (Brown et al. 2015). Indeed, at fixed colour or SFR, the correlation becomes significantly weaker, with galaxies following shallower, parallel relations on the HI gas fraction–stellar mass plane, and star-forming systems being systematically more gas-rich. Thus, this relation is not a direct physically motivated correlation compared to the other correlations with star formation rates or galaxy sizes, and it has a scatter significantly larger (0.5 dex or higher; Catinella et al. 2018).

The unusually small scatter of the Dénes et al. (2014) calibration is simply due to a selection effect—because of its limited sensitivity, HIPASS detects only the most gas-rich galaxies in the local Universe (see also Lutz et al. 2017). As we discuss later in this work, this is a common issue for samples detected by HI-blind surveys, which are primarily biased towards gas-rich galaxies within their volumes (e.g., Huang et al. 2012). The fact that the HI mass versus luminosity/stellar mass scaling relation for a blind HI survey is not representative of the global galaxy population, but offsets towards gas-rich systems, implies that galaxies with normal HI content (according, e.g., to the HG84 definition) may be labelled as HI-deficient. Moreover, from a physical point of view, the use of a deficiency parameter based only on mass/luminosity significantly complicates the interpretation of any trends. As all galaxy properties correlate with stellar mass, it is unclear whether gas deficiency with respect to mass is tracing environmental effects or more simply the bimodality of star-forming properties of galaxies, which has been shown to be well established in all environments (e.g., Baldry et al. 2006).

3.4. Definitions based on specific angular momentum

In recent years, independent works have put forward a new definition of gas deficiency based on the angular momentum properties of galaxies. This idea has been proposed by a few authors throughout the last few decades (e.g., Zasov & Rubtsova 1989; Safonova 2011) and most recently expanded by Li et al. (2020). Their approach is based on the assumption that, for a flat exponential disc with circular rotation, the maximum allowed, stable value of gas fraction strongly depends on the mass and kinematics of the disc. One way to parametrise this is through the dimensionless *global disc stability parameter* q (Obreschkow et al. 2016):

$$q = \frac{j\sigma}{GM}, \tag{4}$$

where j is the baryonic (gas plus stars) specific angular momentum (i.e., angular momentum per unit mass) of the disc, σ is the gas velocity dispersion, M is the total baryonic mass, and G is the gravitational constant. The relation with neutral atomic (HI plus helium) gas fraction, $f_{\rm atm} = M_{\rm atm}/M_{\rm baryons}$, can then be generally approximated by a truncated power law of the form:

$$f_{\rm atm} = \min\left\{1, 2.5q^{1.12}\right\}. \tag{5}$$

While this is arguably a more physically motivated definition of HI deficiency (but see also Romeo & Mogotsi 2018 for some potential limitations of this approach), the basic assumptions are the same behind the original HG84 definition. Indeed, Li et al. (2020) show that (at least in the case of galaxies in the Virgo cluster) the two definitions provide remarkably consistent results.

From a practical point of view, the main short-coming of this technique is that, in addition to being calibrated on pure-disc galaxies only, it requires information on both the two-dimensional distribution and velocity field for at least one baryonic component of galaxies, as well as the total baryonic mass, which is much more difficult to obtain than optical diameter measurements. Regardless, this method implicitly assumes that the process affecting the gas does not change significantly the kinematic properties of the baryons in the galaxy (i.e., the specific angular momentum is not altered), which is not so different from the basic assumption of the optical size-based deficiency. In other words, as already hinted in Section 3.1, this definition can be viewed as a physical explanation for the success of the optical diameter-based approach.

3.5. A direct comparison of different gas deficiency definitions

One of the key reasons why the above limitations have rarely been discussed in the literature is that we are still lacking galaxy samples that simultaneously cover wide ranges of environments (to include both gas-rich and gas-deficient systems), are representative of the local galaxy population (to calibrate reliable scaling relations) and for which sizes, luminosities and angular momentum can be homogeneously estimated (see however HG84, Cortese et al. 2011; Teimoorinia, Ellison, & Patton 2017; Li et al. 2020 for discussions on different gas deficiency definitions and gas predictors in general).

Thus, in order to clarify the points discussed here, we take advantage of the semi-analytic cosmological model of galaxy formation and evolution SHARK (Lagos et al. 2018). The point of this exercise is not to reproduce the observed scaling relations[c] but to show that, even if we calibrate gas deficiency definitions using exactly the same sample and assumptions, major biases still remain.

We compare the optical size, total stellar mass (M_*), specific angular momentum (via the q parameter), and (NUV-r)+μ_*-based approaches for galaxies with stellar masses between 10^9 and 10^{11} $M_\odot$. The first three definitions are calibrated on central galaxies within 1.5σ from the SHARK main sequence of star-forming galaxies, whereas the (NUV-r)+μ_* plane is estimated for all central galaxies with an atomic gas fraction greater than 1%, following Catinella et al. (2010). For the optical size, we use the radius including 50% of the stellar mass of the disc ($R_*(50)$), whereas we estimate q from the total baryonic specific angular momentum and baryonic mass. For each galaxy in the model, we then calculate deficiency as the logarithmic difference between the HI content predicted from each scaling relation and the one given ($DEF_{\rm HI} \equiv \log(M_{\rm HI,pred}) - \log(M_{\rm HI})$). Galaxies with $DEF_{\rm HI} > 2.5$ are set to 2.5 to encapsulate the inability of observations to detect cold gas in extremely gas-poor objects.

The results are shown in Figure 2. As expected, the size and q-based estimates generally agree and are not too offset from the 1-to–1 line (left panel), whereas larger systematic offsets are seen for the stellar mass (middle) and (NUV-r)+μ_* (right) approaches. In particular, a significant fraction of HI-normal galaxies (i.e., $-0.3 < DEF_{HI} < 0.3$, indicated by the grey band) according to the size-based calibration would be classified as HI-deficient using the stellar mass-based calibration (i.e., $DEF_{HI} > 0.5$ to the right of the vertical dotted-dashed line in the middle panel), or even HI-rich or HI-excess galaxies (e.g., $DEF_{HI} < -0.5$). Conversely, many HI-deficient systems according to the size-based approach would appear HI-normal for the gas fraction plane definition (see also Cortese et al. 2011). As mentioned above, this is just due to the different samples used to calibrate the two recipes (all central galaxies with gas fraction above a threshold versus star-forming centrals only). Thus, to first order, HI-deficient galaxies would move along the plane. If we calibrate the plane on just star-forming galaxies, the dependence on star formation disappears almost entirely (simply by selection: i.e., all galaxies have similar SFRs) and the plane becomes equivalent to the gas mass–optical size relation.

In summary, some care must be taken when it comes to the HI deficiency parameter, as its definition and implications for environmental studies may differ significantly from one work to another. As we reviewed in this section, different scaling relations between cold gas content and another galaxy property (or a combination of two or more) can be used to define HI *normalcy*, and offsets from it. The interpretation of such an offset as an indicator of HI deficiency depends critically on three elements: (1) the choice of scaling relation, which implies underlying assumptions on the physical process that removes the gas; (2) the reference sample used to calibrate the scaling relation itself, typically isolated or field galaxies with HI measurements. Clearly, reference samples biased towards gas-rich systems (such as detections from HI-blind surveys) may lead us to misclassify HI-normal systems as HI-deficient ones; (3) the choice of a threshold separating HI-poor from HI-normal systems (typically from 0.3 to 0.5 dex, which is ~1–1.5 times the scatter of these relations, see also Figure 2).

Definitions of HI deficiency based on the size of the stellar disc or on its global-specific angular momentum are most sensitive to stripping processes, which may affect both gas content and star formation, hence are of particular relevance for this review (however, optical sizes are more readily available for large samples of galaxies). Choosing instead NUV-r colour (a proxy for unobscured specific SFR, see Section 3.2) as a scaling parameter implicitly assumes that gas is removed but star formation is not affected. We discourage the use of definitions based on stellar mass or luminosity alone, which have very large scatter (strongly dependent on SFR) and are often inconsistent with the 'classical', size-based HI deficiency, *even when based on the same calibration sample* (Figure 2, middle panel).

---

[c] Indeed, while SHARK shows improvements over previous semi-analytical models in reproducing galaxy scaling relations, there are still clear limitations when it comes to matching the gas properties of galaxies across environments (e.g., Hu et al. 2020).

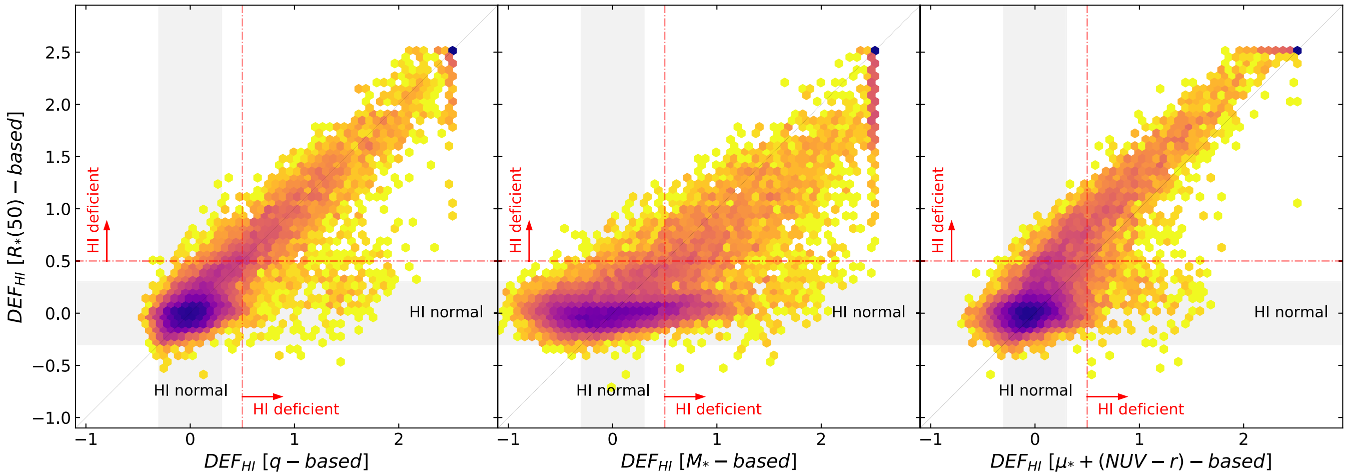

Figure 2. Comparison between different estimates of H I deficiency ($DEF_{\rm HI} \equiv \log(M_{\rm HI,pred}) - \log(M_{\rm HI})$) calibrated on the SHARK semi-analytical model of galaxy formation. From left to right, the panels show the specific angular momentum/stability parameter (q)-based, the stellar mass (M_*)-based, and gas fraction plane-based (($NUV - r$) + μ_*) definitions against the one calibrated on the H I mass versus optical disc size relation. The solid line shows the 1-to-1 relation, the grey band shows the region of 'H I-normalcy' defined by the typical scatter in the scaling relations (i.e., $-0.3 < DEF_{\rm HI} < 0.3$), and the dotted-dashed lines show the threshold of $DEF_{\rm HI}$=0.5 that we use in the rest of this paper to isolate bona-fide H I-deficient galaxies. See Section 3.5 for details on how each parameter has been estimated.

Much of the literature on the effects of environmental processes on the H I content of galaxies makes use of the optical size-based H I deficiency parameter, and this is what we adopt in the rest of this review (using a conservative threshold of 0.5 dex to safely identify H I-deficient galaxies, unless otherwise noted). However, these types of binary classifications, although initially convenient, never capture the complexity of galaxies nor the continuum of properties that we observe, thus we hope that the advent of new large-area blind surveys will see the community abandon this historical terminology and refer instead to offsets with respect to scaling relations, making sure that the calibration samples are representative of the galaxy population.

4. Cold gas removal in nearby clusters—$M_{\rm HALO} > 10^{14}$ M$_\odot$

4.1. The case for H I stripping

We start by focusing on clusters of galaxies, as these are the environments where most of the progress has been made in the last few decades. In reality, as it will become immediately clear, our knowledge of cold gas in these environments is heavily based on studies of one single cluster, Virgo, in particular when it comes to resolved analysis. At a distance of just ∼16–18 Mpc (Mei et al. 2007; Planck Collaboration et al. 2016) from Earth, and sitting in the middle of the northern Spring sky, Virgo has been the primary target of most gas surveys focusing on understanding the role of environment on the gas cycle of galaxies. Given that Virgo may not be the average nearby cluster, at least in terms of accretion history and number of substructures (Sorce, Blaizot, & Dubois 2019), this is something to keep in mind.

The reason for our limited knowledge of gas content in cluster galaxies is that H I-blind surveys, which have provided the largest samples of global H I measurements, only detect the most gas-rich galaxies in their volumes (i.e., the star-forming population), hampering our ability to study systems in the process of being affected by the environment. To demonstrate this point, we take advantage of xGASS (the extended GASS survey; Catinella et al. 2018), a stellar mass-selected, gas fraction-limited survey of ∼ 1 200 galaxies that is the current benchmark for a representative sample in terms of H I properties of nearby galaxies. In Figure 3, we show which parts of the stellar mass-SFR plane are typically detected by H I-blind surveys, in comparison with xGASS (left panel). As a reference for H I-blind surveys, we consider the upcoming Widefield ASKAP L-band Legacy All-sky Blind surveY (WALLABY; Koribalski et al. 2020), which, for unresolved sources, will have a factor ∼2 better sensitivity than the current state of the art, the Arecibo Legacy Fast ALFA (ALFALFA; Giovanelli et al. 2005) survey. We assume a typical root mean square (rms) noise for WALLABY of $\sigma = 1.6$ mJy and, for each distance shown in Figure 3, we plot galaxies that will be detected above a 5σ threshold assuming a typical velocity width of 200 km s^{-1}. Given that not even xGASS detects all passive galaxies, here we take a conservative approach by plotting the upper limits of H I non-detections (triangles). It is clear that, while at the distance of Virgo, both the star-forming and quiescent populations are mapped, beyond ∼60–100 Mpc a WALLABY-like survey will not be able to detect a large number of galaxies below the star-forming main sequence.

From the early works by Davies & Lewis (1973) and Huchtmeier, Tammann, & Wendker (1976), every investigation of clusters of galaxies has found that the late-type population has significantly less H I content than galaxies in isolation at fixed morphology, size, and/or optical luminosity. Most of the early statistical works in this area were carried out with single-dish antennae like the Arecibo and Nançay radio telescopes (e.g., Sullivan & Johnson 1978; Chamaraux et al. 1980; Giovanelli, Chincarini, & Haynes 1981; Giovanelli & Haynes 1985; Haynes & Giovanelli 1986), which simply provided global H I masses, but no information on the spatial distribution of the gas within the galaxy. Despite this limitation, 21-cm-deep surveys of several clusters in the local Universe (e.g., Virgo, Coma, Abell 262, Abell 1367, Cancer, Abell 2147/2151) have shown that H I deficiency is a widespread phenomenon in clusters and that, while deficiency does not strongly correlate with any galaxy or cluster property (see Figure 4), there is a common trend for the degree of deficiency to increase with decreasing distance from the cluster centre.

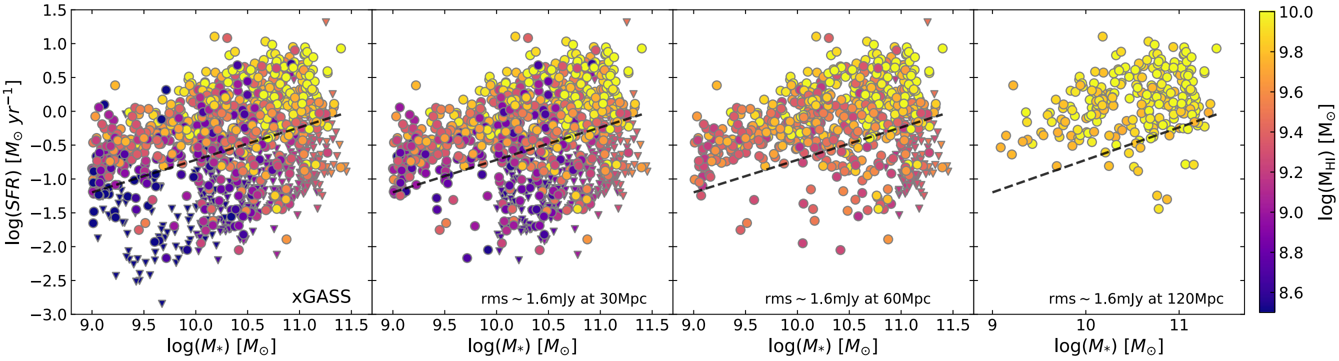

Figure 3. The ability of HI surveys to detect galaxies across the stellar mass versus SFR plane. The left-most panel shows the distribution of galaxies in the xGASS survey, which we use as input. Circles and triangles indicate HI detections and non-detections, respectively. Galaxies are colour-coded according to their HI mass (circles) or provided upper limit (triangles). The dashed line shows 2σ below the star-forming main sequence. The remaining panels show which galaxies would be detected (at 5σ level assuming a velocity width of 200 km s^{-1}) by a survey with 1.6 mJy rms noise (close to the expected sensitivity of the WALLABY survey) for distances varying between 30 and 120 Mpc. We conservatively assume xGASS non-detections at their upper limit. It is clear that, above ∼40–50 Mpc, most of the passive population starts to disappear and at distances higher than ∼100 Mpc only galaxies in the main sequence are detected.

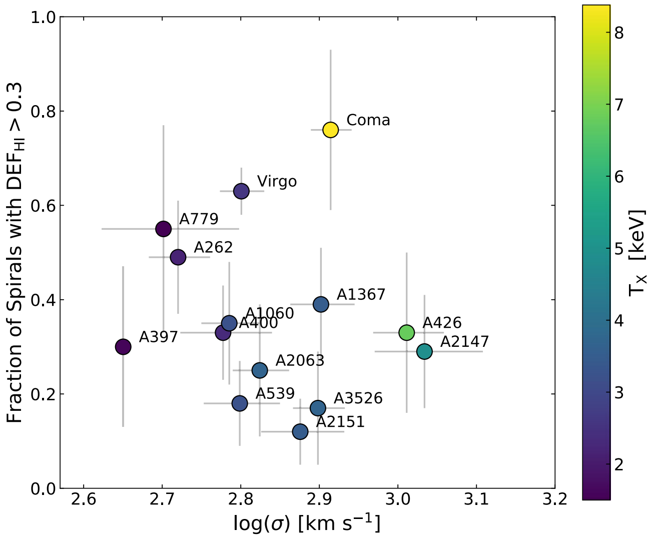

Figure 4. The fraction of HI-deficient spiral galaxies as a function of cluster velocity dispersion (a proxy for cluster mass) for the sample of nearby clusters of galaxies studied in Solanes et al. (2001). Points are colour-coded by X-ray temperature, T_X. It is clear that the fraction of HI-deficient spirals in clusters does not strongly depend on T_X or mass of the cluster.

Nevertheless, the HI deficiency versus cluster-centric distance relation has a large scatter (Solanes et al. 2001; Boselli & Gavazzi 2006), with HI-deficient galaxies observed up to a few Mpc projected distance from the centre, and both the shape and scatter of the correlation appear to depend on the dynamical state of the cluster (e.g., with Coma having a better defined correlation than Virgo). This result, combined with the initial evidence that gas-poor late-type galaxies follow more radial orbits than gas-rich systems (Dressler 1986; Giraud 1986; Solanes et al. 2001), provided the foundation to the idea that, in clusters, atomic hydrogen is directly removed from the disc during the infall, with hydrodynamical effects such as ram pressure being the primary suspect. However, it is worth noting that the same trends could also be explained via galaxy–galaxy interactions (e.g., Valluri & Jog 1990, 1991). In other words, direct stripping of the cold ISM seemed needed to explain the significant lack of gas observed in cluster spirals, but the primary driver remained elusive to single-dish observations.

The advent of radio interferometric observations dramatically improved the situation. Since the first observations of Virgo cluster galaxies by Warmels (1988) and Cayatte et al. (1990), it became clear that not only the total amount of gas, but also its radial distribution changes when galaxies plunge into clusters. HI-deficient cluster galaxies have surface density profiles significantly less extended than their optical sizes, as most of the hydrogen is missing from the outer parts of the disc, whereas the inner regions show little (e.g., within a factor of ∼2) variations in gas surface density. The transition between inner (gas-normal) and outer (gas-deficient) parts of the HI disc is much sharper than observed in field spirals and can drop from a healthy ≥ 5 M$_\odot$ pc^{-2} to less than 1 M$_\odot$ pc^{-2} within just a couple of kiloparsec. This unique feature—generally referred to as truncation of the gas disc—represents one of the clearest (if not the clearest) observational pieces of evidence supporting the idea that gas is directly stripped from the disc. Indeed, it is difficult to imagine a scenario in which a simple cessation of gas infall and/or outflows could produce such a remarkable feature (Boselli et al. 2006), without also affecting the stellar disc, which instead generally shows no sign of strong environmental perturbations in cluster galaxies.

In Figure 5, we take advantage of data from the VLA Imaging of Virgo in Atomic gas (VIVA; Chung et al. 2009) survey to show the strong correlation between HI deficiency and the extent of the HI disc normalised by the optical diameter. HI diameters are iso-density diameters measured at 1 M$_\odot$ pc^{-2} level, while optical ones are measured at the 25th magnitude per square arcsecond from the Third Reference Catalogue of Bright Galaxies (RC3; de Vaucouleurs et al. 1991). This illustrates how high deficiencies are associated with smaller HI discs, confirming that gas removal happens preferentially outside-in. Points are colour-coded by the average HI surface density within the HI size. It is clear that there is not a strong difference in surface densities between HI-deficient and HI-normal galaxies (see also Wang et al. 2016), as surface density appears to regulate the scatter of the relation for *all* deficiency values.

The detailed information provided by the resolved HI maps of Virgo galaxies made it possible to start modelling the interaction with the cluster environment, thus getting closer to isolating

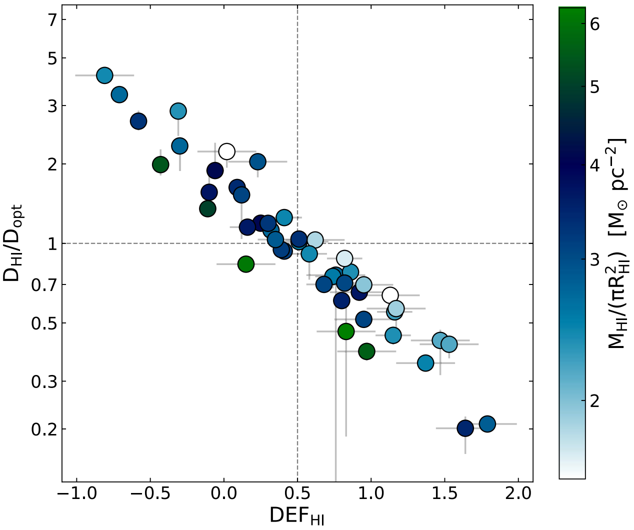

Figure 5. The HI-to-optical isophotal diameter as a function of HI deficiency for galaxies in the Virgo cluster included in the VIVA survey (Chung et al. 2009). Points are colour-coded by average HI surface density. Vertical and horizontal dotted lines are shown to guide the eye and highlight that DEF_{HI} ∼0.5 roughly corresponds to gas removal up to the optical isophotal radius.

the physical mechanism(s) responsible for the observed HI deficiency. Fundamental in this area have been the works carried out by Vollmer et al. (2001, 2004b) and Vollmer (2003) on individual Virgo galaxies, showing that stripping via a hydrodynamical process such as ram pressure is necessary to reproduce the three-dimensional distribution of atomic hydrogen in these systems. A similar conclusion was reached by interferometric studies of other nearby clusters such as Coma and Abell 1367 (Bravo-Alfaro et al. 2000, 2001; Scott et al. 2010). More recently, the discovery of one-headed HI tails, in some cases pointing away from the X-ray centre of clusters, has provided even more direct proof for the importance of stripping in removing cold hydrogen from the star-forming disc (e.g., Oosterloo & van Gorkom 2005; Chung et al. 2007; Ramatsoku et al. 2019; Deb et al. 2020). Indeed, for the typical ICM density of $\sim 10^{-3}$ cm^{-3} inferred from X-ray observations, infalling velocities of ∼1 000 km s^{-1} are enough for ram pressure to strip at least part of the atomic hydrogen content from the star-forming disc of galaxies (Gunn & Gott 1972; Boselli & Gavazzi 2006; Köppen et al. 2018).

While all the observational evidence collected so far indicates that active stripping due to the interaction between the galactic ISM and the ICM is likely the main reason for the lack of HI in disc galaxies, this does not mean that ram pressure is sufficient to explain the transformation of satellite galaxies. We now know plenty of galaxies for which at least one of the alternative environmental mechanisms described in the Introduction needs to be invoked to explain their properties. These include gravitational interactions needed to reproduce the kinematic properties of the stripped gas (e.g., NGC4254, Duc & Bournaud 2008; NGC4438, Vollmer et al. 2005; Kenney et al. 2008; CGCG97-073/79, Gavazzi et al. 2001), and feedback from star formation (e.g., NGC4424, Boselli et al. 2018). Moreover, there are also individual cases where gravitational interactions may be the dominant mechanism responsible for HI stripping (e.g., NGC 4532/DDO 137 in Virgo, Koopmann et al. 2008; NGC1427A in Fornax, Lee-Waddell et al. 2018; the Abell cluster 1367, Scott et al. 2010). This should not come as a surprise, as the pericentre of the orbit of a satellite in a cluster is precisely where ram pressure, cluster tides, and number of high-speed encounters are expected to reach their peak intensity (e.g., Smith et al. 2010a). Once again, this highlights the complexity of galaxy evolution in clusters and, while focusing on a single physical mechanism might still prove useful for individual objects (where a given process might indeed explain the main current features of a galaxy, see e.g. Section 8), it would be reductive to expect that it alone could account for the full galaxy transformation over long times.

4.2. What about molecular hydrogen?

According to our current view of star formation in galaxies, it is now accepted that molecular hydrogen (H_2) is more directly connected to star formation than HI on local (i.e. kiloparsec or smaller) scales (Bigiel et al. 2008; Leroy et al. 2008), with HI simply providing the reservoir out of which molecular clouds are formed. As such, the link between HI stripping and quenching of star formation is not straightforward. Is molecular gas directly stripped as well? Or is this denser phase of the ISM not strongly perturbed by the environment and simply consumed by star formation?

Answering these questions has been challenging because of the lack of molecular gas measurements for large statistical samples of galaxies, spanning different environments. The first complication is that, being a symmetric molecule with low mass, H_2 does not emit at the low temperatures typical of molecular clouds ($T < 50$ K), and thus requires an indirect indicator. The most widely used tracer of H_2 is carbon monoxide (CO), the most abundant molecule after H_2, whose rotational lines are easily excited in cold molecular clouds (see e.g., Bolatto, Wolfire, & Leroy 2013 for an extensive review on this topic). The second complication is that, unlike for HI, there are no large-area, blind surveys of CO emission in the local Universe, and targeted samples are small. At the time of writing, quantification of global H_2 scaling relations is limited to a few hundred galaxies (e.g., Saintonge et al. 2011, 2017; Bothwell et al. 2014; Cicone et al. 2017), a number that drops even more when it comes to resolved properties (Leroy et al. 2009). Luckily, the Atacama Large Millimeter/submillimeter Array (ALMA; Wootten & Thompson 2009) is already having a tremendous impact on this field, especially for galaxies at higher redshift.

The lack of representative samples suitable to define H_2 normalcy for galaxies has meant that any potential quantification of H_2 deficiency is made more challenging, due to selection biases and large scatter in scaling relations (Boselli, Lequeux, & Gavazzi 2002). Nevertheless, all initial investigations suggested that galaxies in rich clusters have on average the same molecular hydrogen content as systems in isolation (e.g., Kenney & Young 1986, 1988; Stark et al. 1986; Casoli et al. 1991, 1998; Boselli et al. 1997). From a theoretical point of view, this is fully consistent with an outside-in stripping scenario, where only the more diffuse gas phase (i.e., HI) in the outer parts of the star-forming disc can be significantly affected by environment. Indeed, it can be easily shown analytically that giant molecular clouds are too dense to be appreciably stripped by the ram pressure wind (e.g., Yamagami & Fujita 2011).

The fact that H_2 is significantly less affected by the cluster environment than HI is evident in Figure 6, where we show H_2-to-HI mass ratios as a function of stellar mass for disc galaxies (S0 or later types) in the Virgo cluster, taken from Boselli,

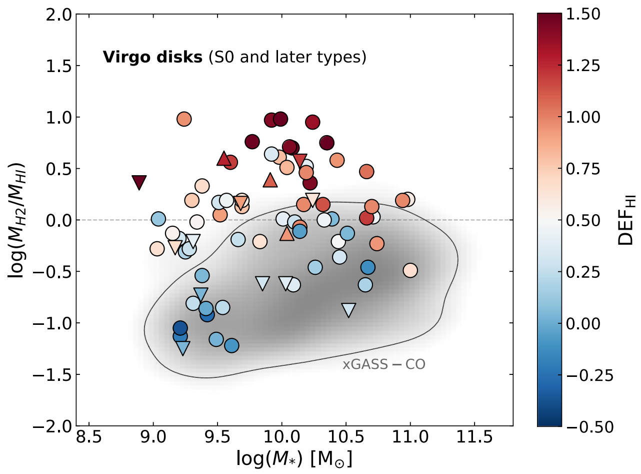

Figure 6. The molecular-to-atomic hydrogen mass ratio for disc galaxies (S0 or later types) in the Virgo cluster (Boselli et al. 2014a). Circles indicate detections in both HI and H_2, upward and downward triangles are upper limits in HI and H_2, respectively. Galaxies are colour-coded by HI deficiency. The grey region in the background shows the typical parameter space covered by local galaxies as traced by the xGASS-CO sample. It is clear that HI-deficient galaxies in Virgo have elevated molecular-to-atomic gas ratios, confirming that HI is much more affected by the cluster environment than H_2.

Cortese, & Boquien (2014a). These are compared with results from xGASS-CO (grey region; Catinella et al. 2018), a representative sample with CO($J = 1 \rightarrow 0$) measurements from xCOLD GASS (the extended CO Legacy Database for GASS survey; Saintonge et al. 2017). While HI-normal galaxies (blue symbols) are consistent with galaxies from xGASS-CO, HI-deficient systems in Virgo (red symbols) are clearly H_2-dominated (see also Mok et al. 2016; Loni et al. 2021). So, is H_2 affected at all, or are cluster galaxies simply not H_2 deficient?

Thanks to improvements of millimeter facilities, recent years have seen growing observational evidence in support of H_2 deficiency being a natural step in the path of satellite galaxies toward quenching. One of the first and best direct examples of H_2 stripping is probably NGC4522 in the Virgo cluster (Vollmer et al. 2008, but see also Vollmer et al. 2005), which shows extraplanar CO emission up to a few kpc from the disc, consistent with displacement due to ram pressure. Fumagalli et al. (2009) extended this work by providing the first statistical evidence for a population of H_2-deficient galaxies in the Virgo cluster. By combining resolved HI and H_2 observations for 47 galaxies across different environments, they showed that, *while HI deficiency by itself is not a sufficient condition for molecular gas depletion, H_2 reduction is associated with the removal of HI inside the galaxy's stellar disc.* This is consistent with the idea that the cold ISM is removed from the disc outside-in and molecular hydrogen, being more centrally concentrated than HI, is affected only when the stripping becomes efficient within the radius of the stellar disc. Intriguingly, they did not interpret H_2 deficiency as evidence for direct stripping of CO, but more as evidence that—when HI is stripped—the remaining atomic gas is at too low column densities to condense and form molecules.

A similar trend was more recently presented by Boselli et al. (2014c), who took advantage of single-dish CO observations for the volume- and K-band-limited Herschel Reference Survey (HRS, Boselli et al. 2010) to quantify H_2 normalcy (based on either stellar mass or size) in a sample of nearby, HI-normal late-type galaxies. They then quantified the degree of H_2 deficiency in Virgo galaxies and showed that the most HI-deficient galaxies are also H_2-deficient. Importantly, galaxies are H_2-deficient only when they have already lost ~80–90% of their original atomic hydrogen reservoir (i.e., $DEF_{\rm HI} > 1$). Contrary to Fumagalli et al. (2009), they interpreted this trend as mainly due to active stripping of CO by ram pressure.

The difference in the interpretation between these two works, despite their similar observational results, reflects the gradual paradigm shift that was beginning to take place in the community a decade ago, based on the growing evidence for individual objects showing direct signs of molecular hydrogen stripping, via the presence of extraplanar CO and/or CO tails (Figure 7; e.g., Corbelli et al. 2012; Scott et al. 2013; Sivanandam, Rieke, & Rieke 2014; Jáchym et al. 2014, 2017, 2019; Lee et al. 2017; Lee & Chung 2018; Chung et al. 2017; Moretti et al. 2018, 2020a). Similar evidence supporting widespread CO stripping has also been reported for galaxies in the Fornax cluster (Zabel et al. 2019). While it is possible that part of the CO observed in the stripped tails was formed in situ (e.g., Jáchym et al. 2014), the fact that these extraplanar features/tails do not show a clear separation from the CO disc suggests that at least part of the CO is being directly stripped from the disc.

Furthermore, it is now clear that cold dust is removed during the interaction with the ICM (e.g., Cortese et al. 2010a,b, 2012a, 2016; Pappalardo et al. 2012; Bianconi et al. 2020) and that global oxygen abundance in the ISM of cluster galaxies shows clear enhancements with respect to isolated systems, with radial profiles sometimes steepening (e.g., Skillman, Kennicutt, & Hodge 1989; Shields, Skillman, & Kennicutt 1991; Petropoulou et al. 2012; Hughes et al. 2013; Gupta et al. 2016). This is consistent with expectations in the case where metal-poor cold hydrogen, mostly found in the outer parts of the star-forming disc, is stripped more preferentially than the metal-enriched ISM, which is typical of the inner parts of the stellar disc. In other words, we now have plenty of evidence that the low density, diffuse, atomic gas is not the only ISM component that is affected by the cluster environment.

How can this conclusion be reconciled with the theoretical expectation that ram pressure can hardly directly strip molecular clouds? A possible explanation is that not all CO emission from galaxies is bound within giant molecular clouds, but a significant fraction of it could trace a diffuse, thick, low-volume density disc, as such more susceptible to environmental effects. While the first evidence for a CO-thick disc associated with a star-forming galaxy dates back nearly three decades (NGC 891; Garcia-Burillo et al. 1992), observational support for this has been growing in recent years. On one side, the detailed analysis of M51 performed as part of the Plateau de Bure+30m Arcsecond Whirlpool Survey (PAWS; Schinnerer et al. 2013) demonstrated that practically 50% of the CO emission originates from structures on spatial scales larger than ~1 kpc, consistent with the presence of a diffuse disc of molecular hydrogen with a typical scale height of ~200 pc (Pety et al. 2013). On the other side, detailed studies of the velocity broadening of the CO line in star-forming discs have shown that the line widths are significantly wider than that expected from a cold, thin molecular disc (i.e., ~10-12 km s^{-1} instead of ~5 km s^{-1}, Caldú-Primo et al. 2013, 2015), and more in line with those observed for the HI component, again suggesting that a significant fraction of the CO emission could come from warmer and more diffuse gas (e.g., $n \sim 100$–500 cm^{-3} and $T \sim 50$–100 K; see also Liszt, Pety, & Lucas 2010) than generally thought. This seems consistent with Milky Way observations, where diffuse CO emission associated with gas at surface densities more typical of HI gas (e.g., <10 M$_\odot$ pc^{-2};

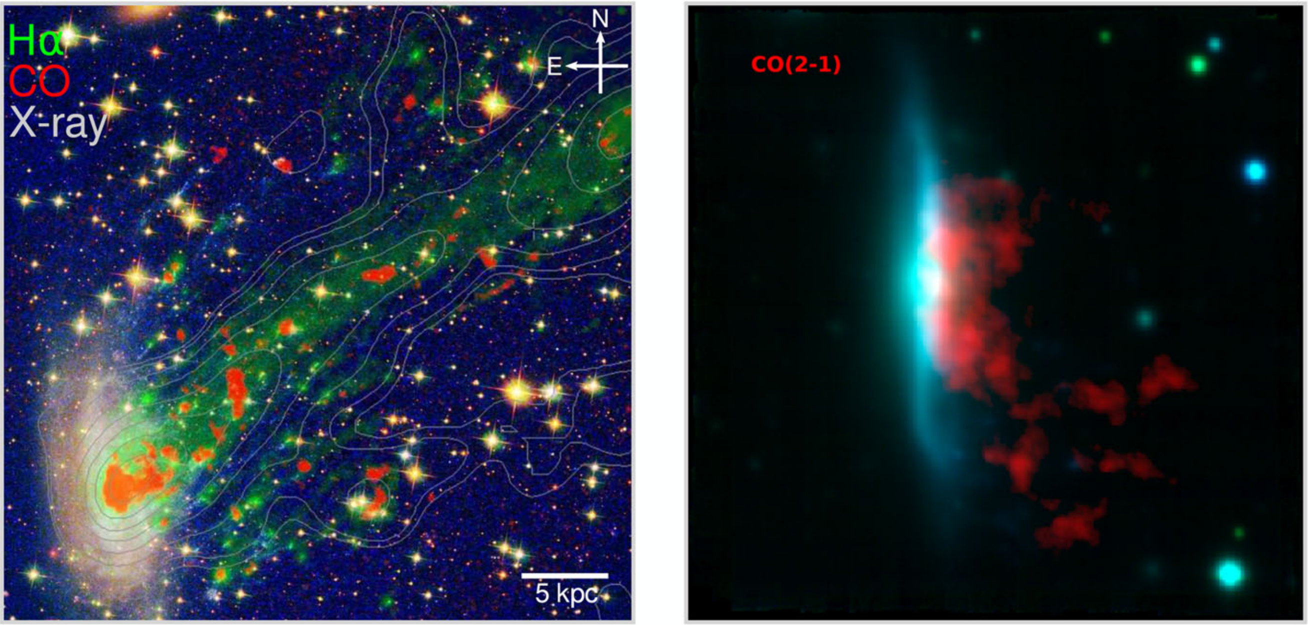

Figure 7. Spectacular examples of stripping of molecular gas, as traced by the CO(2-1) transition line (in red). *Left:* ESO 137-001, a disc galaxy infalling into the Norma Cluster. CO(2-1) emission along with Hα emission in green and X-ray contours are overlaid on a Hubble Space Telescope image (adapted from Figure 3 in Jáchym et al. 2019). *Right:* JW100 in Abell 2626, with CO(2-1) emission overlaid on a composite *V*- (blue) and *I*-band (green) image extracted from Multi-Unit Spectroscopic Explorer (MUSE) observations (adapted from Figure 8 in Moretti et al. 2020a). Images reproduced with permission from the authors. Copyright by AAS.

Roman-Duval et al. 2016) appears to account for $\sim$25% of the total mass of CO-emitting gas, but can even dominate the mass budget at large galactocentric distances (e.g., $>$8 kpc). If so, it would be easy to explain cases of extraplanar CO emission, CO tails, and/or truncated CO discs observed in cluster galaxies. Indeed, this scenario seems to be consistent with recent high-resolution ALMA observations of NGC 4402 in Virgo (Cramer et al. 2020).

However, it is important to acknowledge that there are also cases where no evidence for a significant thick CO component has been found (e.g., M33; Koch et al. 2019), and that we are still missing an extensive investigation of the frequency and properties of CO diffuse, thick discs, primarily due to the lack of CO observations able to trace emission at all physical scales. Moreover, it remains unclear if the fraction of diffuse CO emission maps directly into diffuse H_2 or not, which would clearly impact the overall physical scenario of direct molecular hydrogen stripping. Hopefully, the advent of facilities such as ALMA will soon fill this important gap in the field.

In summary, there is mounting evidence supporting the idea that CO-emitting gas can be directly removed from the disc, even by ram pressure, at least in environments similar to (or harsher than) those of the Virgo cluster. However, it seems clear that satellite galaxies can become H_2-deficient only if environmental processes are strong enough to be efficient within the optical radius of infalling galaxies. Otherwise, despite becoming HI-deficient, satellite galaxies could remain H_2-normal for a long time after infall (i.e., at least a couple of billion years after their first pericentre passage). This fully supports a scenario of outside-in removal of the ISM, where each component is affected differently, primarily depending on its radial distribution across the disc. As discussed below, this is a key element for our current picture of galaxy quenching, and for reconciling apparent contradictions within the literature.

4.3. *The connection between cold gas stripping and star formation quenching*

The evidence for cold gas stripping in clusters presented above may naively suggest that there is a one-to-one correlation between gas deficiency and star formation quenching. As we discuss in this section, the situation is slightly more complicated.

Due to the initial lack of CO observations, most of the early focus of the community has been on the link between HI deficiency and star formation quenching. From the early work by Kennicutt (1983a), and since then gradually confirmed with better data and larger samples (Gavazzi et al. 2002, 2006, 2013), it is now clear that satellite galaxies with at least a factor of $\sim$2–3 less HI than expected from their size and morphology (i.e., $DEF_{\rm HI}$ $\sim$0.3–0.5) have lower global SFRs than isolated systems. However, recent works have highlighted the presence of a significant population of HI-deficient galaxies that still lie on the blue/main sequence of star-forming galaxies (Cortese & Hughes 2009; Boselli et al. 2014b). This nicely confirms what is seen for the molecular hydrogen component of the ISM: that is, as long as the environment is only able to affect the ISM outside the optical radius, its immediate effect ($<$1 Gyr) on star formation is minor or negligible. Indeed, for an outside-in gas removal scenario, those levels of HI deficiency correspond to HI discs affected up to one optical radius (see Figure 5).

However, the clear proof of a direct connection between cold gas stripping and quenching of the star formation comes again from resolved studies. Particularly powerful have been narrowband Hα imaging surveys of nearby clusters of galaxies, which showed that the typical truncation of the gas disc in HI-deficient galaxies is mirrored by a similar truncation in the SFR surface density profile. This field was pioneered by Koopmann & Kenney (2004a,b) and Koopmann, Haynes, & Catinella (2006), who

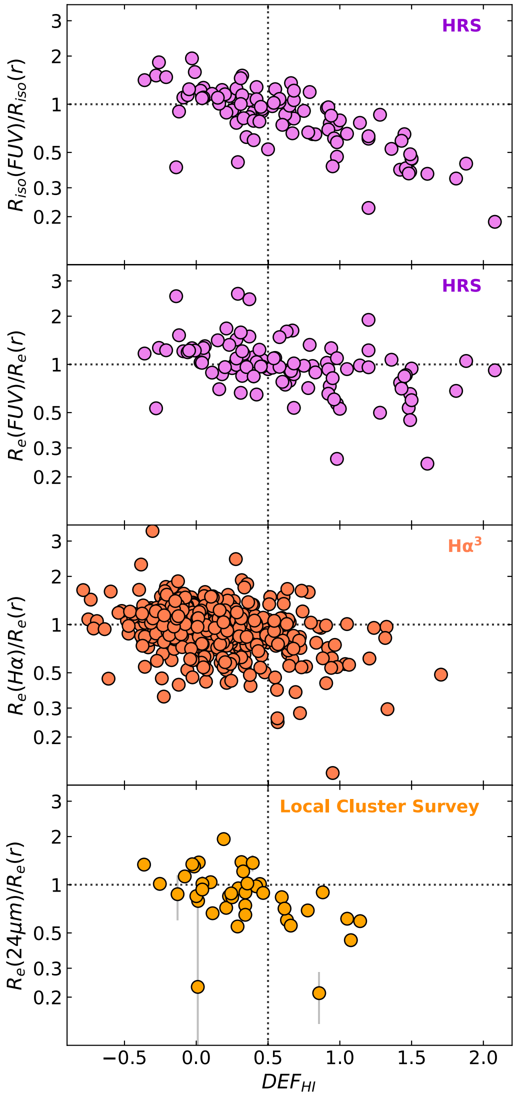

Figure 8. Star-forming-to-optical (*r*-band) disc size ratio as a function of HI deficiency. The panels show different SFR indicators and/or size estimates. Namely, from top to bottom: FUV isophotal and effective radii (Virgo cluster, Cortese et al. 2012a), Hα effective radii (Virgo and Coma supercluster, Fossati et al. 2013), and 24 μm effective radii (Local Cluster Survey, Finn et al. 2018).

surveyed a sample of 55 Virgo cluster galaxies, and showed that their star formation activity is primarily truncated in the outer parts, with the inner parts of the disc showing normal—or sometimes slightly enhanced—SFR surface densities. While, statistically, these results are consistent with active removal of the ISM, they stressed that the physical mechanisms at play might not be the same for all galaxies in their sample.

The existence of a strong correlation between HI deficiency and extent of the SFR density profiles (normalised to the extent of the optical disc) has now been confirmed by several independent works looking at different clusters and using Hα, ultraviolet emission or 24 μm emission as SFR indicators (Rose et al. 2010; Cortese et al. 2012a; Fossati et al. 2013; Finn et al. 2018). However, as shown in Figure 8, the strength of the correlation varies significantly depending on the star formation tracer used and, most importantly, on whether disc sizes are estimated using effective or isophotal radii. The latter generally provide tighter correlations, as a result of being more directly sensitive to variations in SFR surface density in the outer parts of the disc (see also Section 3.1).

It is important to remember that the extent of the star-forming disc alone provides limited information on the actual causes of quenching and cannot be blindly used to discriminate between active environmental stripping and simple cessation of infall of cold gas onto the disc. This is because a reduction of the extent of the star-forming disc can take place even without a change in the shape of the profile (i.e., by systematically reducing SFR across the entire disc, see e.g., Boselli et al. 2006), whereas it is the change in shape and the clear presence of a ‘truncation radius’ that supports the stripping scenario. This is exemplified by the apparent contradiction in the interpretation of Hα morphology of cluster galaxies between Koopmann & Kenney (2004a,b), Moss, Whittle, & Pesce (1998) and Moss & Whittle (2000) on the origin of quenching of the star formation. Both groups reported that, in clusters, star-forming discs are more compact than in the field, but while the latter interpreted this as due to funneling of gas into their centres, feeding star formation primarily in the inner regions, the former argued for a stripping scenario. It is the ability to characterise the radial variation of SFR surface densities across the disc that allowed this debate to be settled, in favour of the stripping scenario. This is something to keep in mind, as the advent of large integral field spectroscopy (IFS) surveys allows us to push these studies beyond the cluster environment (e.g., Schaefer et al. 2017; see Section 5.3) and better isolate the physical mechanisms affecting the shape of SFR surface density profiles in satellites.

4.3.1. How quickly is star formation quenched following cold gas stripping?

The link between gas stripping and quenching has been further reinforced by the ability to time the star formation quenching in the regions of the disc where gas has been stripped. This approach was pioneered by Crowl & Kenney (2008), who combined HI, Hα, and ultraviolet imaging with resolved optical spectroscopy to determine how long ago star formation was quenched (i.e., the quenching *time*) just outside the HI truncation radius for 10 Virgo cluster galaxies. Assuming nearly instantaneous quenching ($\lesssim$50 Myr), they found that, for all galaxies with truncated star-forming discs, the ages of the stellar populations outside the truncation radius are consistent with quenching within the last 0.5 Gyr. Remarkably, these quenching times agree with the time since when the gas was stripped, as estimated independently by, e.g., Vollmer et al. (2004) and Vollmer (2009) using N-body simulations that included the effect of ram pressure stripping. This suggests that quenching is indeed very fast, once the gas has been stripped, and that this happens primarily close to the pericentre of the orbit around the cluster, which coincides with the time of peak intensity of ram pressure.

These results have been corroborated by several independent works (e.g., Pappalardo et al. 2010; Boselli et al. 2016; Ciesla et al. 2016; Fossati et al. 2018; Owers et al. 2019), using different techniques, timescale definitions, and multiwavelength datasets, confirming that in galaxies infalling into a cluster star formation has been quenched relatively recently ($\sim$0.5 Gyr ago) and on short timescales ($\lesssim$100–200 Myr) *after* the cold ISM has been removed from the disc. These techniques generally require knowledge of the location of the HI and/or SFR truncation radius (i.e., 2D resolved maps) and this is why it has so far been applied only to a relatively small number of galaxies.

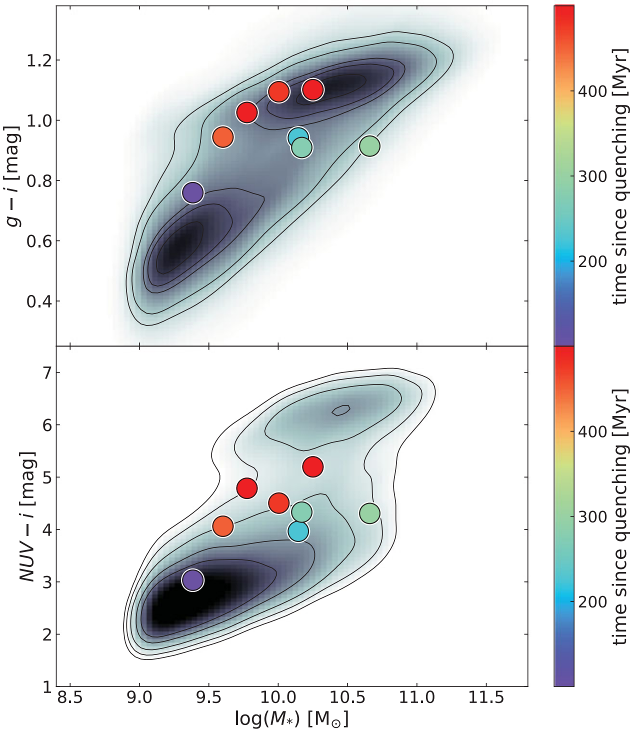

Figure 9. The $g - i$ (top) and $NUV - i$ colour (bottom) versus stellar mass diagrams for the bulk of galaxies in the Crowl & Kenney (2008) sample. Points are colour-coded according to the time since quenching. Stellar masses and colours are taken from Boselli et al. (2014d). Grey-scale and contours show the same relations for a volume-limited sample of nearby galaxies ($0.02 < z < 0.05$) extracted from the SDSS, shown to guide the eye on the location of the blue cloud ($g - i \lesssim 0.8$, $NUV - i \lesssim 4$) and red sequence ($g - i \gtrsim 1$, $NUV - i \gtrsim 5.5$). The region between the two is usually referred to as 'green valley'.

One important point to note is that most of these works assume that, while the outer parts of the discs are consistent with rapid quenching of star formation, the inner parts do not show significant signs of quenching and their stellar populations are not dissimilar from those of unperturbed galaxies. While the sharp truncation seen in both HI and SFR profiles clearly shows that star formation outside and inside the truncation radius proceeds in a different way, it is still unclear if/how environment is able to affect the star formation cycle in the inner parts of galaxies. Is low-density gas stripped and star formation affected also in the inner parts of the disc? Or can environment compress the gas in the disc, thus increasing its star formation efficiency (e.g., Mok et al. 2017)? This is something that only future resolved studies of statistical samples of cluster galaxies will be able to address.

Regardless, it should not be ignored that none of the galaxies analysed by Crowl & Kenney (2008) are fully quenched, as they lie either in the lower part of the main sequence or in the green valley (Cortese & Hughes 2009). This is shown in Figure 9, where we plot the position of most of Crowl & Kenney (2008) sample on the $g - i$ (top) and $NUV - i$ (bottom) colour versus stellar mass diagrams. Galaxies are colour-coded by the time since star formation ceased in the stripped part of the disc. Even after $\sim$0.5 Gyr since quenching occurred beyond the truncation radius, these objects have total $NUV - i$ colours a couple of magnitudes bluer than red sequence objects, while their optical colours are in most cases already consistent with passive galaxies. This is most likely because, even at pericentre, environment is not strong enough to perturb the inner parts of the disc of these relatively massive galaxies ($M_* > 10^{9.5}$ M$_\odot$). Conversely, galaxies that quenched earlier appear to lie already on the optical red sequence. This is just a consequence of the fact that optical colours saturate, therefore galaxies with residual star formation (using ultraviolet indicators) might appear completely passive (Cortese 2012), and shows that optical colours should not be blindly used to time quenching.

While for high stellar mass galaxies full quenching may not occur by the first pericentre passage, it now seems established that, at low stellar masses ($< 10^9$ M$_\odot$), most satellites close to (or past) their first pericentre passage have been fully stripped of their HI reservoir and completely quenched (Boselli et al. 2008, 2014b; Hester et al. 2010). As we discuss in Sections 4.5 and 7, this is a fundamental difference in how massive and dwarf galaxies respond to cold gas stripping mechanisms.

4.3.2. When cold gas stripping triggers star formation

While in the long-term cold gas stripping always leads to local quenching, on short timescales, it is reasonable to wonder whether the high pressure exerted by the ICM on the ISM of satellite galaxies is able to compress the gas and trigger bursts of star formation. Indeed, several theoretical works predict that, under particular conditions (e.g., the right combination of galaxy mass, ISM properties, inclination, infalling velocity and density of the ICM, etc.), the mechanism responsible for the stripping can also briefly enhance (either locally or globally) the star formation (Bekki & Couch 2003; Bekki 2013; Kronberger et al. 2008; Kapferer et al. 2009; Roediger et al. 2014; Steyrleithner, Hensler, & Boselli 2020). While cases of galaxies showing clear examples of bow shocks and asymmetries in their Hα distributions (consistent with star formation triggered by ram pressure) have been known for decades (e.g., Gavazzi et al. 1995; Chanamé, Infante, & Reisenegger 2000) and recent studies have suggested that extreme environmental effects may dramatically increase the efficiency of HI condensation into H$_2$ (Moretti et al. 2020b), the importance of these effects on the enhancement of the global SFRs of galaxies is still unclear, and most likely less than a factor of $\sim$2 (Iglesias-Páramo et al. 2004). This seems in line with recent IFS observations showing that, even in the most extreme cases of ram pressure stripping, the *global* SFR is enhanced on average by less than a factor of 2 (i.e., less than the typical scatter observed in the star-forming main sequence; e.g., Vulcani et al. 2018; Roberts & Parker 2020). Of course, locally this enhancement could be larger, and the advent of large IFS surveys targeting clusters of galaxies should provide some definite quantification of environmentally-driven *local* bursts of star formation (e.g., Vulcani et al. 2020).

An unexpected region where it is now clear that stripping can trigger star formation is in the wake of the gas tail removed from the disc, where turbulence can compress atomic hydrogen, allowing its condensation into molecules and the onset of star formation. The presence of CO emission associated with the tails supports this scenario (e.g., Jáchym et al. 2014, 2019). Galaxies with prominent tails of star-forming knots started to be discovered in the mid 2000s, with probably the first confirmed cases presented by Owen et al. (2006) and Cortese et al. (2007) in clusters at $z \sim 0.2$ (although, as also noted below, evidence for extraplanar HII regions co-located with stripped gas in cluster galaxies had been around for much longer, e.g., Kenney & Koopmann 1999).

Thanks to the improvement of optical and ultraviolet telescopes, the number of these objects (lately dubbed 'jellyfish' galaxies) has increased dramatically, and we now know of more than 100 cases of galaxies showing active star formation in their

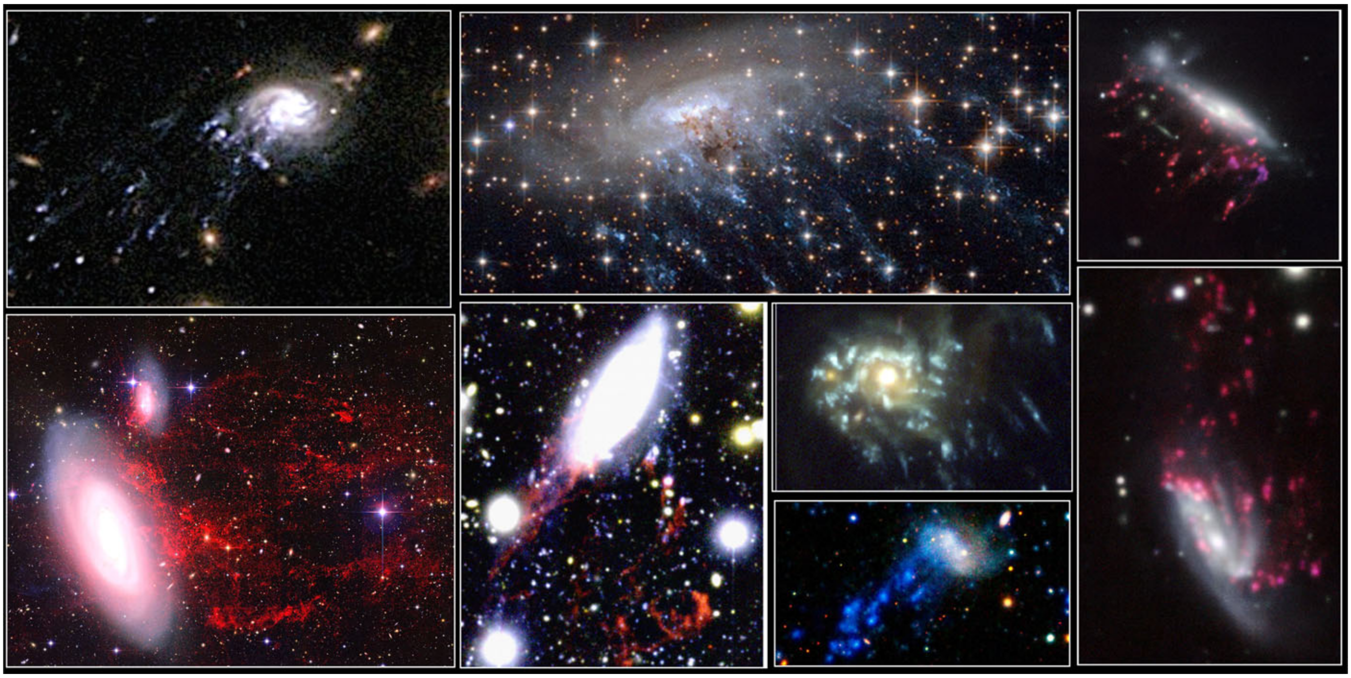

Figure 10. Examples of galaxies where ionised gas and/or active star formation is observed in the stripped gas tail. Red and blue indicate ionised gas (primarily traced by the Hα line) and star-forming regions (traced by ultraviolet or optical continuum emission), respectively. Images show galaxies in different clusters (starting from the top left in clockwise order): Abell 2667 (NASA, ESA, Jean-Paul Kneib[d], see also Cortese et al. 2007), Norma (NASA/ESA/STScI/M. Sun,[e] see also Jáchym et al. 2014), Abell 957 and IIZw108 (ESO/GASP collaboration,[f] see also Poggianti et al. 2017), Abell 2744[g] (see also Owers et al. 2012), IC 3418 in Virgo (NASA/JPL-Caltech[h] see also Hester et al. 2010), Coma (image reproduced with permission from Figure 4 in Yagi et al. 2010, copyright AAS), and NGC 4569 in Virgo (kindly provided by A. Boselli, see also Boselli et al. 2016).

tails (see Figure 10; e.g., Sun, Donahue, & Voit 2007; Yoshida et al. 2008; Smith et al. 2010b; Hester et al. 2010; Owers et al. 2012; Fumagalli et al. 2011; Ebeling, Stephenson, & Edge 2014; McPartland et al. 2016; Poggianti et al. 2019). The increased focus of the community on jellyfish galaxies has also been driven by the 'GAs Stripping Phenomena in galaxies with MUSE' (GASP, Poggianti et al. 2017) survey, which is providing us with one of the most detailed views on the properties of ionised gas and star formation in this unique class of galaxies (e.g., Poggianti et al. 2019; Bellhouse et al. 2019).

Interestingly, the increase in the number of satellite galaxies with star-forming tails, and ensuing popularity of the 'jellyfish' term, has led part of the community to label as such every system showing a hint of a tail of stripped material, regardless of whether this material is star-forming (as in the original definition) or not (e.g., Chung et al. 2009; Boselli et al. 2016, see also Figure 10). If one adopts this broader definition, then the first clear cases of jellyfish galaxies date back at least three decades, with the first detections of radio continuum tails in clusters (Gavazzi & Jaffe 1987; Gavazzi et al. 1995), and it is pretty safe to assume that every satellite galaxy in clusters will go through some kind of jellyfish phase during its evolution.[i]

However, it is still unclear what is the fraction of cases in which the stripped material 'lights-up' and forms stars in the wake of the tail. Indeed, the reason why some gas tails are able to light-up, while others do not is not completely understood. Numerical simulations point to a combination of infalling velocity, ISM density, and ICM density and temperature, with the confining pressure of the ICM surrounding the tail likely playing an important role (Tonnesen, Bryan, & Chen 2011). However, there are still a lot of open questions regarding the complex and intertwined roles of turbulence, magnetic fields, and thermal conduction within the wakes (Tonnesen & Stone 2014; Vijayaraghavan & Sarazin 2017). Multi-phase, high-resolution observations able to resolve individual giant molecular clouds, measure the properties of star-forming complexes in the tails, and trace magnetic fields (Müller et al. 2020) should help with making further progress in this area.

Lastly, it is important to note that, while triggered star formation in the stripped gas tail is expected to be mainly associated with ram pressure, this does not mean that ram pressure is the only mechanism helping to light up the tail. We now know of several examples where gravitational interactions may also play a role. Probably, the best, most generally overlooked example is represented by the Small Magellanic Cloud, whose UV tail is reminiscent of many jellyfish galaxies (see Figure 11), despite the fact that ram pressure is known to be not the only mechanism at play in this case (e.g., D'Onghia & Fox 2016).

4.4 Star formation quenching timescales

As discussed in the previous section, all observational evidence presented so far supports a scenario in which, when cold gas is stripped from the disc, *star formation in the stripped regions* is fully

---

[d] https://www.spacetelescope.org/news/heic0705/.

[e] https://www.spacetelescope.org/news/heic1404/.

[f] https://web.oapd.inaf.it/gasp/.

[g] https://frontierfields.org/2016/11/14/the-hunt-for-jellyfish-galaxies-in-the-frontier-fields/.

[h] http://www.galex.caltech.edu/newsroom/glx2010-02f.html.

[i] Adding to the ambiguity in the definition of a jellyfish system, it is important to remember that the likelihood of detection of a tail is also subject to projection effects.

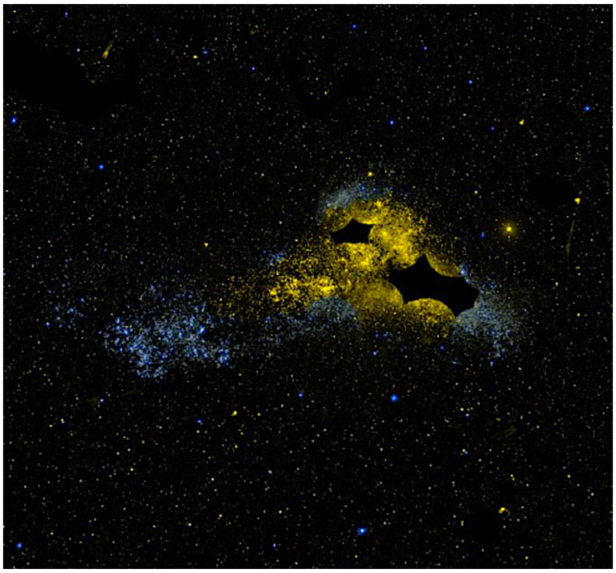

Figure 11. A GALEX far- (blue) and near-ultraviolet (yellow) colour composite image of the Small Magellanic Cloud. The star-forming tail associated with the galaxy closely resembles that of some jellyfish galaxies in clusters. The holes in the inner parts are due to the lack of GALEX pointings for the galaxy centre. Similarly, the yellow colour of most of the main body is simply due to the lack of far-ultraviolet imaging. Credit: GALEX/NASA/JPL-Caltech.[j]

quenched quickly (i.e., on timescales of a few hundreds of Myr or less). This is consistent with the predictions from theoretical modelling of ram pressure stripping, leading many to associate hydrodynamical effects with short *full quenching* timescales. However, as argued below, this assumption is plainly incorrect and, combined with the different definitions of quenching timescales presented in the literature, caused considerable confusion.

The estimate of the time needed by cluster satellites to leave the main sequence of star-forming systems does not require any information on their cold gas content, but primarily a quantification of their stellar ages and/or recent star formation history. Thus, studies focused on timing the quenching of star formation in satellites have been able to benefit, in the last two decades, from the large statistics provided by wide-area photometric and spectroscopic surveys such as the SDSS, inevitably detaching themselves from the approaches adopted in the detailed studies of the few clusters with cold gas information available. In these statistical studies, the goal is not to determine quenching timescales for individual galaxies (something generally challenging with just UV/optical broad-band integrated photometry anyway), but to statistically infer them by matching the predictions of cosmological models of structure formation with the average properties of satellite galaxies, such as their passive fraction, their specific SFR distribution, and/or their 3D position within the cluster (e.g., Balogh, Navarro, & Morris 2000; Wetzel et al. 2013; Haines et al. 2015; Oman & Hudson 2016; Rhee et al. 2020; Oman et al. 2020). The use of merger trees in a cosmological context is the key element that makes this technique orthogonal to the one applied to individual galaxies and described in previous sections.

In order to illustrate the different definitions of quenching timescales adopted in the literature, we refer to Figure 12, which schematically shows the evolution of the SFR with cosmic time for a galaxy, highlighting four key epochs in its evolution: that is, the time when it first becomes a satellite (i.e., crossing the virial radius of a host halo at $t_{1^{\rm st}\ \rm infall}$), the time when it is accreted into an even bigger halo, such as a cluster of galaxies (crossing the cluster virial radius at $t_{\rm cluster\ infall}$), the time when its SFR starts being quenched by the environment (t_q) and when it becomes passive ($t_{\rm passive}$). The present day is indicated as $t_{\rm now}$.

Going back now to the quenching timescales estimated via matching to cosmological merger trees, in this case the clock starts when the galaxy becomes a satellite (either at first infall—$t_q = t_{1^{\rm st}\ \rm infall}$—or when it crosses the virial radius of the current cluster host—$t_q = t_{\rm cluster\ infall}$) and increases with the amount of time spent in the cluster until the object becomes passive. More recently, Oman et al. (2020) introduced a variant in which the clock starts at the time when a satellite reaches its first pericentre passage through the cluster (not shown in the figure).

Conversely, for the technique based on individual galaxies, the timescale is generally measured from $z = 0$ ($t_{\rm now}$) to the time when star formation starts being affected by the environment and is expressed in terms of how long ago the galaxies started quenching. The additional complication here is that sometimes quenching is assumed to be instantaneous, and what is determined is how long ago star formation ceased, instead of a quenching timescale.

It is clear that, with such different assumptions, the two broad approaches can only agree under extremely rare circumstances, for example, if: a) quenching is not assumed to be instantaneous, *and* b) the time of infall corresponds to the time when environmental quenching starts, *and* c) the object crosses the threshold used to divide star-forming from quenched galaxies at the time of the observation (i.e., $t_{\rm passive} = t_{\rm now}$).

Interestingly, the first applications of this technique to SDSS observations of cluster satellites (e.g., Balogh et al. 2000) assumed that quenching starts indeed at the time of first infall and motivated this choice by the fact that, in most semi-analytic models at that time, the primary mechanism for environmentally driven quenching was stripping of the hot halo gas reservoir, which started as soon as a galaxy became a satellite (see also § 8). Under these assumptions, despite significant differences in the technique used to estimate quenching timescales (e.g., definition of virial radius, threshold used to separate star-forming from passive galaxies, observations used to constrain the model), all studies reached the same general conclusion: it takes a few billion years (e.g., from $\sim$2 to $\sim$6 Gyr) for satellites to become passive since the time of their infall (e.g., von der Linden et al. 2010; Weinmann et al. 2010; De Lucia et al. 2012; Wetzel et al. 2013; Hirschmann et al. 2014b; Oman & Hudson 2016).

Such long quenching timescales have always been assumed to be inconsistent with expectations from stripping mechanisms that directly affect the cold ISM in a star-forming disc. Instead, they are more in line with theoretical estimates based on starvation/strangulation, whereby quenching is caused by halting the infall of gas onto the disc.[k] Indeed, regardless of the uncertainties associated with the various techniques, these timescales are arguably much longer than what is observed in the clearest cases of ram pressure stripping. Thus, either the detailed studies of individual galaxies in Virgo provide us with a biased and non-representative view of the quenching pathway followed by

---

[j] https://www.legacysurvey.org/viewer.

[k] We note, however, that some models including only starvation can also lead to short (<1 Gyr) depletion times, as star formation can still be quenched by gas ejection via outflow (i.e., an internal process even for satellites, e.g., Zoldan et al. 2017; Xie et al. 2020).

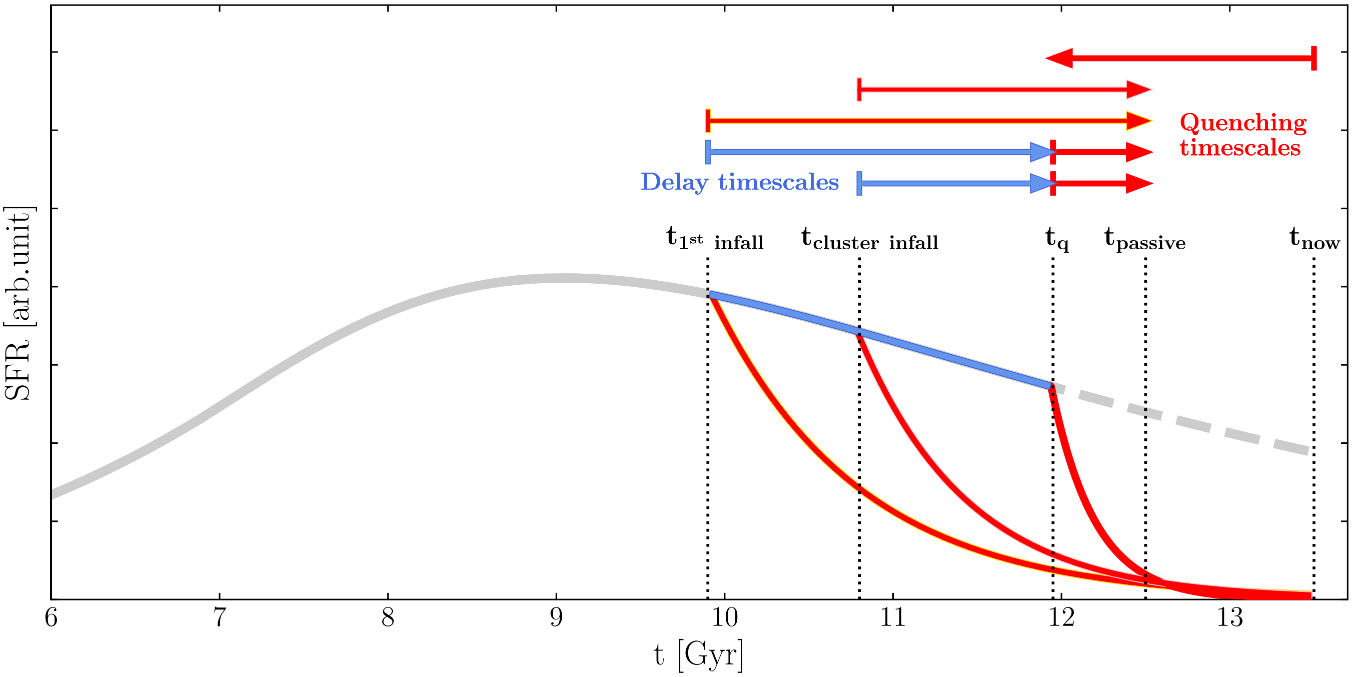

Figure 12. Cartoon illustrating various definitions of satellite quenching timescales found in the literature. The solid plus dashed line shows the expected star formation history for a galaxy with stellar mass $\sim 10^{9.5}$ $M_\odot$ at $z \sim 1$ that stays on the main sequence until $z = 0$. Five key timescales are indicated: $t_{1^{st}\ infall}$ is the time when the galaxy becomes a satellite; $t_{cluster\ infall}$ is the time of infall into its current host (assumed to be a cluster in this case); t_q is the time when environment starts affecting the galaxy's SFR; $t_{passive}$ is the time when the galaxy crosses the SFR or sSFR threshold adopted to separate active and passive systems. The red lines show how its SFR can be affected by the cluster environment, depending on whether t_q corresponds to the time of first infall, to the time of cluster infall, or to some later time. Red and blue arrows show the relative different definitions of delay and quenching timescales, with the direction of the arrow giving an idea of how time is generally assumed to proceed in the timescale estimate.

satellite galaxies, or the basic assumption in the statistical estimates of quenching timescales (i.e., that quenching starts at time of infall and proceeds exponentially since then) is incorrect.

Starting from the work presented by Wetzel et al. (2013), the refinement in the techniques used for the statistical estimate of quenching timescales suggests that the main quenching phase does not start at the time of infall but is significantly delayed (e.g., ∼2–6 Gyr; Haines et al. 2015; Oman & Hudson 2016; Rhee et al. 2020; Oman et al. 2020), as the star formation in satellites is not immediately affected by the environment after infall (indicated in light blue in Figure 12). After this delay phase, quenching proceeds extremely fast, with satellites becoming passive in one billion year or less (the exact value being again heavily model-dependent). Such a delay phase does not imply that the environment is not affecting satellites, but that its effect on star formation is negligible. Indeed, Maier et al. (2019) find that star-forming cluster galaxies show a ∼0.1–0.2 dex enhancement in their oxygen abundance well before a decrease in their SFR. This supports a 'slow-then-rapid' quenching scenario, where the ISM content and/or metal enrichment is affected before the SFR starts decreasing (e.g., infall is stopped and metals are gradually less diluted; see also Section 5.3.2).

Regardless of whether star formation remains constant or drops mildly after infall, it seems now well established that the main quenching phase (i.e., when satellites leave the locus of the star-forming sequence) does not start at the time of infall, but closer to the first cluster pericentre passage. This is a key point that allows us to reconcile different estimates of quenching timescales and build a coherent picture of quenching in clusters of galaxies.

In the rest of this section, we show how tensions between long and short quenching timescales for Virgo cluster galaxies that are clearly affected by ram pressure stripping can be resolved. From the HRS sample, we select late-type (Sa or later types) galaxies with active star formation (as traced by the Hα emission line; Boselli et al. 2015), with observations of both global HI and molecular hydrogen content (as traced by the CO(1-0) transition line; Boselli et al. 2014a), and for which at least one of the two phases has been detected. We then focus on the HI-deficient cluster members ($DEF_{\rm HI} > 0.5$; Cortese et al. 2011). By selection, this sample includes the bulk of Virgo galaxies for which quenching timescales have been directly estimated, all suggesting either instantaneous or fast (a few hundred Myr or less—e.g., Crowl & Kenney 2008; Pappalardo et al. 2010; Boselli et al. 2016; Ciesla et al. 2016; Fossati et al. 2018) quenching timescales.

In the top row of Figure 13, we compare the location of these galaxies (filled circles) with that of non HI-deficient HRS late types (blue spiral symbols) on the total cold gas mass versus stellar mass (left panel) and SFR versus stellar mass (middle) diagrams. The total gas mass is the sum of atomic and molecular gas masses, including a 30% correction for helium. As in Figure 6, we also show the distribution of the xGASS-CO representative sample as a reference for nearby galaxies (grey shaded area). Unsurprisingly, HI-deficient galaxies are also more passive (i.e., offset towards lower SFR at fixed stellar mass) than HI-normal systems but, by selection, none of them have stopped forming stars completely. Only few have already crossed the threshold separating passive from active galaxies, here indicated by the red line as defined in Wetzel et al. (2013).

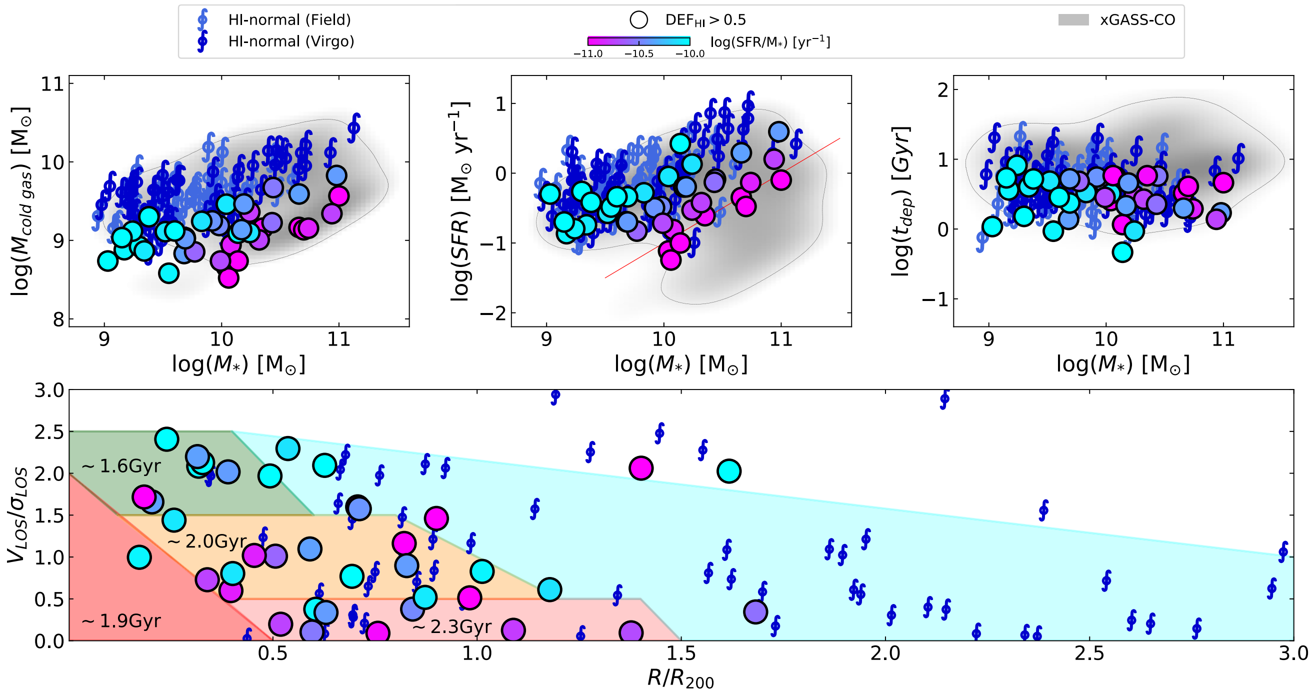

Figure 13. Properties of HI-deficient spiral galaxies in the Virgo cluster. In all plots, large symbols show HRS star-forming, spiral galaxies observed in both HI and H$_2$ and for which at least one of the two phases has been detected, separated into HI-deficient Virgo members ($DEF_{HI} > 0.5$; circles, colour-coded by specific SFR) and HI-normal systems in the Virgo volume and in the field (dark and light blue spiral symbols, respectively). *Top row*. Stellar mass is plotted versus total cold gas mass (left), SFR (middle), and total gas depletion time (i.e., total gas mass-to-SFR; right); grey shaded regions show the corresponding distributions for the xGASS-CO sample (no morphological selection) as a reference. The red line in the middle panel indicates the threshold used by Wetzel et al. (2013) to separate star-forming from passive galaxies. *Bottom row.* Position of Virgo galaxies on the projected phase-space diagram, which is split into five regions as proposed by Rhee et al. (2017); these roughly correspond to increasingly longer infall time (since crossing the virial radius) populations, from first infallers (cyan), to recent and intermediate ones (green, orange, and pink), to ancient infallers/virialised (red). For the latter four regions, we provide typical infall times for the 'Recent Infallers' population as defined in Rhee et al. (2017). Symbols are as in the top row.

The fact that some of these galaxies have short quenching timescales (e.g., $\lesssim$0.2–0.5 Gyr) is not at odds with them not being fully quenched. As already noted, estimates obtained for individual galaxies are either local timescales for complete quenching (i.e., where star formation has already stopped, e.g., Crowl & Kenney 2008; Fossati et al. 2018) or times since star formation started to decrease, regardless of whether the galaxy is already fully quenched (e.g., Ciesla et al. 2016; Boselli et al. 2016). Thus, it is clear that quick—even instantaneous—local (i.e., in the outer disc) quenching via stripping does not automatically imply rapid global quenching of the star formation. This is a key misconception that has led to confusion in the literature. The reason why these galaxies are still star-forming is simple: while they have already lost most of their cold gas reservoir in the outer parts of the disc, cold gas is still present in the inner parts, where star formation is still ongoing. Indeed, as shown in the top right panel of Figure 13, the cold gas global depletion times for these galaxies are not too dissimilar from those observed in main sequence star-forming galaxies, and at least a couple of billion years, without even considering gas recycling (see also Cortese & Hughes 2009 and Boselli et al. 2014d). Thus, without any additional major stripping event, billions of years are needed for these galaxies to become fully passive, despite the fact that they were selected to be HI-deficient.

The next step is to estimate how long ago these galaxies became satellites of the Virgo cluster. To do so, we take advantage of the approach developed by Rhee et al. (2017) and look at the position of our HI-deficient sample on the Virgo phase-space diagram[1], practically extending the analysis recently published by Yoon et al. (2017). By using cosmological hydrodynamic N-body simulations of clusters of galaxies, Rhee et al. (2017) provide an easy statistical way to assign infall timescales to different galaxy populations according to their position on the projected phase-space diagram. This is divided into five different regions, based on the typical fractions and relative infall times of different satellite populations (namely, first infallers, recent infallers, intermediate infallers, and ancient infallers). First infallers have not yet crossed the virial radius for the most part, whereas the other classes are already cluster satellites with gradually increasing infall times.

In the bottom panel of Figure 13, we show the position of the HI-deficient Virgo satellites in phase space, with the coloured boxes highlighting the regions defined by Rhee et al. (2017). By selection, almost all our galaxies are at least recent infallers (i.e., they are already Virgo cluster members) and occupy the three regions (green, orange, and pink) typical of galaxies that are still completing their first orbit into the cluster (i.e., either just before or after first pericentre passage), in agreement with the detailed dynamical modelling of Virgo galaxies by Vollmer (2009). There is a dearth of galaxies in the ‘fully-virialised’ zone at the centre of the cluster (red region). This is simply by selection, as we do not include passive (and thus most likely virialised) galaxies in these plots. It is interesting to note that, when moving from the green to the pink region, the specific SFRs of HI-deficient galaxies tend to decrease from levels typical of the star-forming main sequence (cyan circles) to lower values (violet and purple circles), supporting the idea that less active galaxies have spent longer times in the cluster. According to Rhee et al. (2017), galaxies in these regions have an 80% likelihood to have crossed the cluster virial radius at the very least ∼1–1.5 Gyr ago (i.e., the average value for ‘recent infallers’ varies between ∼1.6 and 2.3 Gyr, see bottom panel of Figure 13), consistently with the typical expectation that it takes ∼1 Gyr for a satellite to get from the virial radius to first pericentre (e.g., Lotz et al. 2019). Intriguingly, the picture emerging from this exercise is qualitatively consistent with recent work by Oman et al. (2020), who combined numerical simulations, SDSS optical data, and ALFALFA HI observations to revisit the connection between HI stripping and full star formation quenching.

---

[1] The phase-space diagram combines information on the projected cluster-centric distance and line-of-sight velocity of a satellite relative to the typical dispersion velocity of the cluster. This is a powerful tool used for decades to identify cluster members and objects at different infall stages (e.g., Kent & Gunn 1982).

In summary, we have shown that the bulk of the Virgo HI-deficient late-type galaxies with residual gas reservoir and star formation in their disc are consistent with stripping of cold (atomic) hydrogen by the cluster environment, they have been cluster satellites for at least 1 Gyr and have enough cold gas to keep forming stars (at the current rate) for at least another couple of billion years. Thus, if we had started the clock at the time of infall into the cluster, we would infer quenching timescales that are significantly longer than what one might expect from a simple ram pressure stripping scenario. In other words, while still a useful quantity, *the global quenching timescale provides us with limited information on the physical process(es) responsible for halting star formation in satellite galaxies.*

4.5. Drawing a coherent picture of the quenching of cluster satellites at z ∼0

Having reconciled the apparent tension between different estimates of quenching timescales, showing that observations of fast ‘local’ stripping are not in contradiction with claims of full quenching timescales of a few Gyr since infall, we can now combine all the evidence summarised above into a coherent picture of the typical pathway to quenching followed by cluster satellite galaxies. For simplicity, here we focus on the simple case of a galaxy becoming satellite for the first time when entering the cluster. We discuss how pre-processing might alter this picture in Section 6, after reviewing the role of cold gas stripping in the quenching of group satellites in Section 5.

First infall. After entering the cluster halo, it takes some time for the star-forming disc to feel the effect of the environment, and star formation does not drop immediately after crossing the virial radius. It is still unclear if gas accretion onto the disc remains active for some time after infall or if it stops immediately.

Approaching pericentre. The first major quenching phase starts only when active stripping of the cold ISM becomes efficient at least in the outer parts of the disc, which generally coincides with a few hundred Myr before pericentre passage. Stripping happens predominantly outside-in, perturbing first the outer parts of the disc that are less bound to the galaxy. While the primary mechanism at play seems to be hydrodynamical, in some cases gravitational interactions and/or internal mechanisms, such as feedback from supernovae or AGN, could increase the stripping efficiency (see e.g., Section 4.1). How far stripping gets inside the optical disc during the first pericentre passage likely depends on the properties of both satellite (e.g., its mass, orbit, ISM properties, etc) and cluster (e.g., ICM density, dynamical state, etc), though we are still missing a detailed characterisation of the physical parameters that determine the gas truncation radius. Moreover, parts of the ISM might be affected by the environment even inside the truncation radius, but testing this requires observations of the inner parts of the cold gas disc of satellite galaxies at kpc or sub-kpc spatial resolution.

Mass-dependent quenching. At least for a Virgo-like cluster, it appears that, to first order, low-mass galaxies ($M_* < 10^9$ M$_\odot$) can be fully stripped at first pericentre (e.g., Boselli et al. 2008), but massive systems ($M_* > 10^{10}$ M$_\odot$) are not, as a significant fraction of their gas reservoir survives in the inner parts of the disc and keeps feeding star formation. This implies that, for massive galaxies, full quenching takes place significantly after the first pericentre passage and that ram pressure stripping alone is likely not enough to explain the properties of passive satellites. This also appears to be consistent with the presence of small molecular gas reservoirs in the inner parts of early-type galaxies in clusters (e.g., Young et al. 2011; Davis et al. 2013). Admittedly, what happens to a galaxy’s remaining gas after pericentric passage is one of the most important missing pieces to the quenching puzzle. While environmental effects may still be playing a role, it is possible that the remaining gas is to a large extent exhausted internally via star formation or expelled/heated by feedback.

We note that a scenario in which low-mass satellites are quenched faster than higher mass ones may appear in contradiction with some claims of longer quenching timescales for low-mass systems (e.g., Wetzel et al. 2013, see also Section 5.4). However, this is again a matter of quenching timescale definitions. First, if the clock starts at time of first infall, it is natural that low-mass galaxies will take longer to be quenched as, on average, they spend longer in smaller groups before infalling into a cluster (De Lucia et al. 2012). Second, the use of a simple threshold in specific SFR to separate passive and active galaxies may introduce systematic effects in the estimate of quenching timescales (e.g., Pasquali et al. 2019; Rhee et al. 2020). Indeed, even on the star-forming main sequence, high-mass galaxies have lower specific SFRs than low-mass ones. As such, once star formation stops, their specific SFR will reach any fixed threshold sooner than lower mass systems, even if the rate of quenching is the same. Indeed, when individual star formation histories are examined, both observations and simulations seem to agree that low-mass galaxies are quenched more rapidly (e.g., Pasquali et al. 2019; Lotz et al. 2019; Smith et al. 2019).

Is stripping of cold ISM from the disc sufficient to halt star formation? The availability of cold gas in the inner part of massive discs that continues to feed star formation implies that, at high masses, direct stripping of the cold ISM from the disc of satellite galaxies is a *necessary but not always sufficient* condition to halt star formation. At face value, this means that neither the stripping of the cold ISM (e.g., ram pressure) nor the cessation of infall (e.g., starvation) alone is sufficient to explain the quenching of massive galaxies in clusters, but that both are required: environmental effects strip part of the cold gas *and* are responsible for

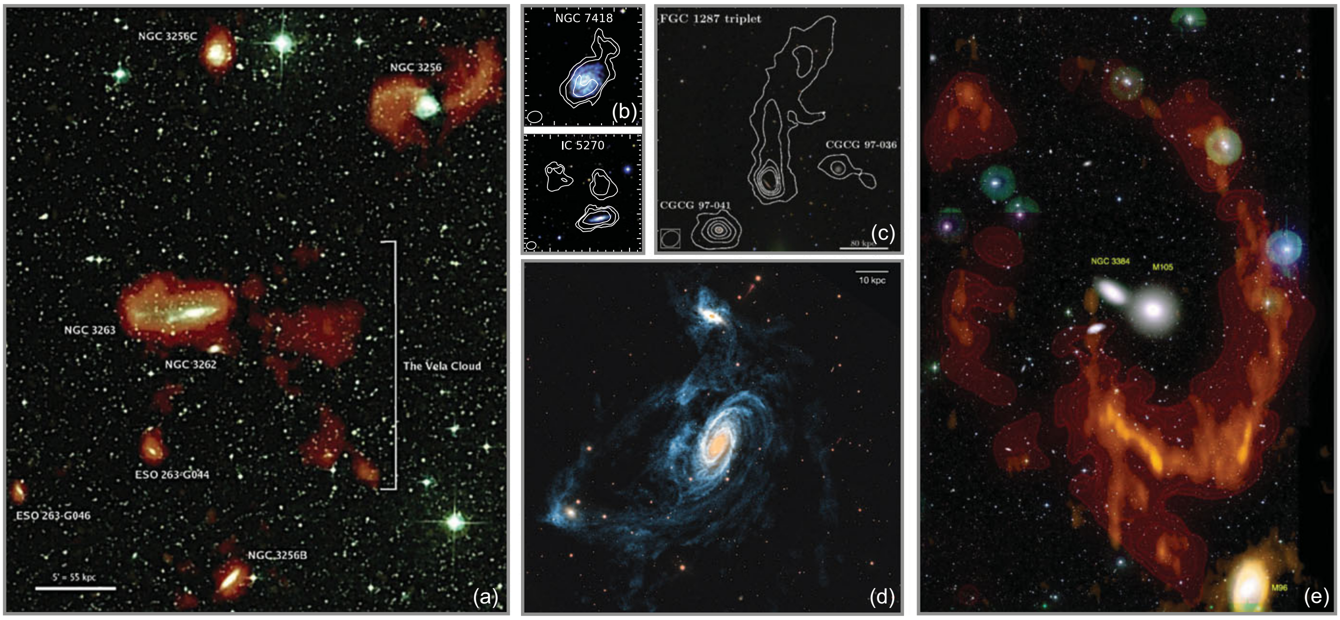

Figure 14. Examples of HI stripping in galaxy groups. In all panels, HI emission (in orange, blue, or white contours) is superposed on optical colour images. The images show the Vela group (a; from Figure 1 in English et al. 2010), the galaxy group IC1459 (b; from Figure 6 in Serra et al. 2015), the FGC1287 triplet (c; from Figure 1 in Scott et al. 2012), the M81/M82 group (d; from Figure 6 in de Blok et al. 2018), and the Leo ring (e; from Figure 1 in Michel-Dansac et al. 2010). All images are reproduced with permission. Copyright by AAS or the authors.

stopping the infall of gas, but gas consumption via star formation likely affects the inner parts of the disc, where environment is less effective. In addition, it is possible that feedback may further contribute to emptying the inner cold gas reservoir of galaxies (see also Section 8). This highlights, once more, how inadequate it would be to invoke one single mechanism as the sole responsible for star formation quenching.

5. Cold gas removal in groups—$M_{\rm halo} < 10^{14}$ $M_\odot$

The observational evidence for a direct connection between stripping of the cold ISM and quenching for satellites in groups with $M_{\rm halo} < 10^{14}$ $M_\odot$ is significantly less rich than in the case of clusters of galaxies. As discussed in Section 4.1, this is primarily due to the limitations of current HI surveys, which are not sensitive enough to probe the HI-deficient regime for large numbers of galaxies (including those in groups). The situation is worse for H_2 studies, which have not well characterized even the star-forming regime across environments, as the largest sample currently available comprises ∼500 galaxies, nearly half of which are non-detections (e.g., Saintonge et al. 2017, see Section 4.2).

While some of the conclusions drawn for clusters may be valid also for massive groups (e.g., $M_{\rm halo} \sim 10^{13.5}$ $M_\odot$), it is natural to expect some potentially major changes due to the different conditions experienced by satellites in groups. On one side, the temperature and density of the intra-group medium (ρ), as well as the orbital velocity (v) of the satellites, are lower than in clusters; hence, the efficiency of ram pressure (proportional to ρv^2, see also Section 5.2) may significantly decrease. On the other side, thanks to the lower relative velocities of group members, gravitational interactions become more efficient than in clusters at fixed satellite mass. Despite these differences, as we discuss in this section and summarise in Section 7, the overall picture emerging in Section 4.5 seems to be applicable also to galaxies in groups.

5.1. *HI stripping in groups*

Intriguingly, the first evidence for stripping of cold atomic hydrogen in groups emerged before that for clusters of galaxies. Since the first interferometric observations of the Magellanic Clouds (Kerr, Hindman, & Robinson 1954; Hindman, Kerr, & McGee 1963), and of pairs and group galaxies in our nearest neighborhoods (Roberts 1968; Rots 1975), it was clear that environment can directly remove HI and create striking trails and streams. As showcased in Figure 14, we currently have a plethora of examples of HI stripping in groups, with most of the evidence pointing towards gravitational interactions as primarily responsible for creating these features (e.g., Yun, Ho, & Lo 1994; Hibbard et al. 2001; Williams, Yun, & Verdes-Montenegro 2002; Koribalski, Gordon, & Jones 2003; Kantharia et al. 2005; English et al. 2010; Michel-Dansac et al. 2010; Serra et al. 2013, 2015; Leisman et al. 2016; Hess et al. 2017; de Blok et al. 2018; Lee-Waddell et al. 2019). This is due to the fact that, in most cases, stellar tidal features and/or peculiar optical morphologies are also clearly visible in these systems, suggesting a prominent role of tidal forces in affecting both their gas and stellar distributions.

However, one fundamental difference between the evidence for direct stripping in group versus cluster environment is that the vast majority of the galaxies in groups for which HI streams and tails have been detected are still actively star-forming and not HI-deficient (regardless of the exact definition of deficiency). This is primarily a selection effect, because interferometric observations of groups very rarely probe the HI-poor regime, and thus preferentially pick gas-rich (or gas-normal) systems, whose outer gas discs are easily perturbed by the gravitational pull from other group members. Moreover, given the mild level of stripping, in some cases it is unclear how much of the displaced gas is no longer bound to the galaxy and will not 'rain down' onto the disc (or accrete onto another satellite), as we know of at least a few examples where this seems to be the case (e.g., Hibbard & Mihos 1995; Struck & Smith 2003; Koribalski & Dickey 2004). Thus, these might not be examples of a direct link between stripping and quenching in groups. Access to the critical gas-poor regime is still primarily limited to single-dish telescopes, at the cost of losing spatial information. Even so, in the past few decades, a consistent picture is starting to emerge from HI studies.

Since the late 20th century, there have been claims of the presence of HI-deficient galaxies in loose or compact groups (e.g., Gerin & Casoli 1994; Huchtmeier 1997; Verdes-Montenegro et al. 2001), but the installation of the multibeam receiver on the 64-m Parkes telescope and the HIPASS HI-blind survey made large statistical studies more feasible, allowing us to quantify the HI content of galaxies in different types of groups (e.g., Hickson 1982 compact groups, loose groups, X-ray selected groups, etc.; Stevens et al. 2004; Omar & Dwarakanath 2005; Sengupta & Balasubramanyam 2006; Kilborn et al. 2009). The vast majority of these works found evidence for HI-deficient galaxies in groups (but see e.g., Stevens et al. 2004 for an opposite view), suggesting that, even in halos smaller than those of clusters, environmental processes are able to remove a significant fraction of the cold ISM from star-forming discs. Although different definitions of HI deficiency (see Section 3) make quantitative comparisons difficult, all major statistical studies (Verdes-Montenegro et al. 2001; Sengupta & Balasubramanyam 2006; Kilborn et al. 2009) agree that HI-deficient galaxies are preferentially found in X-ray bright groups and that, while HI-poor galaxies are more common in the inner parts of groups, there is no strong correlation between gas content and distance from the centre of the group. This is not entirely surprising, given that such a correlation is weak even in clusters, as well as strongly affected by projections effects.

Interestingly, while both Verdes-Montenegro et al. (2001) and Kilborn et al. (2009) support gravitational interactions as the primary driver for HI deficiency in groups, Sengupta, Balasubramanyam, & Dwarakanath (2007) show that the HI morphology of gas-deficient galaxies is similar to that observed in clusters and propose a scenario in which hydrodynamical mechanisms such as ram pressure may play an important role in removing cold gas from the disc. Similarly, Rasmussen, Ponman, & Mulchaey (2006), Rasmussen et al. (2008, 2012) claim that ram pressure is needed to explain the HI properties of group galaxies, although it may not always be the dominant stripping mechanism.

At the same time, a similar picture emerged from studies of the Local Group, which showed a dramatic transition between gas-rich and gas-poor satellites across the virial radius of the Milky Way (Grebel, Gallagher, & Harbeck 2003; Grcevich & Putman 2009; Spekkens et al. 2014; Westmeier et al. 2015; Putman et al. 2021), with very little or no HI found in satellites inside the virial radius. This was shown to be consistent with the expectation for ram pressure stripping by the Milky Way halo, although it is possible that gravitational interactions, supernova winds, and heating by the cosmic ultraviolet background could contribute by increasing the stripping efficiency (e.g., Mayer et al. 2007; Kazantzidis et al. 2017).

More recently, the advent of deep targeted HI surveys such as xGASS and the REsolved Spectroscopy Of a Local VolumE (RESOLVE) atomic gas survey (Stark et al. 2016), along with the second-generation HI-blind ALFALFA survey, have made it possible to extend studies of atomic hydrogen in groups to significantly larger samples and take advantage of the overlap with wide-area optical surveys such as SDSS. Perhaps the first evidence supporting the idea that HI deficiency may be widespread in groups across a wide range of halo masses came from GASS (Catinella et al. 2013), a representative sample of ~800 galaxies with stellar masses greater than 10^{10} $M_\odot$, limited an HI-to-stellar mass fraction of ~1.5%, which was later extended to smaller stellar masses (xGASS). Catinella et al. (2013) showed that satellites in groups have significantly lower gas content than central galaxies of the same stellar mass and/or stellar mass surface density. Similar results were found by Stark et al. (2016) using RESOLVE, a targeted HI survey designed to be baryonic (i.e., stellar plus atomic hydrogen) mass limited, as opposed to stellar mass selected as GASS/xGASS. Intriguingly, as shown in Figure 15 (left), the agreement between RESOLVE and xGASS is also quantitative, as both surveys provide a consistent view of the decrease of gas fraction at fixed halo mass from low- to high-mass groups. Unfortunately, most of the satellite population in large groups is still not detected even in these deep surveys, making it difficult to gain insights into the physical drivers of the observed trends.

Similarly, works based on galaxies detected by ALFALFA (Hess & Wilcots 2013; Yoon & Rosenberg 2015; Odekon et al. 2016) found that the fraction of HI-detected systems gradually decreases towards the centre of groups, with the effect being stronger in more massive halos. However, as also pointed out by Yoon & Rosenberg (2015), environmental studies based on HI detections alone have limited informative power apart from simply confirming the presence of a morphology–density relation, thus providing little evidence for the presence of stripping and any links with star formation quenching.

The real breakthrough in this field came from spectral stacking, a technique used to constrain the statistical properties of a population of galaxies that lack individual detections in a survey. When applied to an HI-blind survey, spectral stacking is a powerful tool to reach sensitivities well below the nominal one, provided that independent redshift measurements are available for large numbers of galaxies in the survey's sky footprint. Briefly, this requires to extract individual HI spectra at the known positions of the galaxies (regardless of whether these are formally detected or not), align in redshift and co-add (or *stack*)—the spectrum thus obtained gives an estimate of the total and average HI content of the sample that was co-added. By binning galaxies according to a given property (e.g., stellar mass, colour, morphology, etc.) and stacking the corresponding HI spectra in each bin, it is possible to study gas scaling relations (e.g., Fabello et al. 2011, 2012; Geréb, Morganti, & Oosterloo 2014; Brown et al. 2015, 2017; Healy et al. 2019; Guo et al. 2020; Hu et al. 2020).

Naturally, the gain in sensitivity afforded by spectral stacking comes at a cost, in terms of two important drawbacks. First, we only know the average HI content of the population that was co-added, and nothing about its dispersion (although the scatter of a relation can be explored by binning according to multiple properties simultaneously, if the sample is large enough). Second, stacking is an intrinsically *linear* operation, thus only provides linear averages. This is in contrast to scaling relations based on targeted observations, which are typically presented in terms of medians or logarithmic averages (reflecting the fact that almost all galaxy properties follow a log-normal distribution). This is illustrated in Figure 15, where we show both medians and linear averages for xGASS and RESOLVE: the two averaging techniques do not provide the same answer, hence one cannot blindly compare results from targeted observations (left panel) with stacking (right panel), or even values for single galaxies with averages

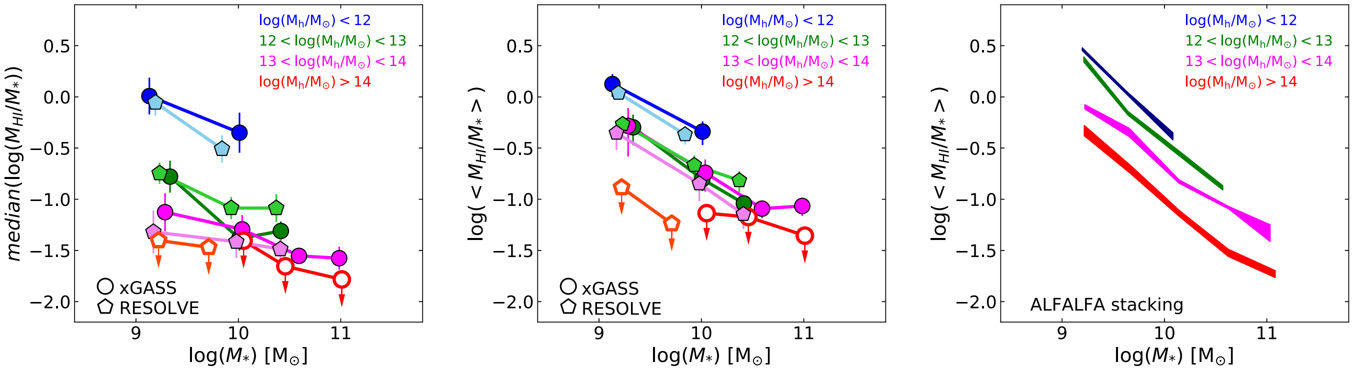

Figure 15. The HI-to-stellar mass ratio versus stellar mass relation for satellite galaxies as a function of mass of their host group halo. Results from targeted single-dish HI surveys are shown in the left and middle panel, with circles and pentagons indicating xGASS (Catinella et al. 2018) and RESOLVE (Stark et al. 2016), respectively. Colours correspond to different halo masses (as noted on the top-right corner of each panel), with arrows indicating bins dominated by upper limits. Only bins with at least 10 galaxies are shown. While the left panel shows medians values, the middle panel shows linear averages in each bin. The right panel shows the same plot obtained by Brown et al. (2017) via stacking of ALFALFA galaxies. By construction, this technique only provides linear averages and cannot be blindly compared with median scaling relations.

derived from stacking. This means that the power of spectral stacking for scaling relations lies in the determination of *relative offsets between various samples or subsets*, and that care must be taken when comparing scaling relations (and their detailed shape) from stacking with ones based on targeted observations and/or predictions from theoretical models.

Despite its limitations, stacking has provided us with the strongest observational evidence supporting cold gas stripping in groups. Fabello et al. (2012) first applied this technique to a sample of $\sim 5\,000$ galaxies with stellar mass $M_* > 10^{10}$ $M_\odot$ and redshift $0.025 < z < 0.05$, extracted from the overlap between ALFALFA and SDSS surveys. They found that, for galaxies with $M_* < 10^{10.5}$ $M_\odot$, the HI-to-stellar mass ratio decreases with increasing local environmental density faster than the specific SFR, suggesting that galaxies first lose their cold gas and then have their star formation reduced. They interpreted this result as evidence for outside-in gas stripping/star formation quenching, favouring a scenario in which hydrodynamical mechanisms like those observed in clusters of galaxies play a role even in groups with halo masses down to $\sim 10^{13}$ $M_\odot$.

This work was further extended by Brown et al. (2017), who stacked the ALFALFA HI spectra of $\sim 10\,600$ satellite galaxies extracted from the SDSS-based group catalogue of Yang, Mo, & van den Bosch (2009) to quantify the variation of HI content as a function of halo mass and galaxy-projected density. They confirmed that at fixed stellar mass, or stellar mass surface density, or specific SFR, the HI-to-stellar mass ratio of satellites monotonically decreases when moving from low to high halo masses and/or projected galaxy densities (Figure 15, right panel). Incidentally, the fact that similar trends are present at fixed specific SFR or stellar surface density (a proxy for morphology) implies that the results shown in Figure 15 are not simply a consequence of the well-known morphology/star formation rate–density relation (i.e., the fact that, at fixed stellar mass, groups have a higher fraction of gas-poorer, early-type galaxies than the field).

Very interestingly, the large number statistics allowed Brown et al. (2017) to go one step further and look for variations in HI content as a function of environment and more than one galaxy property at the same time. First, they showed that HI content decreases from small to larger halos even when controlling for *both mass and SFR*, which confirms that their findings are genuinely tracing environmentally-driven gas removal. They interpreted this trend as evidence that HI is removed without any strong effects on star formation over timescales of <1 Gyr. They also showed that the decrease in HI content depends more strongly on halo mass than local density, suggesting that the physical mechanism at work is more closely related to the size of the halo, rather than the galaxy distribution within it—again favouring active outside-in stripping, most likely by ram pressure, initiating the quenching phase of satellite galaxies.

It is important to note that, while qualitatively the results of the ALFALFA stacking agree with linear averages from xGASS and RESOLVE, there are still systematic differences, as clearly seen by comparing the middle and right panels of Figure 15. While the origin of such differences is still unclear, this highlights how more work in this area is much needed.

In summary, we have now plenty of evidence that cold HI stripping is ubiquitous also in the group environment, although the degree of HI deficiency is on average significantly lower than in clusters. However, the physical mechanism responsible for the removal of the gas remains unclear. Historically, gravitational interactions were the preferred option, as the dramatic effect of galaxy–galaxy encounters on the HI distribution is very easy to spot in groups. In recent years, though, the popularity of hydrodynamical mechanisms as a cause for HI stripping in groups has been increasing. But should we really expect ram pressure to be efficient in the group environment?

5.2. Is ram pressure efficient in the group environment?

Unlike in galaxy clusters, the observational evidence in support of ram pressure playing a significant role in groups is, arguably, circumstantial. The higher frequency of optically disturbed systems (highlighting the importance of gravitational interactions), combined with the lack of large samples of highly HI-deficient galaxies, prompted the question of whether the interaction with the intragroup medium is strong enough to strip any gas from the satellites, in particular in groups without an IGM component detected in X-rays.

As mentioned above, perhaps the best case of ram pressure-driven gas deficiency in groups is our Local Group, where the lack of HI detections in any of the dwarf satellites within the virial radius of the Milky Way is fully consistent with the predictions from a simple ram pressure stripping model (e.g., Gatto et al. 2013; Spekkens et al. 2014; Caproni et al. 2017). This indicates that, for dwarf galaxies, ram pressure can be efficient even for IGM densities of $\sim$1–2 $\times$ 10^{-4} cm^{-3}, as expected for the corona of the Milky Way. This also seems to be consistent with the presence of H I tails seen in isolated Local Group dwarf galaxies (e.g., McConnachie et al. 2007). Outside the Local Group, similar or even lower IGM densities have been shown to be sufficient to explain the H I asymmetries and/or kinematic disturbances observed in group galaxies (e.g., Bureau & Carignan 2002; Bernard et al. 2010; Westmeier, Braun, & Koribalski 2011; Elagali et al. 2019), but admittedly it is not clear if ram pressure is powerful enough to reproduce the observed trends between H I gas fractions and group halo mass.

The lack of an X-ray emitting IGM in many groups with clear signs of gas stripping has been commonly used to argue against ram pressure stripping (e.g., Scott et al. 2012), on the basis that they are thought to lack a dense medium that could provide enough ram pressure to remove cold ISM from star-forming discs. However, this is definitely not the case. Indeed, individual groups with halo mass smaller than $\sim 10^{13}$ M$_\odot$ are still partially out of reach of current X-ray missions (e.g., Mulchaey 2000; Finoguenov et al. 2009; Miniati et al. 2016) and can also host dense IGM at lower temperatures (e.g., $10^{5\text{-}6}$ K) than larger groups and clusters. Interestingly, indirect proof of the presence of a significant IGM component in X-ray faint groups comes from the work of Freeland & Wilcots (2011), who looked for bent-double radio sources in groups and estimated the density of the IGM, under the assumption that the radio jets are bent by ram pressure (see also the X-ray stacking results of Anderson, Bregman, & Dai 2013; Anderson et al. 2015). They probed projected group distances between $\sim$20 kpc and 2 Mpc and targeted groups with velocity dispersions between 250 and 570 km s^{-1}, finding clear evidence for a significant IGM even at large group-centric distances, with volume densities between 3×10^{-3} and 2×10^{-4} cm^{-3}—that is, a factor of $\sim$1–10 lower than the typical density observed in the centre of clusters such as Virgo and Coma (e.g. Boselli & Gavazzi 2006). While maybe not enough to fully strip a Milky Way-size galaxy in a group, these densities should be sufficient to remove the outer parts of the H I disc, as well as a significant fraction of the gas reservoir of dwarf galaxies. To show this, we rewrite the standard Gunn & Gott (1972) formalism for ram pressure ($\rho v^2 \geq 2\pi G\Sigma_g\Sigma_s$, where ρ is the volume density of the IGM, v is the orbital velocity of the galaxy, G is the gravitational constant, and Σ_g, Σ_s are the surface densities of gas and stars) by rescaling it to the conditions typical of the outer disc of a galaxy in a group:

$$\frac{\rho[\mathrm{cm}^{-3}]}{5\times10^{-4}}\left(\frac{v[\mathrm{km\,s}^{-1}]}{250}\right)^2 \geq 0.88\,\frac{\Sigma_g[\mathrm{M}_\odot\,\mathrm{pc}^{-2}]}{5}\,\frac{\Sigma_s[\mathrm{M}_\odot\,\mathrm{pc}^{-2}]}{5}. \tag{6}$$

It is clear that, for surface densities typically observed at a galaxy's optical radius (e.g., Leroy et al. 2008; Sánchez Almeida 2020), ram pressure can be strong enough, even for IGM densities a factor of a few smaller and orbital velocities five times slower than for galaxies passing through the centre of massive clusters (see also the modelling presented by Hester 2006 and Köppen et al. 2018).

In summary, H I stripping by hydrodynamical processes such as ram pressure can be a viable scenario to explain the H I properties of group galaxies and should not be dismissed simply based on a lack of an X-ray emitting IGM. However, even more than in clusters of galaxies, multiple physical mechanisms are likely playing a significant role in removing cold gas from the disc, and it is plausible that the primary mechanism responsible varies depending on the properties of the individual group and its satellites. Nevertheless, as discussed so far, it is clear that direct stripping of the cold ISM from the disc is widespread even in groups. So, the next step is to determine whether stripping is physically linked, or even driving, the quenching of star formation in group satellite galaxies.

5.3. Does cold gas stripping cause star formation quenching in groups?

The limited amount of H I observations available for groups, combined with the lower efficiency of stripping, makes it more challenging to obtain direct observational proof of a tight connection between cold gas stripping and quenching. As will soon become clear in this section, this issue is made even worse by the lack of adequate molecular hydrogen information *and* resolved studies of star formation activity for large statistical samples of group galaxies. Thus, in addition to considering H$_2$ and SFR properties of satellites in groups (as we did for galaxy clusters in Section 4), we are forced to resort to more indirect tracers, such as gas and stellar metallicities, in order to tease out the impact of environmental effects on the star formation cycle of galaxies in groups, and establish a connection between H I gas stripping and quenching.

5.3.1. Molecular hydrogen in groups

Molecular hydrogen investigations for representative samples of satellite galaxies in groups are almost non-existent. So far, CO observations have primarily focused on pre-selected samples of Hickson/compact groups. In these environments, molecular hydrogen appears significantly less affected (if at all) than atomic hydrogen, cases of H$_2$ deficiency are rare, and star formation efficiency appears to be the same as observed in isolated systems (e.g. Lisenfeld et al. 2014, 2017; Martinez-Badenes et al. 2012). In some cases, galaxies whose star formation has already been significantly reduced show significant H$_2$ reservoirs but low star formation efficiencies, perhaps suggesting that H$_2$ suppression (either by stripping or starvation) may not always be needed to quench star formation (Alatalo et al. 2015), but higher turbulence and/or gas heating may reduce the efficiency with which gas is turned into stars. However, it is still unclear if these findings are applicable to the average satellite galaxy in a group. Thus, it is still impossible to directly connect H I to H$_2$ in groups in a statistical sense and to use observations of cold gas in groups as direct evidence for star formation quenching.

5.3.2. SFR surface density profiles

The situation is slightly better when it comes to the resolved star formation properties of satellites. While we lack representative samples for which both resolved H I and SFR maps are available, the advent of large optical IFS surveys is gradually providing us with important insights on how group environment affects the SFR surface density profiles of satellites. Intriguingly, while pretty much all studies so far (e.g., Schaefer et al. 2017, 2019a; Medling et al. 2018; Lian et al. 2019; Spindler et al. 2018; Coenda et al. 2019; Bluck et al. 2020 but see also Eigenthaler et al. 2015 for a narrow-band-based approach) suggest that the SFR density distribution in group satellites is significantly less affected by environment than

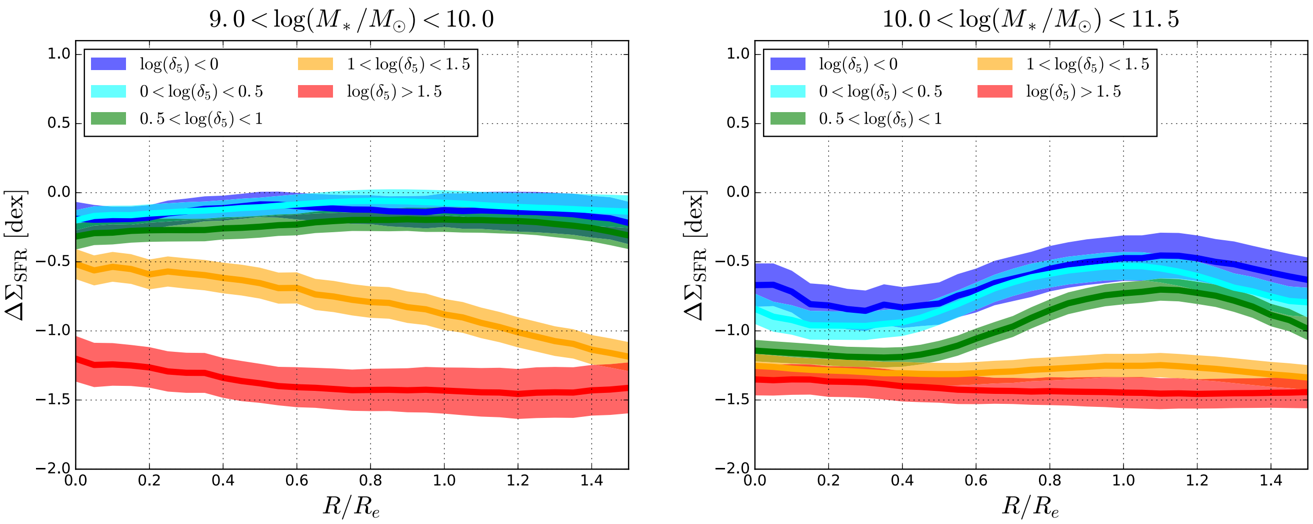

Figure 16. SFR surface density radial profiles for satellite galaxies in different environments. SFR surface density is expressed in terms of deviation from the resolved star-forming main sequence ($\Delta\Sigma_{\rm SFR}$), with $\Delta\Sigma_{\rm SFR} = 0$ indicating regions that are forming stars as expected for their stellar mass surface density. Median $\Delta\Sigma_{\rm SFR}$ radial profiles for low-mass ($9 < \log(M_*/M_\odot) < 10$, left panel) and high-mass ($10 < \log(M_*/M_\odot) < 11.5$, right panel) galaxies are split into ranges of local galaxy over-density evaluated at the 5th nearest neighbour (δ_5). The width of each coloured region indicates the 1σ uncertainty on the population average. While low-mass satellites show gradual 'outside-in' quenching, high-mass satellites are more consistent with either flat radial profiles or even 'inside-out' quenching. Adapted from Bluck et al. (2020) and kindly provided by A. Bluck.

observed in nearby clusters, the agreement between these works stops here. Schaefer et al. (2017) take advantage of the Sydney-AAO Multi-Object Integral-Field Spectrograph (SAMI) Galaxy Survey (Bryant et al. 2015) to show that the Hα SFR profiles of galaxies (with no distinction between centrals and satellites) become steeper with increasing environmental density at fixed stellar mass, consistently with what is expected if star formation is quenched outside-in. This trend is particularly strong for massive ($M_\star > 10^{10}$ M$_\odot$) systems. In other words, they suggest that quenching is due to a milder version of the same process acting in clusters. This work is further expanded by Schaefer et al. (2019a) to show that massive satellite galaxies in groups ($M_h > 10^{12.5}$ M$_\odot$) have star formation more concentrated in their inner regions than what observed in central/isolated galaxies, whereas lower mass satellites do not show any evidence of SFR concentration.

Conversely, Spindler et al. (2018) perform a similar analysis using data from the Mapping Nearby Galaxies at Apache Point Observatory (MaNGA; Bundy et al. 2015) survey and find no variation in the SFR (or specific SFR) profiles of centrals and satellite galaxies, nor a variation in the SFR density profiles with environmental density. This seems confirmed by a more recent analysis of MaNGA presented by Lian et al. (2019), where a correlation between environmental density and shape of SFR profiles may be present, but not at a statistically significant level. Intriguingly, the only stellar mass bin where the correlation may be significant covers the range $9 < \log(M_*/M_\odot) < 9.7$, in contradiction with the SAMI-based results. Similar findings have been reported by Coenda et al. (2019) using the Calar Alto Legacy Integral Field Area (CALIFA; Sánchez et al. 2012) survey, who find that the specific SFR profiles of group satellites are not different from those of field galaxies, except for galaxies in the stellar mass range $9 < \log(M_*/M_\odot) < 10$, where they find evidence for outside-in quenching.

Apart from potential differences in datasets and environmental metrics used, there are some key limitations associated with the use of Hα SFR profiles extracted from IFS data, which are most likely behind the differences between the investigations discussed above. By selection, most of these works are primarily focused on the high SFR surface density regime (i.e., $> 10^{-3}$ M$_\odot$ yr^{-1} kpc^{-2}), thus mainly tracing galaxies that are still on the main sequence. This is due not only to the sensitivity of the observations, but also to the fact that, below the star-forming main sequence, the dominant source of ionisation in the ISM is no longer star formation, but either more evolved stars, shocks, and/or accreting super-massive black holes. This makes it very challenging to derive SFR density profiles for a representative sample of satellite galaxies below the main sequence (Belfiore et al. 2017). Thus, it is not too surprising that actively star-forming satellites do not show strong signs of environmental perturbation (note that a similar conclusion would be reached also for cluster galaxies), and that those studies pushing into the passive population do find more tantalising evidence for outside-in quenching in group satellites.

Excitingly, Bluck et al. (2020) have recently been able to push the analysis of resolved star formation in satellite galaxies to lower SFRs with a two-stage approach: that is, using Hα emission where available, and the strength of the 4 000 Å break otherwise. Their findings seem to confirm that low-mass ($M_* < 10^{10}$ M$_\odot$) satellites are quenched outside-in, whereas higher mass systems may be more consistent with inside-out quenching (see Figure 16). Moreover, they argue that environment may not even play a significant role in the quenching of high-mass satellites, potentially driven by 'internal mechanisms'. This technique is very promising and could become a powerful tool for establishing how star formation is quenched in group satellites.

In summary, the star formation in the inner parts (i.e., within ∼1–1.5 effective radii) of the optical disc of group satellite galaxies does not seem to be significantly affected by environmental effects. This is in contrast to the outer parts of the disc, where the quenching of the star formation seems to be consistent with the evidence for stripping of the cold ISM up to the optical radius. Thus, it remains unclear whether there is a direct connection between stripping of H I in the outer parts of the disc and full quenching of

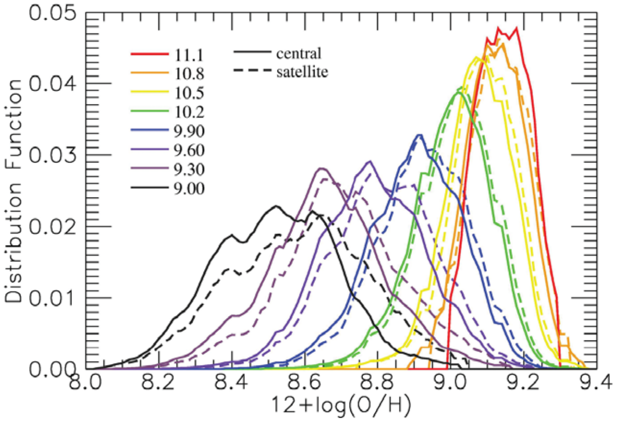

Figure 17. Gas-phase oxygen abundance distribution for star-forming centrals (solid lines) and star-forming satellites (dashed lines) for different stellar mass bins (coloured lines), based on SDSS. At the same stellar mass, the average metallicity of satellites is higher than that of centrals, especially at low stellar masses. Image reproduced with permission from Figure 2 in Peng & Maiolino (2014). Copyright by the authors.

the star formation. In order to gain more insights into this matter, we next discuss what gas-phase and stellar metallicities can tell us about the recent and past enrichment history of the ISM.

5.3.3. Gas-phase metallicities

It is now well established that, even when still forming stars at rates typical of what is observed in the star-forming main sequence, satellite galaxies in groups show gas-phase metallicities significantly higher ($\sim$0.1–0.2 dex) than central galaxies of the same stellar mass. This increase in metallicity of the ISM has been reported by studies based on both fibre spectroscopy (e.g., Pasquali, Gallazzi, & van den Bosch 2012; Peng & Maiolino 2014; Wu et al. 2017) and IFS data (e.g., Lian et al. 2019; Schaefer et al. 2019b) and appears to become more and more prominent with decreasing galaxy stellar mass (see Figure 17). While these observational findings are overall in agreement with results from clusters of galaxies and generally interpreted as evidence for the cessation of infall of pristine gas and stripping of cold ISM from the outer disc (see Sections 4.2 and 4.4), for satellites in groups multiple scenarios have been proposed. Most importantly, it is still debated whether such an increase in metallicity is directly linked to stripping. Pasquali et al. (2012) put forward a scenario in which, at the same time, (a) the halting of gas infall prevents the galaxy from accreting pristine gas; (b) ram pressure removes the gas in the outer disc and prevents radial inflow of low-metallicity gas into the disc, and (c) metal-enriched outflows are prevented due to the external pressure of the IGM. A similar conclusion was reached by Wu et al. (2017), who linked the increase in metallicity to the lack of cold gas in satellites in high-density environments.

Conversely, Peng & Maiolino (2014) argued that the increase in gas-phase metallicity has little to do with stripping or halting of gas inflow, but that it is primarily a consequence of the fact that satellites in groups accrete preferentially metal-enriched gas. They used the gas regulator model presented by Lilly et al. (2013) to show that a metallicity enhancement at fixed mass and SFR can simply be obtained by assuming that, in denser environments, the IGM is more metal enriched and, therefore, its infall into satellites would boost the metal content in their ISM. One of the key elements of their argument is indeed the presence of a clear metallicity offset between centrals and satellites having the same SFR. A similar conclusion was recently reached by Schaefer et al. (2019b), who looked at the resolved mass gas-phase metallicity of satellite and central galaxies extracted from the MaNGA survey.

The recent analysis presented by Lian et al. (2019), and based again on MaNGA data, may provide an avenue to gradually discriminate between the different scenarios presented above. They found that, at least at low stellar masses ($9 < \log(M_*/\mathrm{M}_\odot) < 9.7$), the enhancement in gas-phase metallicity is associated with a gradual flattening of metallicity gradients with increasing environmental density. This is accompanied by a weak steepening of the SFR density profiles. Using a chemical evolution model, they showed that the observed changes in SFR and gas-phase metallicity profiles are more consistent with outside-in quenching and halting of gas infall primarily in the outer parts of the star-forming disc, rather than accretion of pre-enriched material. However, they stressed that larger number statistics is needed to fully reject the metal-enriched gas accretion scenario.

As argued by Schaefer et al. (2019b), the Lian et al. (2019) sample extends to lower SFRs than the one used in other works, suggesting that they are much more sensitive to environmental effects than analyses focused on satellites that are pre-selected to lie on the star-forming main sequence. In other words, there may be multiple channels affecting the enrichment of satellite galaxies and our ability to trace them may heavily depend on sample selection criteria.

Intriguingly, a similar debate has recently emerged also from the analysis of cosmological simulations. For example, Bahé et al. (2017) take advantage of the Evolution and Assembly of GaLaxies and their Environments (EAGLE; Schaye et al. 2015) simulation to show that gas-phase metallicity enhancements are directly linked to environmental quenching, and due to the removal of metal-poor gas from the outskirts of the star-forming disc and suppression of gas inflows. Conversely, Gupta et al. (2018) show that ILLUSTRIS-TNG (Pillepich et al. 2018) satellite galaxies in groups accrete more pre-enriched gas than galaxies in isolation and suggest that this can easily account for the observed difference in gas-phase metallicity between satellites and centrals. However, as extensively discussed in Bahé et al. (2017), even in the case of theoretical simulations, the selection criteria used to match simulated and observed data can significantly influence the results.

In summary, while further analysis is needed to determine the origin of the gas-phase metallicity enhancement observed in satellite galaxies, all evidence suggests that stripping of HI can directly affect the outer parts of the star-forming disc, whereas for most of the optical disc changes in star formation activity and ISM enrichment appear more consistent with just a reduction of the gas infall rate onto the disc. This is particularly true for galaxies with stellar masses $M_* \geq 10^{10}\ \mathrm{M}_\odot$.

5.3.4. Stellar metallicities

A scenario in which cold gas stripping marginally affects the inner star formation activity of group satellites appears consistent with the stellar abundance properties of satellite galaxies (e.g., Pasquali et al. 2010; Peng et al. 2015). In particular, Peng et al. (2015) show that passive satellite galaxies have higher stellar metallicities than star-forming ones at fixed stellar mass (see also Bluck et al. 2020; Trussler et al. 2020). They argue that this is consistent with a scenario in which star formation is quenched slowly, allowing significant further enrichment of stellar populations after infall (see also Bahé et al. 2017 for a theoretical view on this). This appears also in line with the lack of any difference in the shape of stellar age and stellar metallicity gradients in galaxies as a function of environment (e.g., Goddard et al. 2017; Zheng et al. 2017) and the fact that already quenched satellite galaxies rarely support an outside-in quenching of their star formation within ∼1–1.5 effective radii (e.g., Lin et al. 2019). One potential caveat in trying to link studies of stellar metallicities with those focused on SFRs, gas-phase metallicites, and cold gas is that these two approaches generally target different populations, with gas studies focusing on star-forming satellites only, while stellar ones also including galaxies that are already quenched and have likely spent most of their life as satellites (e.g., Pasquali et al. 2019; Smith et al. 2019). Thus, the two approaches may be sensitive to different physical processes and infall times.

5.4. Star formation quenching timescales in the group environment

It should be now clear to the reader that, even in groups, the picture emerging on the potential connection between stripping and quenching is not dramatically different from what we have seen for clusters. Thus, the key points on quenching timescales highlighted in Section 4.4 are applicable also to the group environment. However, here it is worth going into greater detail on issues that are directly relevant to group satellites.

Even in groups, it is natural to expect that, for low-mass galaxies ($\lesssim 10^8$ M$_\odot$), ram pressure is strong enough to remove all the cold gas reservoir soon after the crossing of the virial radius or at first pericentre passage. Thus, for these objects, quenching timescales (measured from the time of infall until the time of quenching) should be relatively short (i.e., ∼1 Gyr).

This is indeed the consistent picture emerging from all estimates of quenching timescales for galaxies in the Local Group (e.g., Fillingham et al. 2015, 2019; Wetzel, Tollerud, & Weisz 2015). Excitingly, with the advent of the Gaia mission (Gaia Collaboration et al. 2016), it has even become possible to reconstruct the orbits of satellites around the Milky Way and determine quenching timescales with unprecedented accuracy. By doing so, Fillingham et al. (2019) find quenching timescales (measured from the time when the galaxy crossed the virial radius of the Milky Way halo) <2 Gyr for all Milky Way satellites with stellar masses lower than $M_* \sim 10^8$ M$_\odot$. Moreover, as expected, the exact timescale strongly depends on the detailed orbital parameters of each satellite, with orbits with unusually large pericentre passages corresponding to significantly longer (i.e., several Gyr) quenching timescales. Interestingly, Wetzel et al. (2015) report a trend of increasing quenching timescale with increasing stellar mass, consistent with the idea that the efficiency of the quenching mechanism decreases with increasing mass, as in the case of ram pressure stripping.

It would be natural to assume that, at fixed group mass, the trend of increasing quenching timescale with increasing mass can be extrapolated to higher stellar masses. However, the picture appears a bit more complicated. If we combine all most popular estimates of quenching timescales in satellites (see e.g., Wheeler et al. 2014; Fillingham et al. 2015, 2016; Wetzel et al. 2015) an unexpected trend emerges, where quenching timescales increase with stellar mass of up to ∼6–8 Gyr for stellar masses of $\sim 10^9$ M$_\odot$ and start decreasing for higher stellar masses. The favoured interpretation of this trend is that $M_* \sim 10^9$ M$_\odot$ represents the transition mass above which stripping of the cold ISM becomes inefficient and starvation becomes dominant. Thus, the decrease in quenching timescale at higher masses is supposedly just a consequence of shorter total gas depletion times in more massive galaxies (e.g., depletion time scaling with $M_*^{-0.3}$; Davé, Oppenheimer, & Finlator 2011).

While future investigations are needed to settle this issue, we recommend caution in interpreting such trends at face value. Not only are different group masses combined but, as discussed in Section 4.4, there are many caveats in the use of quenching timescales to isolate physical processes driving quenching, and mass trends could be a simple by-product of the threshold used to separate passive and active galaxies. Moreover, longer timescales may not mean less efficient quenching, but different orbital parameters/accretion histories. Quenching likely does not start at the time of crossing the virial radius, and there is evidence suggesting that it is this time delay between infall and onset of quenching that drives the mass dependency of quenching timescales in both groups and clusters (e.g., Wetzel et al. 2013; Rafieferantsoa, Davé, & Naab 2019). Indeed, as already mentioned, when quenching timescale estimates do not depend on assumptions on delay time, mass dependencies either disappear or revert back to less massive systems being quenched faster (e.g., Smethurst et al. 2017; Pasquali et al. 2019). This conclusion appears in line with the recent findings by Oman et al. (2020), who provide an extensive discussion on the biases and limitations of the various techniques used so far to infer quenching timescales and on how these could artificially introduce mass dependencies.

From a quantitative point of view, a more detailed analysis is required to determine whether a decrease in quenching timescale of a factor of ∼4 from stellar masses of 10^9 to 10^{11} M$_\odot$ (e.g., from 8 to 2 Gyr; Fillingham et al. 2015) can be explained with just a variation in depletion time. At the time of writing, any mass dependence in the total gas depletion time observed in nearby galaxies rarely surpass a factor of ∼2, with a large scatter (see also Figure 13). Indeed, previous works have reported total gas depletion times even increasing with decreasing specific SFR (Boselli et al. 2014d), and molecular gas depletion times monotonically increasing with increasing mass and decreasing specific SFR (Saintonge et al. 2017), that is, opposite to what is expected if cold gas depletion times drive quenching timescales.

Regardless of the exact mass dependence of quenching timescales for stellar masses larger than $\sim 10^9$ M$_\odot$, it is clear that in groups, as in clusters, a few billion years (i.e., multiple pericentre passages) are needed to fully quench intermediate- and high-mass satellites. Most importantly, even in groups, it seems clear that both stripping of the cold ISM (for dwarf galaxies and the outer parts of discs in more massive systems) and slower quenching, at least partially associated with the halting of gas accretion onto the star-forming disc, are playing a role in driving satellites out of the star-forming main sequence.

6. Pre-processing and the role large-scale structure

So far, we have looked at satellites in groups and clusters under the hidden assumption that they spend all their life as satellites in the host halo in which they are found at $z \sim 0$. This is definitely useful to set the scene and provide an overview of the observational evidence supporting the link between cold gas removal and quenching. This is also motivated by the fact that we are still lacking the ability to trace environmental effects on cold gas beyond $z \sim 0.1$. However, it is important to note that this is an oversimplification.

In a hierarchical framework, structures grow through accretion of lower mass halos. Thus, satellites observed today in massive groups and clusters may have spent a significant part of their past evolutionary history as satellites of smaller groups and may have been affected by nurture in environments different from those they currently inhabit, a scenario generally referred to as *galaxy pre-processing* (e.g., Zabludoff & Mulchaey 1998; Fujita 2004). Similarly, galaxy groups are not isolated entities but are embedded into the large-scale structure of the Universe and, during their growth, move along cosmic filaments. Growing support is emerging from cosmological simulations for a potential physical connection between cold gas accretion, disc spin orientation, and location of galaxies within filaments (e.g., Codis et al. 2012; Dubois et al. 2014; Kraljic et al. 2020).

Thus, it is important to review the current observational evidence for the role of pre-processing and large-scale structure on cold gas stripping and discuss how this fits into the picture emerging from the previous sections.

6.1. Pre-processing

Given the focus of this review on the quenching of star-forming satellites, here we are interested in the potential role of pre-processing in starting (but not completing) the quenching phase of satellites before their infall into the current cluster (or large group; for simplicity, we refer only to clusters in the rest of this section). Indeed, while important for understanding the variation of the passive satellite fraction with environment and mass (e.g., De Lucia et al. 2012; Wetzel et al. 2013; Haines et al. 2015), pre-processed satellites infalling into the cluster already fully quenched are irrelevant for what was discussed in Section 4, and their quenching history (as well as the role of pre-processing) is fully encapsulated in Section 5, where we have seen how groups can quench star formation in their satellites.

From a theoretical point of view, there is general agreement that roughly ∼30–40% of the satellite population found in cluster-size halos (e.g., 10^{14} $M_\odot$) fell into the cluster as a satellite of a halo of mass $\sim 10^{13}$ $M_\odot$ (e.g., McGee et al. 2009; De Lucia et al. 2012; Han et al. 2018). However, this fraction strongly depends on stellar mass, with more massive galaxies having an increased likelihood of infalling into clusters as centrals than lower mass systems (De Lucia et al. 2012; Wetzel et al. 2013). Most importantly, the time spent as a satellite before infalling into the cluster can vary dramatically (e.g., from just ∼0.1 to 8 Gyr or more) but is generally ∼2–3 Gyr or less (e.g., see Figure 18). This is of the same order of magnitude, or even shorter, than the typical delay time before the onset of the major quenching phase in satellites (∼2–6 Gyr). In this time frame, pre-processing could definitely impact on the ability of satellites to accrete new gas and could also contribute to the removal of cold gas from the very outer discs. But it seems unlikely that, for the bulk of star-forming galaxies infalling into today's clusters (which are the focus of this review), pre-processing plays a key role in their path towards quenching. This is simply because they are still in the star-forming main sequence when they reach the cluster environment and, by definition, their star formation activity has not yet been significantly affected by the environment experienced before infall.

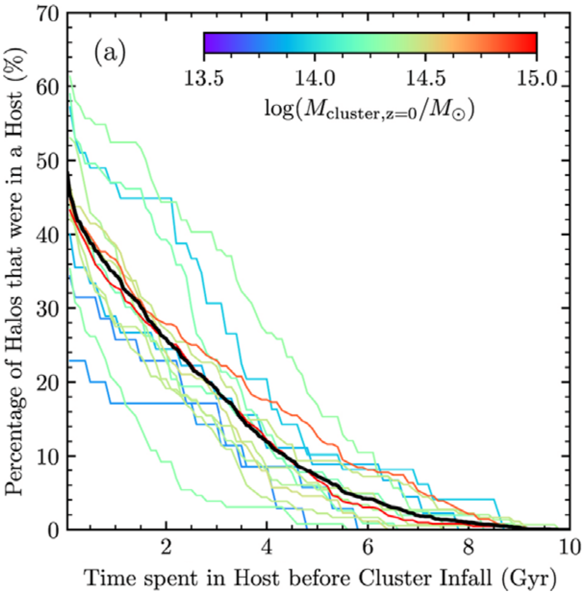

Figure 18. Cumulative percentage of cluster satellites at $z=0$ that have spent more than a certain amount of time in a host before infall, as predicted by the Yonsei Zoom-in Cluster hydrodynamic simulation. The thick dark line shows the percentage of all members in the 15 clusters studied, while thinner lines (colour-coded by cluster mass) show individual clusters. Image reproduced with permission from Figure 2 in Han et al. (2018). Copyright by AAS.

Indeed, from an observational point of view, apart from peculiar cases of groups infalling into clusters (e.g., Cortese et al. 2006; Džudžar et al. 2019), the few observational pieces of evidence suggesting an effect of pre-processing on the gas reservoir of infalling star-forming satellites indicate just very small variations in HI content (∼0.1–0.2 dex, e.g., Yoon & Rosenberg 2015; Odekon et al. 2016). These are generally within the typical variation in the HI content of galaxies on the star-forming main sequence (Janowiecki et al. 2020) and, indeed, the bulk of the population of infalling satellites in clusters has SFR and HI content within ∼0.2 dex of those observed in isolated systems (e.g., Cortese & Hughes 2009; Boselli et al. 2014d).

Admittedly, the limitation of current HI and H_2 surveys makes it impossible to further investigate the role of pre-processing in any detail and quantify its effect on cold gas content and SFR *simultaneously* as a function of group and satellite mass. However, it is clear that, when star-forming satellites infall into cluster-size halos (∼10^{14} $M_\odot$ or higher), the key paths driving the quenching of the star formation are those summarised in Section 4.5 (i.e., outside-in stripping and quenching), with group pre-processing potentially only making them more efficient.

6.2. Large-scale structure filaments

Even more circumstantial is the observational evidence for a connection between cold gas content, star formation quenching, and position of galaxies within filaments. Only a handful of studies have investigated the correlation between HI mass and distance from the spine of large-scale structure filaments, and samples are still relatively small and generally biased towards gas-rich systems. While there seems to be common agreement that gas richness may vary with distance from the filaments (Kleiner et al. 2017; Crone Odekon et al. 2018; Blue Bird et al. 2020), additional work is needed to properly quantify these differences and their dependence on galaxy properties. For example, while Crone Odekon et al. (2018) find an increase of HI content with increasing distance from the spine of the large-scale structure, Kleiner et al. (2017) report the opposite trend for galaxies with stellar masses greater than 10^{11} $\mathrm{M}_{\odot}$. Perhaps more importantly for the focus of this review, both theoretical and observational studies seem to imply that the overall effect of filaments on gas content and star formation (at fixed group environment) should be relatively small (< 0.3 dex) and well within the scatter in properties observed for the star-forming galaxy population (indeed, the large-scale environment could well be one of the contributing causes of this scatter).

However, much like in the case of pre-processing, understanding the role played by filaments is most likely critical in regulating the inflow rate of gas into star-forming discs. We still know very little about how cold gas gets into the disc and whether, for fixed satellite and group properties, large-scale structure plays an important role in regulating when and how accretion occurs and stops. Looking ahead, it will be first necessary to carefully control for the effect of the group environment, in order to isolate filament-driven effects.

7. A unified view on the role of cold gas stripping in satellite quenching

The observational evidence presented in this review suggests that stripping of the cold ISM is practically *always* associated with quenching. So far, we have never observed a clear example of quenching in a satellite galaxy where there was no removal of at least the very outer parts of the HI disc. Thus, we can at least exclude the 'stability' scenario described in Section 2 as a key pathway for satellite galaxies. At the same time, active stripping rarely appears sufficient to fully quench galaxies, unless *all* the cold gas is stripped during the first orbit through the centre of the parent halo. For a typical Milky Way-like galaxy, the inner parts of the cold disc remain bound to the galaxy and can continue to feed star formation for at least a few billion years longer.

Cold gas stripping: key parameters. The mass of the satellite and of the parent halo are most likely the two primary parameters determining whether or not full gas stripping is efficient, as testified by the fact that all Local Group dwarf satellites within the virial radius of the Milky Way are fully quenched, whereas massive discs (i.e., $M_* > 10^{10}$ $\mathrm{M}_{\odot}$) in Virgo are able to retain a significant amount of gas in their disc after the first pericentre passage. However, the value of the stellar mass threshold below which gas is fully stripped, and its dependence on halo mass, is still to be determined. In addition, it is natural to expect that the orbital properties of satellites as well as the accretion history of the groups may play a secondary, yet significant, role.

Outside-in gas removal. Stripping of cold gas is preferentially outside-in, with the outer parts of the star-forming disc quenched first. This does not necessarily imply that the inner parts of the disc are immune from environmental effects, as diffuse/extraplanar gas may still be affected within the truncation radius. But, more simply, it means that the overall stripping efficiency varies significantly with galactocentric distance. The details also depend on the physical mechanism(s) responsible for the stripping and, while hydrodynamical processes are clearly the dominant players when the ISM is affected within the optical disc, multiple physical processes (e.g., including gravitational interactions) are most likely at work when gas is removed only from the outer edges of the HI disc, and their relative role and efficiency still need to be quantified. This is something that may even be nearly impossible as they often occur simultaneously.

Starvation and stripping. One key implication of the widespread presence of cold ISM stripping is that the physical mechanism(s) responsible for removing the cold gas from the disc also prevent the accretion of new gas onto the disc. Thus, both quenching channels (i.e., active cold gas removal and cessation of gas infall) are happening at the same time and may even be driven by the same physical processes. What changes is primarily the importance of the two channels for full quenching, depending on how far inside the optical disc is stripping efficient.

In this regard it is clear that, at least for star-forming satellites with $M_* \sim 10^{10}$ $\mathrm{M}_{\odot}$ in a typical galaxy group (e.g., $M_h \sim 10^{13}$ $\mathrm{M}_{\odot}$), their cold gas content is almost never fully stripped after one pericentre passage. Thus, star formation will be fully quenched only gradually (i.e., over timescales of at least a few billion years after crossing the virial radius of their host halo), most likely due to the consumption of gas via star formation and lack of additional infall. Pre-processing in smaller groups might make stripping and quenching more efficient but, at least at $z \sim 0$, its role appears secondary.

It is important to stress that the fate of the inner parts of the star-forming disc (where stripping cannot be dominant) is probably one of the most important unknowns in the picture emerging from this work. While the general assumption in the literature is, indeed, that star formation will be quenched gradually and the galaxy will starve, this still needs to be proven as it is possible that other processes (e.g., outflows) may additionally contribute to regulating the last stages of the quenching phase.

In summary, as already hinted by several studies (e.g., Cortese & Hughes 2009; Fillingham et al. 2016; Roberts et al. 2019), satellite galaxies in groups at $z \sim 0$ seem to follow a well-defined path towards full quenching, where both direct stripping and halting of infall play a key and *simultaneous* role and might even be driven by the *same* physical process(es). The main variable is how deep into the star-forming disc does stripping affect the cold ISM, which determines its relative importance with respect to gas exhaustion via star formation in driving full quenching, and in the end sets the timescale needed for satellites to transition from the active to the passive population.

8. The theoretical perspective

Before concluding, it is natural to wonder if the observationally motivated scenario presented here is in line with the predictions from theoretical models of galaxy formation and evolution. While it is beyond the scope of this paper to review all the theoretical work on this topic carried out in the last decades, we believe that is important to provide the reader with an overview of how current simulations fit in the observational picture that we have put forward. Hence, we specifically focus only on three key points: (a) whether cold gas stripping is ubiquitous in satellites galaxies; (b) if theoretical models can help identify the driving physical mechanism stripping the gas, and (c) if satellites are fully stripped, and thus quenched, after the first pericentre passage.

8.1. Do we need cold gas stripping?

In the last two decades, one of the most popular tools for studying the gas content of galaxy populations in a cosmological context has been semi-analytical models (SAMs). Most modern SAMs take the merger trees of dark matter only cosmological N-body simulations *to follow the growth of structure through gravitational instability* and then include a semi-analytical treatment of the various physical processes affecting the evolution of baryons (e.g., gas cooling, star formation, feedback, etc) to derive the properties of galaxies hosted within their dark matter halos. Because of the limited computational cost, they are extremely efficient at exploring large parameter space and investigating wide simulated volumes (e.g., Baugh 2006; Somerville & Davé 2015).

The vast majority of early SAMs implemented gas loss in satellite galaxies by removing only the hot gas content of galaxies instantly after they become satellites (Baugh, Cole, & Frenk 1996; Springel et al. 2001; Lagos, Cora, & Padilla 2008). However, it soon became clear that the combination of instantaneous stripping with very efficient supernova feedback produced galaxies that tended to use up (or eject) their remaining cold disc gas too rapidly, resulting in fractions of red galaxies in groups and clusters that were too high compared to observations (Weinmann et al. 2006; Baldry et al. 2006; Kimm et al. 2009). This also explains why early efforts to include ram pressure stripping of the cold ISM in SAMs (e.g., Okamoto & Nagashima 2003; Lanzoni et al. 2005) reported no significant improvements in the ability of models to match the star formation properties of satellites (i.e., galaxies were quenched before ram pressure stripping of cold gas could play a role).

As a result, McCarthy et al. (2008) provided new recipes derived from hydrodynamical simulations describing gradual hot gas stripping that, combined with an improved treatment of how the gas is re-heated by feedback, improved the match with observations (e.g., Font et al. 2008; Lagos et al. 2014; De Lucia et al. 2019). However, these changes were still insufficient to match the observed passive fractions (e.g., see Guo et al. 2011; Hirschmann et al. 2014b; Henriques et al. 2015). Intriguingly, more recent work focused on the relative effect of hot gas stripping on the atomic-to-molecular hydrogen ratio has also highlighted that hot stripping alone would produce satellite galaxies with lower H_2-to-HI ratios than star-forming centrals of the same stellar mass (e.g., Xie et al. 2018, 2020), contrary to what is observed in clusters.

These issues, combined with the increasing number of observational constraints on HI and H_2 properties of satellite galaxies, have prompted several groups to include recipes for cold gas stripping in their SAMs (e.g., Tecce et al. 2010; Stevens & Brown 2017; Cora et al. 2018; Xie et al. 2020). To do so, the general approach is to calculate the cold gas stripping radius analytically by balancing the galaxy's restoring forces against the drag expected from ram pressure. Commonly, the hot halo gas shields the cold disc until it has been stripped, although the exact implementation varies somewhat between studies, as do the timescales for the gas to be removed, generally related to the time resolution of the simulation.

Although these studies concur that hot gas stripping is still the primary factor dictating the strength of quenching in most galaxies,[m] some works are starting to suggest that the inclusion of recipes for cold stripping is necessary for improving the match to observed quenching fractions (at least in clusters, e.g., Xie et al. 2020), supporting the idea that cold gas stripping is important for the evolution of satellite galaxies. More generally accepted is the fact that gas stripping appears indispensable to better reproduce the HI content of satellites, the variation of HI deficiency with cluster-centric distance, and the increase of H_2/HI fractions in clusters (e.g., Cora et al. 2018; Stevens et al. 2018; Xie et al. 2020). Nevertheless, the match between observations and SAMs when it comes to multi-phase gas properties of satellite galaxies is not yet perfect (e.g., it is still challenging to match the HI and H_2 content of satellites simultaneously, across all ranges of halo masses; Xie et al. 2020), implying that more work is needed to understand the interplay between stripping and quenching in these models.

In parallel to SAMs, in the last decade, large-scale hydrodynamical cosmological simulations have become a commonly used tool to study the evolving gas content of galaxy populations, with a clear explosion in the number of simulations readily available for a comparison with observations (e.g., EAGLE, Schaye et al. 2015; ILLUSTRIS, Vogelsberger et al. 2014; ILLUSTRIS-TNG, Pillepich et al. 2018; HORIZON-AGN, Dubois et al. 2014; MAGNETICUM, Hirschmann et al. 2014a). As opposed to SAMs, cosmological hydrodynamical simulations follow gravitational and hydrodynamical processes in a self-consistent manner, so that cold gas stripping is inherently built-in to these simulations. Nevertheless, their typical resolution is still insufficient to trace the formation of the cold gas phase of the ISM, hence they have to rely on subgrid prescriptions to separate the atomic and molecular cold gas phases.

Contrary to SAMs, in cosmological hydrodynamical simulations, we cannot simply switch on and off cold stripping in order to answer the question 'is cold stripping required to better match observations?' What we can determine is whether cold gas stripping commonly happens in the path of a satellite towards quenching. Not surprisingly, the answer to this question appears to be a resounding 'yes' for both cosmological (e.g., Bahé et al. 2013; Bahé & McCarthy 2015; Cen 2014; Marasco et al. 2016; Jung et al. 2018; Arthur et al. 2019; Stevens 2019a, 2020; Yun et al. 2019; Rafieferantsoa et al. 2019) and controlled hydrodynamical simulations (e.g., Quilis, Moore, & Bower 2000; Abadi, Moore, & Bower 1999, Roediger & Hensler 2005; Roediger & Brüggen 2007; Bekki 2009, 2014; Tonnesen & Bryan 2009). However, while hydrodynamical simulations include stripping by default, admittedly they have not always been able to fully reproduce the properties of satellites, yet.

Tremendous progress has been made in matching the global gas scaling relations of galaxies (i.e., the properties of centrals; e.g., see Davé et al. 2020), but in many instances satellite galaxies appear over-stripped and/or over-quenched (e.g., Brown et al. 2017; Davé, Rafieferantsoa, & Thompson 2017; Stevens 2019a; Xie et al. 2020; Donnari et al. 2020). The mismatch between simulations and observations varies as a function of both host and satellite mass, and the exact dependency changes if we consider quenching fractions instead of gas fractions, as well as varying from model to model. The reasons for such a mismatch are still unclear and can be multiple. Most certainly, too efficient feedback that would eject a large fraction of the ISM out of the disc (e.g., Stevens et al. 2019a) and/or insufficient resolution (i.e., 1 kpc or lower), which makes it impossible to conduct a proper partition between the different cold gas phases in order to trace the denser (and more difficult to strip) gas within the multi-phase ISM of their discs (e.g., Hu et al. 2016), are among some of the most likely issues.

Thus, as in the case of SAMs, we are finding general support for the idea that cold gas stripping is part of a satellite's pathway towards quenching, though more work is clearly needed to improve the ability of cosmological hydrodynamical simulations to match the observed properties of satellites.

---

[m] However, we note the caveat that, due to hot halo shielding of the cold gas, it is difficult to directly see the effect of each mechanism independently. For instance, if hot halo stripping is switched off, it will disable cold stripping as well.

8.2. Do simulations provide insight on mechanisms behind cold gas stripping?

Keeping in mind the limitations described above, it is nevertheless tempting to see if current simulations can provide insights on the nature of the mechanism(s) responsible for cold gas stripping.

In the case of SAMs, even if hydrodynamical mechanisms cannot be directly implemented, processes like stripping due to ram pressure appear to be preferred to tidal stripping by a host's potential well. Indeed, SAMs typically calculate a tidal stripping radius and a ram pressure stripping radius for their satellite halos as they orbit through their hosts. These radii mark the boundary beyond which each stripping mechanism is effective, and most works (including those based on hydrodynamical simulations) agree that the ram pressure radius is typically smaller than the tidal stripping radius (McCarthy et al. 2008; Font et al. 2008; Bahé & McCarthy 2015; Cora et al. 2018). This implies that, by the time a galaxy reaches the region within its host halo at which tidal stripping becomes efficient, ram pressure has typically already removed most of the gas.

Naively, we might expect that hydrodynamical cosmological simulations should provide the best opportunity to clearly isolate the physical processes responsible for cold gas stripping, given that detailed information about all of a galaxy's mass components, and their time evolution is, in principle, available. However, the ability to self-consistently trace multiple and interconnected physical processes makes it even more challenging to pin-point what observers would call the 'dominant mechanism' at play. For example, the implementation of internal mechanisms such as star formation consumption and various forms of feedback may contribute to the stripping efficiency of different environmental mechanisms, meanwhile external factors such as the background UV field, tidal interactions, or hydrodynamical processes may all influence each other's abilities to remove cold gas in complex and non-linear ways.

The complexity of this problem was clearly showcased by Marasco et al. (2016), who tried to identify the responsible for cold gas stripping in groups and cluster galaxies (see also Xie et al. 2020 for a similar approach from the SAMs point of view). While they emphasise that, at $z \sim 0$, ram pressure is the most common physical process stripping H I from satellites, they also highlighted the importance of satellite–satellite encounters in stripping H I from the disc (especially at large cluster-centric distances and higher redshift) and showed that there is rarely a single cold gas stripping mechanism acting individually in a cosmological context. Instead, the most frequent source of H I gas mass loss is a combination of simultaneous ram pressure and satellite–satellite encounters (see Figure 19), with the balance between the two processes changing as a function of redshift (i.e., satellite–satellite interactions more important at earlier epochs; see also Hwang et al. 2018). Interestingly, this suggests that ram pressure is efficient also in groups of halo masses of $\sim 10^{13}$ M$_\odot$, consistently with what found in other cosmological (e.g., Bahé et al. 2013; Bahé & McCarthy 2015) and non-cosmological simulations (e.g., Bekki 2009, 2014). Overall, this is in line with the key message of this review: that is, environmental mechanisms that influence cold gas content are typically most efficient at the highest densities, for example, near the pericentre passage. Therefore, they tend to peak in strength at the same time and rarely occur in isolation.

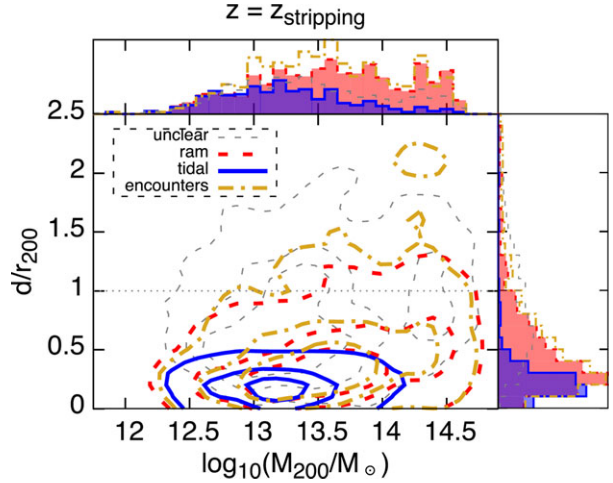

Figure 19. The halo mass (M_{200}) versus group-centric distance (d/r_{200}) distribution of H I-poor satellites in the EAGLE simulation, evaluated at the time of H I loss (i.e., $z = z_{\rm stripping}$). Lines show the parameter space occupied by satellites affected by different environmental processes: that is, tidal stripping by the host halo (blue solid), ram pressure stripping by the IGM (red thick dashed), satellite–satellite interactions (yellow dot-dashed), or none of the above (thin dashed), with contours enclosing 30%, 60%, and 90% of the satellites. Only systems with stellar mass (at $z = 0$) larger than 10^9 M$_\odot$ are considered. Image reproduced with permission from Figure 13 in Marasco et al. (2016). Copyright by the authors.

A potential (and complementary) way forward to break this complexity is provided by controlled hydrodynamical simulations. Their controlled nature means that the effect of just one individual mechanism can be isolated. For example, in ram pressure stripping-only simulations (e.g., Roediger & Hensler 2005; Roediger & Brüggen 2007; Tonnesen & Bryan 2009; Steinhauser, Schindler, & Springel 2016), it has been possible to clearly identify long, one-sided gas tails as observed in cluster satellites, providing some of the strongest theoretical support for the key role played by ram pressure in removing cold gas from star-forming satellite galaxies. By systematically adjusting input parameters, it has also been possible to quantify how the effects of ram pressure depend on disc inclination and orbits (Vollmer et al. 2001; Roediger & Brüggen 2007), presence of a bulge (Steinhauser et al. 2012), or cluster dynamical state (Vijayaraghavan & Ricker 2013; Roediger et al. 2012). This approach has been crucial for the development of accurate analytical recipes of gas stripping mechanisms, which can then be implemented in SAMs (Font et al. 2008), or used to identify when a mechanism plays a dominant role in hydrodynamical cosmological simulations (Marasco et al. 2016).

By limiting the simulation volume and duration, controlled simulations can also reach higher resolution or consider complex physics that would be otherwise computationally prohibitive. As such, they have been able to model and highlight the potential importance of viscous, turbulent stripping (Roediger & Hensler 2005; Roediger & Brüggen 2007), a multiphase treatment of the ISM (Tonnesen et al. 2011), the interplay between thermal evaporation and magnetic fields (Tonnesen & Stone 2014; Vijayaraghavan & Sarazin 2017), and the importance of mixing (Tonnesen & Bryan 2021) for the overall cold gas stripping process. This clearly confirms that, even when only stripping by hydrodynamical processes is considered, a complex set of poorly understood processes interact, including turbulence and magnetic fields, meaning that such modelling is highly challenging. Of course, as with every approach, even controlled simulations are limited by how well they are able to properly include and interconnect all the key physical processes at play.

In summary, theoretical models are overall providing a view consistent with that emerging from observations, where multiple physical processes generally act simultaneously on the cold gas reservoir in the ISM. While hydrodynamical stripping mechanisms appear to be the most efficient in Virgo-like and more massive clusters (at least at $z \sim 0$), in smaller structures the picture is much more complex and additional work is required to characterise the net effect of the various physical processes affecting the ISM in satellite galaxies.

8.3. Are satellites fully stripped after first pericentre passage?

While the general scenario emerging from both SAMs and hydrodynamical simulations is that cold gas stripping is widespread in satellites and is needed to reproduce the observed properties of group and cluster galaxies, this does not necessarily imply that satellites are fully stripped (and then quenched) after first pericentre passage. Indeed, as for observations, models cast doubts that stripping completely halts star formation after one pericentre passage, even in Virgo-like clusters.

High-resolution controlled simulations suggest that ∼Milky Way mass spirals would typically lose a substantial amount of their cold gas in a cluster but would become completely stripped only in extreme cases, with the amount of stripping being a sensitive function of galaxy orbit (e.g., Roediger & Hensler 2005; Roediger & Brüggen 2007). Similarly, Steinhauser et al. (2016) find that discs galaxies with $V_{\rm circ} \sim 110$–170 km s^{-1} are only fully stripped for very plunging orbits ($R_{\rm peri} \sim 100$ kpc), while star formation is only weakly affected for the rest of the orbits. Moving to cosmological simulations, Brüggen & De Lucia (2008) applied the results found by Roediger & Brüggen (2007) to the Millenium simulation and showed that only a minority of disc galaxies with $V_{\rm circ}$>200 km s^{-1} are expected to be fully stripped in clusters (∼11–32% dependent on cluster mass), but that more than half (∼54–64%) would be heavily stripped. This is also consistent with the results by Cen (2014), who finds that in hydrodynamical simulations most of the cold gas within the inner parts of satellite galaxies (at least above $M_* \sim 3 \times 10^9$ M$_\odot$) is unaffected by environmental effects.

Nevertheless, some cosmological simulations do seem to provide a different picture. For example, Jung et al. (2018) find that almost half of their galaxies lose their cold gas before reaching the cluster pericentre, although many are already gas poor prior to cluster infall due to pre-processing. Using the MAGNETICUM simulation, Lotz et al. (2019) report the removal of all the gas in more than 90% of cluster satellites after a single pericentre passage, with only some of their most massive galaxies (i.e., stellar masses a few times 10^{11} M$_\odot$) able to remain star forming for more than 1 Gyr after infall. It is not yet clear what is the origin of these differences in cold gas stripping efficiency. Simulation resolution may play a role, limiting the ability to resolve both the denser phases of the ISM and the hydrodynamical stripping processes themselves. Moreover, differences in the treatment of subgrid physics such as feedback are also likely important, affecting both the density of ICM that galaxies pass through and the ease with which the cold disc gas can be removed.

Thus, while there is not a complete agreement between different theoretical models, we can conclude that the fact that full stripping is not widespread even in clusters does appear as a possible (if not likely) scenario. Thus, it is natural to ask how—in models—the remaining cold gas stops feeding star formation. Curiously, to our knowledge, there are few simulation papers specifically focused on this issue in the context of satellite galaxies in clusters, but we can use results obtained on quenching in a broader context to provide some insights on this issue.

It has been shown that enhanced star formation, either as a result of tidal shocking near pericentre or due to compression of one side of the gas disc by ram pressure (Bekki 2014; Steinhauser et al. 2016; Lotz et al. 2019; Troncoso-Iribarren et al. 2020; Lee et al. 2020), can potentially aid cold gas consumption. However, as discussed in Section 4.3.2, observationally such bursts appear to be relatively minor and thus unlikely to consume a significant fraction of the gas reservoir left in the disc. Feedback could also play a key role. SAMs already crucially rely on reheating and ejection of gas via supernova feedback with an efficiency that depends on redshift in order to reproduce stellar mass functions at high redshift (Hirschmann et al. 2014b; Cora et al. 2018). Stellar feedback may also heat cold disc gas into more easily stripped and/or less star-forming phases or push the gas from inside the truncation radius to radii where it can be stripped, although so far this has only been modelled in the context of Local Group dwarf galaxies (Kazantzidis et al. 2017, but also see Emerick et al. 2016), whose shallow potential wells may enhance the amount of material lost in this manner. In more massive galaxies, AGNs triggered in ram pressure stripped galaxies may also provide a source of feedback to the remaining cold disc gas (Ricarte et al. 2020). Finally, it should not be excluded that a more continuous loss of cold gas from the disc may also occur after pericentre passage via viscous and turbulent stripping at the ICM/disc boundary, as modelled for cluster satellites (Roediger & Brüggen 2007).

In conclusion, while numerical simulations generally agree that cold gas stripping is a normal path for satellite galaxies towards quenching, there are still many open questions also from the theory side. Specifically, the relative importance of various physical processes in driving gas stripping, as well as when and how the cold gas reservoirs of satellites stop forming stars are still highly debated questions, which are also model-dependent. In the case of hydrodynamical simulations, significant improvement will hopefully come from a more realistic multi-phase treatment of the ISM, including the role of magnetic fields, which should provide interesting clues on these open questions. At the same time, in the case of SAMs, the development of new analytical prescriptions, such as a more multi-phase treatment of the ISM (Tonnesen & Bryan 2009), differing treatment of sub- and super-sonic discs (Roediger & Hensler 2005), and inclusion of continuous gas mass loss mechanisms (Roediger & Brüggen 2007) could potentially reduce some of the tensions currently present between observations and simulations.

What is definitely already clear is that understanding the individual significance of the physical processes driving stripping in simulations remains at least as challenging as it is for observations. This is an area in which controlled simulations may yet provide the missing key for improving cosmological runs and our understanding of what can be learnt from them. On one side, they can help developing better prescriptions for SAMs and investigate issues of numerical convergence. On the other side, their higher spatial and mass resolutions, combined with their versatility, make controlled simulations able to include (and switch between) various complex baryonic physics that might be numerically unfeasible (or have unexpected consequences) in cosmological simulations, but could be critical for understanding environmental effects.

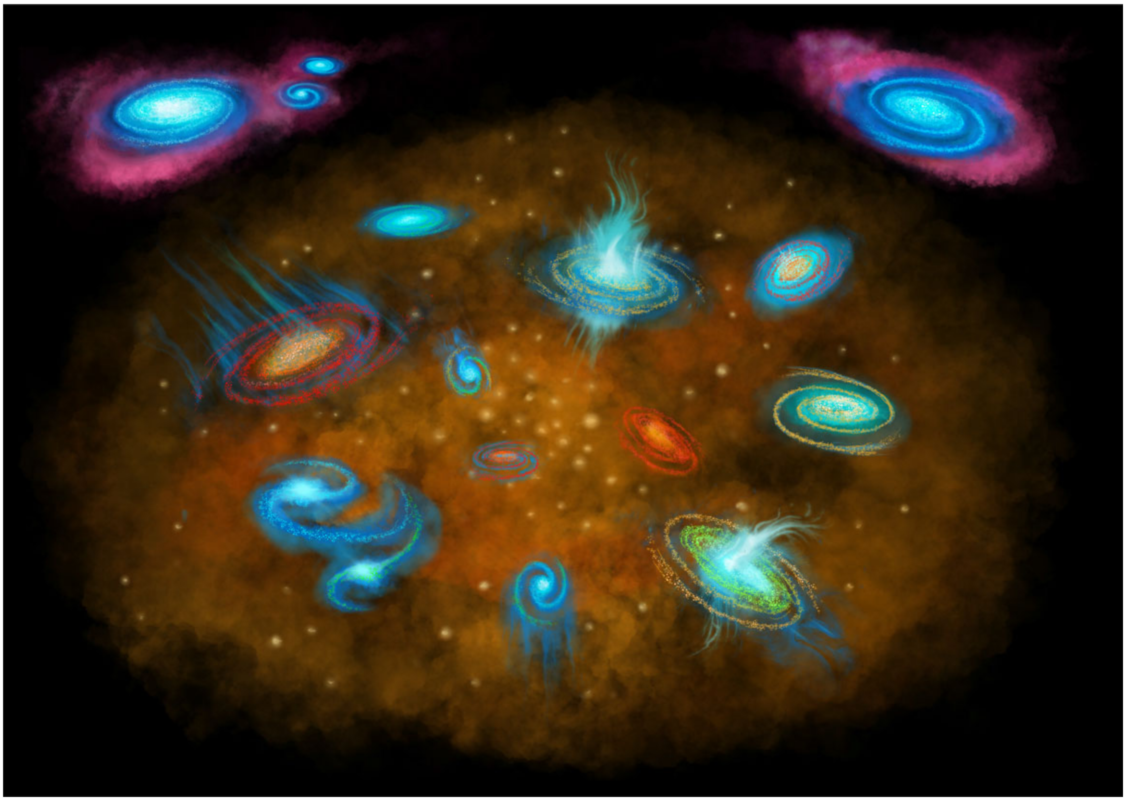

Figure 20. Illustration summarising the picture emerging from this review. When galaxies become satellites, their access to CGM gas (pink) is removed, and cold gas stripping appears widespread. However, there is no single physical mechanism driving the loss of gas and, consequently, quenching. Instead, multiple mechanisms can be at play, sometimes even simultaneously.

9. Closing thoughts and outlook

In this work, we have discussed *how*, *when*, and *for how long* the gas star formation cycle in satellite galaxies at $z\sim0$ is affected by the environment. Specifically, we have reviewed the observational evidence for the stripping of cold gas from the disc of star-forming satellite galaxies and argued that this is a necessary step towards quenching their star formation activity. However, both observations (e.g., Sections 4 and 5) and numerical simulations (Section 8) suggest a complex picture, where different physical processes may act simultaneously and identifying a single culprit is neither feasible nor correct (see Figure 20). While hydrodynamical mechanisms—such as ram pressure stripping—are likely dominant in the central regions of galaxy clusters, gravitational interactions (i.e., the interaction with the central host and/or satellite–satellite encounters) must play an important role in the lower-density environments of groups, and what regulates the balance between various stripping mechanisms remains unclear. While, locally, quenching is fast (hundreds of Myr or less) *after* the cold gas has been stripped, it is clear that stripping alone does not always lead to full quenching, as not all the gas is stripped in one orbit. This means that: (a) timescales for full quenching can be long (e.g., a few Gyrs, in particular if the clock starts at time of infall) and (b) other physical processes such as gas consumption by star formation or feedback can play an important role in fully quenching satellites after the first pericenter passage.

Despite substantial progress having taken place in the past decades on this topic, much remains to be explored before we can obtain a complete picture of the effects of nurture on satellite galaxies. This is in large part due to the difficulty in mapping such an extended and complex parameter space, which requires a detailed knowledge of the various components of the ISM and star formation properties for large, representative samples of galaxies spanning all the different environments. As discussed in several points throughout this review, differences in sample selections, quantification of cold gas normalcy/poorness, and definitions of quenching (and related timescales) have led to apparently conflicting results and misconceptions. But even taking all this into account, existing samples lack the *statistics, spatial resolution, and sensitivity* required to quantify the impact of environmental processes on galaxies, critically on their cold gas component, and to link this to quenching of their star formation.

The need for statistical samples stems from the fact that environment not only spans orders of magnitude of density, but is also a second-order effect, thus it is necessary to control for stellar mass or another property scaling with galaxy size. Spatial resolution is key to understand the physics on a local basis, allowing for instance to investigate in detail what happens to the metallicity and star formation activity in a region where the gas has just been stripped, and whether an adjacent region has been affected at all. Sensitivity is critical to detect small amounts of cold gas in galaxies below the star-forming sequence, on their way to becoming passive. State-of-the-art, representative cold gas samples not only are still limited to global measurements, but are not sensitive enough to probe the gas-poor regime across all stellar masses and environmental densities, simultaneously.

Fortunately, the facilities on the horizon in the next decade will allow giant leaps forward by addressing at least some of the above limitations. This was indeed the main motivation behind this work, as it seemed timely to review the current state of the field and highlight future challenges before the next-generation radio and optical facilities begin accumulating new data. Below, we briefly focus on a few areas where progress seems particularly promising.

The fate of the inner parts of star-forming discs. Perhaps the most important unknown in the picture emerging from this work is what happens to the cold gas residing in the inner parts of galaxies (within the truncation radius), where the effects of stripping might be negligible. As previously discussed (see Section 5.4), stripping (regardless of the exact physical process responsible for it) appears not efficient enough to completely remove the cold gas disc in galaxies with $M_* > 10^8$ $M_\odot$ in groups like our Local Group, and $M_* > 10^{10}$ $M_\odot$ in clusters such as Virgo, at first pericentre passage (see Sections 4, 5 and 7). As a result, part of the cold gas remains available after the first passage through the group/cluster, where it can sustain residual star formation for at least a few billion years. It is generally assumed that star formation will gradually cease and the galaxy will starve, as its ability to acquire new gas from the surrounding CGM and IGM has been negated by the environmental process that stripped the gas.

However, given the length of the timescales involved and the fact that most satellites remain embedded in their group/cluster after the first pericentre passage, it seems unlikely that their inner parts will remain completely shielded from any environmental effects. In this scenario, it becomes particularly important to understand what is the interplay between atomic and molecular hydrogen, whether H_2 is directly stripped, or the formation of H_2 is simply inhibited by the partial removal of atomic hydrogen from the outer parts of the disc. Unfortunately, a *simultaneous* characterisation of both H_2 and SFR surface density distributions (e.g., radial profiles) for large statistical samples of satellites across environments is still missing. As highlighted in this review, large IFS surveys like MaNGA and SAMI are arguably advancing this field, but they have not been able to properly investigate the outer parts of the star-forming discs, where most of the observational signatures of environmental effects (particularly in groups) may be found. This is an area where wide-field IFS, such as MUSE (Bacon et al. 2014), have helped and will likely continue to do so. Moreover, next-generation large statistical IFS surveys such as HECTOR (Bryant et al. 2018) may be key in pushing to the outer parts of discs and to start investigating the second-order effects, as satellites remain a small fraction of the population targeted by any of these surveys.

Nevertheless, there is still a crucial lack of any resolved surveys of H_2 content in satellites, even in clusters. While the situation is slowly improving for clusters like Fornax and Virgo, where ALMA programmes such as the ALMA Fornax Cluster Survey (AlFoCS, Zabel et al. 2019) and the Virgo Environment Traced in CO (VERTICO[n]) survey should provide important insights into the interplay between cluster environment and H_2, nothing is on the horizon when it comes to molecular hydrogen properties of satellite galaxies outside clusters. This is a major issue that will most likely hamper our ability to make progress in this field. Our hope is that state-of-the-art millimetre facilities will be able to provide us with surveys of satellite galaxies with a number statistics and spatial resolution on a par with what IFS optical surveys have produced in the last decade.

A more physically-motivated characterisation of environment for cold gas studies. When it comes to the cold gas properties of satellites, much of the observational work so far, and hence this review, has focused on the distinction between groups and clusters of galaxies. Indeed, contrary to optical surveys that have provided stellar masses, sizes and SFR estimates for millions of galaxies across a wide redshift range, atomic and molecular gas studies of satellites are still limited to the very local Universe and have imaged galaxies only in well-known nearby groups or a handful of clusters.

However, this is clearly an oversimplification. There is no obvious threshold between large groups and clusters, clusters often contain substructures with densities that are typical of groups, and most importantly environment is more complex than what a simple dichotomy might suggest: groups and clusters are embedded in a cosmic web of large-scale filaments and structures where dark and baryonic matter flow, bringing along energy and angular momentum. This requires the adoption of environmental descriptors that are continuous and more physically motivated (such as halo mass, local density, distance from the spine of a filament, and so on), thus are more suitable to capture the complexity of the real Universe. Such indicators are also more directly comparable to numerical simulations and studies at other wavelengths which, thanks to the sheer amount of available data, are typically concerned with statistical studies of environmental effects. At the same time, as discussed at the beginning of this review, we need to move beyond the HI-normal versus HI-deficient dichotomy and treat the HI (and H_2) content of satellites as a continuum.

While the observational optical community has made these transitions nearly two decades ago thanks to the advent of large-area surveys such as the SDSS, this *paradigm shift* has yet to happen for HI and H_2 studies of satellite galaxies in the local Universe. Undoubtedly, surveys such as ALFALFA and xGASS have already started such a change, but we will most likely have to wait for the completion of large-area surveys with the SKA precursor facilities (e.g., the Australian SKA Pathfinder, ASKAP, Johnston et al. 2008; MeerKAT in South Africa, Jonas & MeerKAT Team 2016) to see HI studies routinely taking advantage of the number statistics and quality of ancillary data that has become so normal for optical and near-infrared investigations. Notably for local Universe studies, the WALLABY survey alone is expected to image HI emission from ~5 000 galaxies and detect ~600 000 systems with z <0.26 (Koribalski et al. 2020). This will be particularly critical to investigate the 10^{13}–10^{14} $M_\odot$ halo mass regime and more accurately quantify how much (and under which conditions) HI is stripped from the star-forming disc of satellite galaxies.

Connecting the ISM and CGM. Somewhat related to the large-structure environment, it is generally accepted that star formation in galaxies is fed by inflowing gas from the surrounding CGM (Tumlinson, Peeples, & Werk 2017). However, how gas is accreted onto the galaxies and reaches their ISM is still an open question. We argued that, if gas accretion is indeed widespread in star-forming galaxies, it must be stopped in order for satellite galaxies to become passive. While this argument sounds plausible, it is worth clarifying that this is just an assumption, as there is no direct observational evidence showing what physical process is responsible for halting gas accretion, how and when it operates, how long does it take, what regulates the rate of inflowing gas, and so on. As discussed in the Introduction to this review, this is a crucial issue because the exchange of gas between ISM and CGM via inflows, outflows, and recycling is what regulates how galaxies form and evolve.

---

[n] https://sites.google.com/view/verticosurvey/home.

The SKA pathfinders will potentially provide the means to trace the flow of baryons into galaxies, by combining exquisite sensitivity with wide-field capability to image atomic hydrogen down to the low-column densities (e.g., 10^{17} cm^{-2}), supposedly needed to trace cold gas flows in and out of star-forming discs. However, while with ASKAP and MeerKAT this will be possible already for the Milky Way (e.g. with the Galactic ASKAP—GASKAP—survey, Dickey et al. 2013) and nearby galaxies (e.g., with the MeerKAT HI Observations of Nearby Galactic Objects; Observing Southern Emitters—MHONGOOSE—survey, de Blok et al. 2016), only the first phase of the SKA may eventually allow us to target large samples of satellite galaxies at a similar depth.

In the meantime, we believe that significant progress in understanding the interplay between accretion, CGM, and ISM in satellite galaxies could come in the next 5 to 10 years from the combination of absorption- and emission-line studies across the ultraviolet, optical, and radio regimes. This is a rapidly growing field and, despite the limited amount of data currently available, it is already clear that the combination of wide-area integral-field spectrographs such as MUSE and KCWI (Morrissey et al. 2018) with facilities such as ALMA and ASKAP will provide us with important insights on the interplay between different gas phases flowing in and out of galaxies (e.g., Borthakur et al. 2019; Frye et al. 2019; Péroux et al. 2019). Indeed, not surprisingly the picture emerging is already a complex one where, for example, accretion may not always be halted immediately after infall but may depend on the detailed properties of the group and infalling orbit.

In conclusion, the topic of this review is a piece of a larger puzzle to understand how gas flows in and out of galaxies, regulates their evolution, and what are the physical processes that affect this balance and transform them into passive systems. Probably, the most important limitation that hampers our attempts to obtain a complete picture of galaxy evolution is our inability to trace multiple gas phases at the required depth and resolution, for the same samples of galaxies and across the whole parameter space, even in the local Universe. Another important challenge for the future will be to connect detailed studies of gas and star formation that are currently possible only in nearby systems, to kpc-scale and global studies, linking galaxies to their surroundings and tracing all this back to their progenitors at higher redshift. At the same time, making sense of the avalanche of data expected from the next-generation surveys with SKA, 30-m class telescopes, and space telescopes will be extremely challenging if not daunting, but undoubtedly this is a stimulating challenge for the future, with lots of exciting, and potentially unexpected, discoveries on the horizon.

Acknowledgements. We thank the Editorial Board of PASA, and in particular Stas Shabala, for inviting us to contribute this work to the Dawes Review series. We thank two anonymous referees for useful comments that helped improve the clarity of this review. We thank Peter Ryan for designing the two illustrations presented in Figures 1 and 20 of this review. We thank Claudia Lagos for providing the data from the SHARK model used to create Figure 2; Aeree Chung for help with the VIVA data used for Figure 5; Matteo Fossati and Rose Finn for providing the data used in Figure 8, Alessandro Boselli for providing part of the data used in Figure 9 and an updated image of NGC 4569 used in Figure 10; Jinsu Rhee for help with Figure 13; Toby Brown and David Stark for sharing the ALFALFA and RESOLVE data used for Figure 15; and Asa Bluck for providing Figure 16. We thank Alessandro Boselli, Benedetta Vulcani, Gabriella de Lucia, and Stephanie Tonnesen for providing comments on a draft of this review, Paula Calderón Castillo for a careful proofreading, and Claudia Lagos for useful discussions.

Parts of this research were conducted by the Australian Research Council Centre of Excellence for All Sky Astrophysics in 3 Dimensions (ASTRO 3D), through project number CE170100013. LC is the recipient of an Australian Research Council Future Fellowship (FT180100066) funded by the Australian Government. We also acknowledge support by the Australian Government through the Australia-Korea Foundation of the Department of Foreign Affairs and Trade (‘Galaxy evolution across environments: linking Australian observatories and Korean simulations’ -AKF00601).

This research made use of Astropy,[o] a community-developed core Python package for Astronomy (Astropy Collaboration et al. 2013, 2018); and of NASA’s Astrophysics Data System Bibliographic Services.

References

Abadi, M. G., Moore, B., & Bower, R. G. 1999, MNRAS, 308, 947
Alatalo, K., et al. 2015, ApJ, 812, 117
Anderson, M. E., Bregman, J. N., & Dai, X. 2013, ApJ, 762, 106
Anderson, M. E., Gaspari, M., White, S. D. M., Wang, W., & Dai, X. 2015, MNRAS, 449, 3806
Anglés-Alcázar, D., Faucher-Giguère, C.-A., Kereš, D., Hopkins, P. F., Quataert, E., & Murray, N. 2017, MNRAS, 470, 4698
Arthur, J., et al. 2019, MNRAS, 484, 3968
Astropy Collaboration, et al. 2013, A&A, 558, A33
Astropy Collaboration, et al. 2018, AJ, 156, 123
Bacon, R., et al. 2014, Msngr, 157, 13
Bahé, Y. M., McCarthy, I. G., Balogh, M. L., & Font, A. S. 2013, MNRAS, 430, 3017
Bahé, Y. M., & McCarthy, I. G. 2015, MNRAS, 447, 969
Bahé, Y. M., Schaye, J., Crain, R. A., McCarthy, I. G., Bower, R. G., Theuns, T., McGee, S. L., & Trayford, J. W. 2017, MNRAS, 464, 508
Baldry, I. K., Balogh, M. L., Bower, R. G., Glazebrook, K., Nichol, R. C., Bamford, S. P., & Budavari, T. 2006, MNRAS, 373, 469
Balogh, M. L., & Morris, S. L. 2000, MNRAS, 318, 703
Balogh, M. L., Navarro, J. F., & Morris, S. L. 2000, ApJ, 540, 113
Barnes, D. G., et al. 2001, MNRAS, 322, 486
Baugh, C. M. 2006, RPP, 69, 3101
Baugh, C. M., Cole, S., & Frenk, C. S. 1996, MNRAS, 283, 1361
Bekki, K. 2009, MNRAS, 399, 2221
Bekki, K. 2013, MNRAS, 432, 2298
Bekki, K. 2014, MNRAS, 438, 444
Bekki, K., & Couch, W. J. 2003, ApJ, 596, L13
Belfiore, F., et al. 2017, MNRAS, 466, 2570
Bellhouse, C., et al. 2019, MNRAS, 485, 1157
Bernard, J.-P., et al. 2010, A&A, 518, L88
Bianconi, M., Smith, G. P., Haines, C. P., McGee, S. L., Finoguenov, A., & Egami, E. 2020, MNRAS, 492, 4599
Bigiel, F., & Blitz, L. 2012, ApJ, 756, 183
Bigiel, F., Leroy, A., Seibert, M., Walter, F., Blitz, L., Thilker, D., & Madore, B. 2010b, ApJ, 720, L31
Bigiel, F., Leroy, A., Walter, F., Blitz, L., Brinks, E., de Blok, W. J. G., & Madore, B. 2010a, AJ, 140, 1194
Bigiel, F., Leroy, A., Walter, F., Brinks, E., de Blok, W. J. G., Madore, B., & Thornley, M. D. 2008, AJ, 136, 2846
Binney, J., & Tremaine, S. 1987, Galactic dynamics

---

[o] http://www.astropy.org.

Birnboim, Y., Dekel, A., & Neistein, E. 2007, MNRAS, 380, 339
Blitz, L., & Rosolowsky, E. 2006, ApJ, 650, 933
Bluck, A. F. L., et al. 2020, MNRAS, 499, 230
Blue Bird, J., et al. 2020, MNRAS, 492, 153
Boissier, S., & Prantzos, N. 2000, MNRAS, 312, 398
Bolatto, A. D., Wolfire, M., & Leroy, A. K. 2013, ARA&A, 51, 207
Borthakur, S., Momjian, E., Heckman, T. M., Catinella, B., Vogt, F. P. A., & Tumlinson, J. 2019, ApJ, 871, 239
Boselli, A., Boissier, S., Cortese, L., & Gavazzi, G. 2008, ApJ, 674, 742
Boselli, A., Boissier, S., Cortese, L., Gil de Paz, A., Seibert, M., Madore, B. F., Buat, V., & Martin, D. C. 2006, ApJ, 651, 811
Boselli, A., et al. 2010, PASP, 122, 261
Boselli, A., Cortese, L., & Boquien, M. 2014a, A&A, 564, A65
Boselli, A., Cortese, L., Boquien, M., Boissier, S., Catinella, B., Gavazzi, G., Lagos, C., & Saintonge, A. 2014c, A&A, 564, A67
Boselli, A., Cortese, L., Boquien, M., Boissier, S., Catinella, B., Lagos, C., & Saintonge, A. 2014b, A&A, 564, A66
Boselli, A., et al. 2014d, A&A, 570, A69
Boselli, A., Fossati, M., Gavazzi, G., Ciesla, L., Buat, V., Boissier, S., & Hughes, T. M. 2015, A&A, 579, A102
Boselli, A., et al. 2016, A&A, 596, A11
Boselli, A., et al. 2018, A&A, 620, A164
Boselli, A., & Gavazzi, G. 2006, PASP, 118, 517
Boselli, A., & Gavazzi, G. 2009, A&A, 508, 201
Boselli, A., Gavazzi, G., Donas, J., & Scodeggio, M. 2001, AJ, 121, 753
Boselli, A., Gavazzi, G., Lequeux, J., Buat, V., Casoli, F., Dickey, J., & Donas, J. 1997, A&A, 327, 522
Boselli, A., Lequeux, J., & Gavazzi, G. 2002, A&A, 384, 33
Bothwell, M. S., et al. 2014, MNRAS, 445, 2599
Bottinelli, L., & Gouguenheim, L. 1974, A&A, 36, 461
Bouché, N., et al. 2010, ApJ, 718, 1001
Bravo-Alfaro, H., Cayatte, V., van Gorkom, J. H., & Balkowski, C. 2000, AJ, 119, 580
Bravo-Alfaro, H., Cayatte, V., van Gorkom, J. H., & Balkowski, C. 2001, A&A, 379, 347
Brinchmann, J., Charlot, S., White, S. D. M., Tremonti, C., Kauffmann, G., Heckman, T., & Brinkmann, J. 2004, MNRAS, 351, 1151
Brown, T., Catinella, B., Cortese, L., Kilborn, V., Haynes, M. P., & Giovanelli, R. 2015, MNRAS, 452, 2479
Brown, T., et al. 2017, MNRAS, 466, 1275
Brüggen, M., & De Lucia, G. 2008, MNRAS, 383, 1336
Bryant, J. J., et al. 2015, MNRAS, 447, 2857
Bryant, J. J., et al. 2018, in Society of Photo-Optical Instrumentation Engineers (SPIE) Conference Series, Vol. 10702, Ground-based and Airborne Instrumentation for Astronomy VII, ed. C. J. Evans, L. Simard, & H. Takami, p. 107021H, 10.1117/12.2309893
Bundy, K., et al. 2015, ApJ, 798, 7
Bureau, M., & Carignan, C. 2002, AJ, 123, 1316
Byrd, G., & Valtonen, M. 1990, ApJ, 350, 89
Caldú-Primo, A., Schruba, A., Walter, F., Leroy, A., Sandstrom, K., de Blok, W. J. G., Ianjamasimanana, R., & Mogotsi, K. M. 2013, AJ, 146, 150
Caldú-Primo, A., Schruba, A., Walter, F., Leroy, A., Bolatto, A. D., & Vogel, S. 2015, AJ, 149, 76
Caproni, A., Amaral Lanfranchi, G., Campos Baio, G. H., Kowal, G., & Falceta-Gonçalves, D. 2017, ApJ, 838, 99
Casoli, F., Boisse, P., Combes, F., & Dupraz, C. 1991, A&A, 249, 359
Casoli, F., et al. 1998, A&A, 331, 451
Catinella, B., et al. 2010, MNRAS, 403, 683
Catinella, B., et al. 2013, MNRAS, 436, 34
Catinella, B., et al. 2018, MNRAS, 476, 875
Cayatte, V., van Gorkom, J. H., Balkowski, C., & Kotanyi, C. 1990, AJ, 100, 604
Cen, R. 2014, ApJ, 781, 38
Chamaraux, P., Balkowski, C., & Gerard, E. 1980, A&A, 83, 38
Chanamé, J., Infante, L., & Reisenegger, A. 2000, ApJ, 530, 96
Chung, A., van Gorkom, J. H., Kenney, J. D. P., Crowl, H., & Vollmer, B. 2009, AJ, 138, 1741
Chung, A., van Gorkom, J. H., Kenney, J. D. P., & Vollmer, B. 2007, ApJ, 659, L115
Chung, E. J., Yun, M. S., Verheijen, M. A. W., & Chung, A. 2017, ApJ, 843, 50
Cicone, C., et al. 2017, A&A, 604, A53
Ciesla, L., et al. 2016, A&A, 585, A43
Codis, S., Pichon, C., Devriendt, J., Slyz, A., Pogosyan, D., Dubois, Y., & Sousbie, T. 2012, MNRAS, 427, 3320
Coenda, V., Mast, D., Martínez, H. J., Muriel, H., & Merchán, M. E. 2019, A&A, 621, A98
Cole, S., Lacey, C. G., Baugh, C. M., & Frenk, C. S. 2000, MNRAS, 319, 168
Cora, S. A., et al. 2018, MNRAS, 479, 2
Corbelli, E., et al. 2012, A&A, 542, A32
Cortese, L. 2012, A&A, 543, A132
Cortese, L., & Hughes, T. M. 2009, MNRAS, 400, 1225
Cortese, L., et al. 2006, ApJ, 637, 242
Cortese, L., et al. 2007, MNRAS, 376, 157
Cortese, L., et al. 2010a, A&A, 518, L49+
Cortese, L., et al. 2010b, A&A, 518, L63+
Cortese, L., Catinella, B., Boissier, S., Boselli, A., & Heinis, S. 2011, MNRAS, 415, 1797
Cortese, L., et al. 2012a, A&A, 540, A52
Cortese, L., et al. 2012b, A&A, 544, A101
Cortese, L., et al. 2016, MNRAS, 459, 3574
Cowie, L. L., & Songaila, A. 1977, Nature, 266, 501
Cramer, W. J., Kenney, J. D. P., Cortes, J. R., Cortes, P. C. Vlahakis, C., Jáchym, P., Pompei, E., & Rubio, M. 2020, ApJ, 901, 95
Crone Odekon, M., Hallenbeck, G., Haynes, M. P., Koopmann, R. A., Phi, A., & Wolfe, P.-F. 2018, ApJ, 852, 142
Croton, D. J., et al. 2006, MNRAS, 365, 11
Crowl, H. H., & Kenney, J. D. P. 2008, AJ, 136, 1623
Davé, R., Crain, R. A., Stevens, A. R. H., Narayanan, D., Saintonge, A., Catinella, B., & Cortese L. 2020, MNRAS, 497, 146
Davé, R., Oppenheimer, B. D., & Finlator, K. 2011, MNRAS, 415, 11
Davé, R., Rafieferantsoa, M. H., & Thompson, R. J. 2017, MNRAS, 471, 1671
Davies, R. D., & Lewis, B. M. 1973, MNRAS, 165, 231
Davies, L. J. M., et al. 2019, MNRAS, 483, 5444
Davis, T. A., et al. 2013, MNRAS, 429, 534
Davis, T. A., et al. 2014, MNRAS, 444, 3427
de Blok, W. J. G., et al. 2016, in MeerKAT Science: On the Pathway to the SKA, 7 (arXiv:1709.08458)
de Blok, W. J. G., et al. 2018, ApJ, 865, 26
Deb, T., et al. 2020, MNRAS, 494, 5029
Dekel, A., et al. 2009, Nature, 457, 451
De Lucia, G., Hirschmann, M., & Fontanot, F. 2019, MNRAS, 482, 5041
De Lucia, G., Springel, V., White, S. D. M., Croton, D., & Kauffmann, G. 2006, MNRAS, 366, 499
De Lucia, G., Weinmann, S., Poggianti, B. M., Aragón-Salamanca, A., & Zaritsky, D. 2012, MNRAS, 423, 1277
Dénes, H., Kilborn, V. A., & Koribalski, B. S. 2014, MNRAS, 444, 667
de Vaucouleurs, G., de Vaucouleurs, A., Corwin Jr., H. G., Buta, R. J., Paturel, G., & Fouque, P. 1991, Third Reference Catalogue of Bright Galaxies
Dewdney, P. E., Hall, P. J., Schilizzi, R. T., & Lazio, T. J. L. W. 2009, IEEE PROC, 97, 1482
Dickey, J. M., et al. 2013, PASA, 30, e003
Donnari, M., Pillepich, A., Nelson, D., Marinacci, F., Vogelsberger, M., & Hernquist, L. 2020, arXiv e-prints, p. arXiv:2008.00004
D'Onghia, E., & Fox, A. J. 2016, ARA&A, 54, 363
Dressler, A. 1986, ApJ, 301, 35
Dubois, Y., et al. 2014, MNRAS, 444, 1453
Duc, P.-A., & Bournaud, F. 2008, ApJ, 673, 787
Džudžar, R., Kilborn, V., Murugeshan, C., Meurer, G., Sweet, S. M., & Putman, M. 2019, MNRAS, 490, L6
Ebeling, H., Stephenson, L. N., & Edge, A. C. 2014, ApJ, 781, L40
Eigenthaler, P., Ploeckinger, S., Verdugo, M., & Ziegler, B. 2015, MNRAS, 451, 2793
Elagali, A., et al. 2019, MNRAS, 487, 2797

Emerick, A., Mac Low, M.-M., Grcevich, J., & Gatto, A. 2016, ApJ, 826, 148

English, J., Koribalski, B., Bland-Hawthorn, J., Freeman, K. C., & McCain, C. F. 2010, AJ, 139, 102

Fabello, S., Catinella, B., Giovanelli, R., Kauffmann, G., Haynes, M. P., Heckman, T. M., & Schiminovich, D. 2011, MNRAS, 411, 993

Fabello, S., Kauffmann, G., Catinella, B., Li, C., Giovanelli, R., & Haynes, M. P. 2012, MNRAS, 427, 2841

Fillingham, S. P., Cooper, M. C., Pace, A. B., Boylan-Kolchin, M., Bullock, J. S., Garrison-Kimmel, S., & Wheeler, C. 2016, MNRAS, 463, 1916

Fillingham, S. P., Cooper, M. C., Wheeler, C., Garrison-Kimmel, S., Boylan-Kolchin, M., & Bullock, J. S. 2015, MNRAS, 454, 2039

Fillingham, S. P., et al. 2019, arXiv e-prints, p. arXiv:1906.04180

Finn, R. A., et al. 2018, ApJ, 862, 149

Finoguenov, A., et al. 2009, ApJ, 704, 564

Font, A. S., et al. 2008, MNRAS, 389, 1619

Fossati, M., et al. 2013, A&A, 553, A91

Fossati, M., et al. 2018, A&A, 614, A57

Fraternali, F., & Binney, J. J. 2008, MNRAS, 386, 935

Freeland, E., & Wilcots, E. 2011, ApJ, 738, 145

Frye, B. L., Bowen, D. V., Tripp, T. M., Jenkins, E. B., Pettini, M., & Ellison, S. L. 2019, ApJ, 872, 129

Fujita, Y. 2004, PASJ, 56, 29

Fumagalli, M., Gavazzi, G., Scaramella, R., & Franzetti, P. 2011, A&A, 528, A46

Fumagalli, M., Krumholz, M. R., Prochaska, J. X., Gavazzi, G., & Boselli, A. 2009, ApJ, 697, 1811

Gaia COLLABORATION, et al. 2016, A&A, 595, A1

Garcia-Burillo, S., Guelin, M., Cernicharo, J., & Dahlem, M. 1992, A&A, 266, 21

Gatto, A., Fraternali, F., Read, J. I., Marinacci, F., Lux, H., & Walch, S. 2013, MNRAS, 433, 2749

Gavazzi, G., Boselli, A., Cortese, L., Arosio, I., Gallazzi, A., Pedotti, P., & Carrasco, L. 2006, A&A, 446, 839

Gavazzi, G., Boselli, A., Mayer, L., Iglesias-Paramo, J., Vlchez, J. M., & Carrasco, L. 2001, ApJ, 563, L23

Gavazzi, G., Boselli, A., Pedotti, P., Gallazzi, A., & Carrasco, L. 2002, A&A, 396, 449

Gavazzi, G., Contursi, A., Carrasco, L., Boselli, A., Kennicutt, R., Scodeggio, M., & Jaffe, W. 1995, A&A, 304, 325

Gavazzi, G., Fumagalli, M., Fossati, M., Galardo, V., Grossetti, F., Boselli, A., Giovanelli, R., & Haynes, M. P. 2013, A&A, 553, A89

Gavazzi, G., & Jaffe, W. 1987, A&A, 186, L1

Geréb, K., Catinella, B., Cortese, L., Bekki, K., Moran, S. M., & Schiminovich, D. 2016, MNRAS, 462, 382

Geréb, K., Janowiecki, S., Catinella, B., Cortese, L., & Kilborn, V. 2018, MNRAS, 476, 896

Geréb, K., Morganti, R., & Oosterloo, T. A. 2014, A&A, 569, A35

Gerin, M., & Casoli, F. 1994, A&A, 290, 49

Giovanelli, R., Chincarini, G. L., & Haynes, M. P. 1981, ApJ, 247, 383

Giovanelli, R., & Haynes, M. P. 1985, ApJ, 292, 404

Giovanelli, R., et al. 2005, AJ, 130, 2598

Giraud, E. 1986, A&A, 167, 25

Glover, S. C. O., & Clark, P. C. 2012, MNRAS, 421, 9

Gnedin, N. Y., & Kravtsov, A. V. 2011, ApJ, 728, 88

Goddard, D., et al. 2017, MNRAS, 465, 688

Grand, R. J. J., et al. 2019, arXiv e-prints, p. arXiv:1909.04038

Grcevich, J., & Putman, M. E. 2009, ApJ, 696, 385

Grebel, E. K., Gallagher John, S. I., & Harbeck, D. 2003, AJ, 125, 1926

Gunn, J. E., & Gott, J. R. I. 1972, ApJ, 176, 1

Guo, Q., et al. 2011, MNRAS, 413, 101

Guo, H., Jones, M. G., Haynes, M. P., & Fu, J. 2020, ApJ, 894, 92

Gupta, A., Yuan, T., Tran, K.-V. H., Martizzi, D., Taylor, P., & Kewley, L. J. 2016, ApJ, 831, 104

Gupta, A., et al. 2018, MNRAS, 477, L35

Haines, C. P., et al. 2015, ApJ, 806, 101

Han, S., Smith, R., Choi, H., Cortese, L., Catinella, B., Contini, E., & Yi, S. K. 2018, ApJ, 866, 78

Haynes, M. P., & Giovanelli, R. 1984, AJ, 89, 758

Haynes, M. P., & Giovanelli, R. 1986, ApJ, 306, 466

Healy, J., Blyth, S. L., Elson, E., van Driel, W., Butcher, Z., Schneider, S., Lehnert, M. D., & Minchin, R. 2019, MNRAS, 487, 4901

Heckman, T. M., Armus, L., & Miley, G. K. 1990, ApJS, 74, 833

Henriques, B. M. B., White, S. D. M., Thomas, P. A., Angulo, R., Guo, Q., Lemson, G., Springel, V., & Overzier, R. 2015, MNRAS, 451, 2663

Hess, K. M., Cluver, M. E., Yahya, S., Leisman, L., Serra, P., Lucero, D. M., Passmoor, S. S., & Carignan, C. 2017, MNRAS, 464, 957

Hess, K. M., & Wilcots, E. M. 2013, AJ, 146, 124

Hester, J. A. 2006, ApJ, 647, 910

Hester, J. A., et al. 2010, ApJ, 716, L14

Hibbard, J. E., & Mihos, J. C. 1995, AJ, 110, 140

Hibbard, J. E., van Gorkom, J. H., Rupen, M. P., & Schiminovich, D. 2001, An HI Rogues Gallery, 657

Hickson, P. 1982, ApJ, 255, 382

Hindman, J. V., Kerr, F. J., & McGee, R. X. 1963, AuJPh, 16, 570

Hirschmann, M., De Lucia, G., Wilman, D., Weinmann, S., Iovino, A., Cucciati, O., Zibetti, S., & Villalobos, Á. 2014b, MNRAS, 444, 2938

Hirschmann, M., Dolag, K., Saro, A., Bachmann, L., Borgani, S., & Burkert, A. 2014a, MNRAS, 442, 2304

Hopkins, P. F., Hernquist, L., Cox, T. J., & Kereš, D. 2008, ApJS, 175, 356

Hu, C.-Y., Naab, T., Walch, S., Glover, S. C. O., & Clark, P. C. 2016, MNRAS, 458, 3528

Hu, W., Catinella, B., Cortese, L., Staveley-Smith, L., Lagos, C. d. P., Chauhan, G., Oosterloo, T., & Chen, X. 2020, MNRAS, 493, 1587

Huang, S., Haynes, M. P., Giovanelli, R., & Brinchmann, J. 2012, ApJ, 756, 113

Huchtmeier, W. K. 1997, A&A, 325, 473

Huchtmeier, W. K., Tammann, G. A., & Wendker, H. J. 1976, A&A, 46, 381

Hughes, T. M., Cortese, L., Boselli, A., Gavazzi, G., & Davies, J. I. 2013, A&A, 550, A115

Hwang, J.-S., Park, C., Banerjee, A., & Hwang, H. S. 2018, ApJ, 856, 160

Iglesias-Páramo, J., Boselli, A., Gavazzi, G., & Zaccardo, A. 2004, A&A, 421, 887

Jáchym, P., Combes, F., Cortese, L., Sun, M., & Kenney, J. D. P. 2014, ApJ, 792, 11

Jáchym, P., et al. 2017, ApJ, 839, 114

Jáchym, P., et al. 2019, ApJ, 883, 145

Janowiecki, S., Catinella, B., Cortese, L., Saintonge, A., & Wang, J. 2020, MNRAS, 493, 1982

Johnston, S., et al. 2008, ExA, 22, 151

Jonas, J., & MeerKAT TEAM 2016, in MeerKAT Science: On the Pathway to the SKA, 1

Jones, M. G., et al. 2018, A&A, 609, A17

Jung, S. L., Choi, H., Wong, O. I., Kimm, T., Chung, A., & Yi, S. K. 2018, ApJ, 865, 156

Kantharia, N. G., Ananthakrishnan, S., Nityananda, R., & Hota, A. 2005, A&A, 435, 483

Kapferer, W., Sluka, C., Schindler, S., Ferrari, C., & Ziegler, B. 2009, A&A, 499, 87

Karachentseva, V. E. 1973, Soobshcheniya Spetsial'noj Astrofizicheskoj Observatorii, 8, 3

Kazantzidis, S., Mayer, L., Callegari, S., Dotti, M., & Moustakas, L. A. 2017, ApJ, 836, L13

Kenney, J. D. P., & Koopmann, R. A. 1999, AJ, 117, 181

Kenney, J. D., & Young, J. S. 1986, ApJ, 301, L13

Kenney, J. D., & Young, J. S. 1988, ApJS, 66, 261

Kenney, J. D. P., Tal, T., Crowl, H. H., Feldmeier, J., & Jacoby, G. H. 2008, ApJ, 687, L69

Kennicutt, R. C. J. 1983a, AJ, 88, 483

Kennicutt, R. C. 1983b, ApJ, 272, 54

Kent, S. M., & Gunn, J. E. 1982, AJ, 87, 945

Kereš, D., Katz, N., Weinberg, D. H., & Davé, R. 2005, MNRAS, 363, 2

Kerr, F. J., Hindman, J. F., & Robinson, B. J. 1954, AuJPh, 7, 297

Kilborn, V. A., Forbes, D. A., Barnes, D. G., Koribalski, B. S., Brough, S., & Kern, K. 2009, MNRAS, 400, 1962

Kimm, T., et al. 2009, MNRAS, 394, 1131

Kleiner, D., Pimbblet, K. A., Jones, D. H., Koribalski, B. S., & Serra, P. 2017, MNRAS, 466, 4692

Knapp, G. R., Turner, E. L., & Cunniffe, P. E. 1985, AJ, 90, 454

Koch, E. W., Rosolowsky, E. W., Schruba, A., Leroy, A., Kepley, A., Braine, J., Dalcanton, J., & Johnson, M. C. 2019, MNRAS, 485, 2324

Koopmann, R. A., Haynes, M. P., & Catinella, B. 2006, AJ, 131, 716

Koopmann, R. A., & Kenney, J. D. P. 2004a, ApJ, 613, 851

Koopmann, R. A., & Kenney, J. D. P. 2004b, ApJ, 613, 866

Koopmann, R. A., et al. 2008, ApJ, 682, L85

Köppen, J., Jáchym, P., Taylor, R., & Palouš, J. 2018, MNRAS, 479, 4367

Koribalski, B., & Dickey, J. M. 2004, MNRAS, 348, 1255

Koribalski, B., Gordon, S., & Jones, K. 2003, MNRAS, 339, 1203

Koribalski, B. S., et al. 2020, Ap&SS, 365, 118

Kraljic, K., et al. 2020, MNRAS, 491, 4294

Kronberger, T., Kapferer, W., Ferrari, C., Unterguggenberger, S., & Schindler, S. 2008, A&A, 481, 337

Krumholz, M. R., Leroy, A. K., & McKee, C. F. 2011, ApJ, 731, 25

Krumholz, M. R., McKee, C. F., & Tumlinson, J. 2009, ApJ, 693, 216

Lagos, C. D. P., Cora, S. A., & Padilla, N. D. 2008, MNRAS, 388, 587

Lagos, C. D. P., Davis, T. A., Lacey, C. G., Zwaan, M. A., Baugh, C. M., Gonzalez-Perez, V., & Padilla, N. D. 2014, MNRAS, 443, 1002

Lagos, C. D. P., Tobar, R. J., Robotham, A. S. G., Obreschkow, D., Mitchell, P. D., Power, C., & Elahi, P. J. 2018, MNRAS, 481, 3573

Lanzoni, B., Guiderdoni, B., Mamon, G. A., Devriendt, J., & Hatton, S. 2005, MNRAS, 361, 369

Larson, R. B., 1972, Nature, 236, 21

Larson, R. B., & Tinsley, B. M. 1978, ApJ, 219, 46

Larson, R. B., Tinsley, B. M., & Caldwell, C. N. 1980, ApJ, 237, 692

Lee-Waddell, K., et al. 2018, MNRAS, 474, 1108

Lee-Waddell, K., et al. 2019, MNRAS, 487, 5248

Lee, B., et al. 2017, MNRAS, 466, 1382

Lee, J., Kimm, T., Katz, H., Rosdahl, J., Devriendt, J., & Slyz, A. 2020, arXiv e-prints, p. arXiv:2010.11028

Lee, B. & Chung, A. 2018, ApJ, 866, L10

Leisman, L., Haynes, M. P., Giovanelli, R., Józsa, G., Adams, E. A. K., & Hess, K. M. 2016, MNRAS, 463, 1692

Leroy, A. K., Walter, F., Brinks, E., Bigiel, F., de Blok, W. J. G., Madore, B., & Thornley, M. D. 2008, AJ, 136, 2782

Leroy, A. K., et al. 2009, AJ, 137, 4670

Li, J., Obreschkow, D., Lagos, C., Cortese, L., Welker, C., & Džudžar, R. 2020, MNRAS, 493, 5024

Lian, J., Thomas, D., Li, C., Zheng, Z., Maraston, C., Bizyaev, D., Lane, R. R., & Yan, R. 2019, MNRAS, 489, 1436

Lilly, S. J., Carollo, C. M., Pipino, A., Renzini, A., & Peng, Y. 2013, ApJ, 772, 119

Lin, L., et al. 2019, ApJ, 872, 50

Lisenfeld, U., Appleton, P. N., Cluver, M. E., Guillard, P., Alatalo, K., & Ogle, P. 2014, A&A, 570, A24

Lisenfeld, U., Alatalo, K., Zucker, C., Appleton, P. N., Gallagher, S., Guillard, P., & Johnson, K. 2017, A&A, 607, A110

Liszt, H. S., Pety, J., & Lucas, R. 2010, A&A, 518, A45

Longmore, S. N., et al. 2013, MNRAS, 429, 987

Loni, A., et al. 2021, arXiv e-prints, p. arXiv:2102.01185

Lotz, M., Remus, R.-S., Dolag, K., Biviano, A., & Burkert, A. 2019, MNRAS, 488, 5370

Lutz, K. A., et al. 2017, MNRAS, 467, 1083

Maddox, N., Hess, K. M., Obreschkow, D., Jarvis, M. J., & Blyth, S. L. 2015, MNRAS, 447, 1610

Maier, C., Ziegler, B. L., Haines, C. P., & Smith, G. P. 2019, A&A, 621, A131

Marasco, A., Crain, R. A., Schaye, J., Bahé, Y. M., van der Hulst, T., Theuns, T., & Bower, R. G. 2016, MNRAS, 461, 2630

Marinacci, F., Binney, J., Fraternali, F., Nipoti, C., Ciotti, L., & Londrillo, P. 2010, MNRAS, 404, 1464

Martig, M., Bournaud, F., Teyssier, R., & Dekel, A. 2009, ApJ, 707, 250

Martinez-Badenes, V., Lisenfeld, U., Espada, D., Verdes-Montenegro, L., García-Burillo, S., Leon, S., Sulentic, J., & Yun, M. S. 2012, A&A, 540, A96

Mayer, L., Kazantzidis, S., Mastropietro, C., & Wadsley, J. 2007, Nature, 445, 738

McCarthy, I. G., Frenk, C. S., Font, A. S., Lacey, C. G., Bower, R. G., Mitchell, N. L., Balogh, M. L., & Theuns, T. 2008, MNRAS, 383, 593

McConnachie, A. W., Venn, K. A., Irwin, M. J., Young, L. M., & Geehan, J. J. 2007, ApJ, 671, L33

McGee, S. L., Balogh, M. L., Bower, R. G., Font, A. S., & McCarthy, I. G. 2009, MNRAS, 400, 937

McPartland, C., Ebeling, H., Roediger, E., & Blumenthal, K. 2016, MNRAS, 455, 2994

Medling, A. M., et al. 2018, MNRAS, 475, 5194

Mei, S., et al. 2007, ApJ, 655, 144

Michel-Dansac, L., et al. 2010, ApJ, 717, L143

Miniati, F., Finoguenov, A., Silverman, J. D., Carollo, M., Cibinel, A., Lilly, S. J., & Schawinski, K. 2016, ApJ, 819, 26

Mo, H. J., Mao, S., & White, S. D. M. 1998, MNRAS, 295, 319

Mok, A., et al. 2016, MNRAS, 456, 4384

Mok, A., Wilson, C. D., Knapen, J. H., Sánchez-Gallego, J. R., Brinks, E., & Rosolowsky, E. 2017, MNRAS, 467, 4282

Moore, B., Katz, N., Lake, G., Dressler, A., & Oemler, A. 1996, Nature, 379, 613

Moretti, A., et al. 2018, MNRAS, 480, 2508

Moretti, A., et al. 2020a, ApJ, 889, 9

Moretti, A., et al. 2020b, ApJ, 897, L30

Morrissey, P., et al. 2018, ApJ, 864, 93

Moss, C., & Whittle, M. 2000, MNRAS, 317, 667

Moss, C., Whittle, M., & Pesce, J. E. 1998, MNRAS, 300, 205

Mulchaey, J. S. 2000, ARA&A, 38, 289

Müller, A., et al. 2021, Nature Astronomy, 5, 159

Nelson, D., et al. 2018, MNRAS, 475, 624

Nilson, P. 1973, Nova Acta Regiae Soc. Sci. Upsaliensis Ser. V, p. 0

Noeske, K. G., et al. 2007, ApJ, 660, L43

Nulsen, P. E. J. 1982, MNRAS, 198, 1007

Obreschkow, D., Glazebrook, K., Kilborn, V., & Lutz, K. 2016, ApJ, 824, L26

Odekon, M. C., et al. 2016, ApJ, 824, 110

Okamoto, T., & Nagashima, M. 2003, ApJ, 587, 500

Oman, K. A., Bahé, Y. M., Healy, J., Hess, K. M., Hudson, M. J., & Verheijen, M. A. W. 2020, arXiv e-prints, p. arXiv:2009.00667

Oman, K. A., & Hudson, M. J. 2016, MNRAS, 463, 3083

Omar, A., & Dwarakanath, K. S. 2005, JApA, 26, 71

Oort, J. H. 1970, A&A, 7, 381

Oosterloo, T., van Gorkom, J. 2005, A&A, 437, L19

Owen, F. N., Keel, W. C., Wang, Q. D., Ledlow, M. J., & Morrison, G. E. 2006, AJ, 131, 1974

Owers, M. S., Couch, W. J., Nulsen, P. E. J., & Rand all, S. W. 2012, ApJ, 750, L23

Owers, M. S., et al. 2019, ApJ, 873, 52

Pappalardo, C., Lançon, A., Vollmer, B., Ocvirk, P., Boissier, S., & Boselli, A. 2010, A&A, 514, A33

Pappalardo, C., et al. 2012, A&A, 545, A75

Pasquali, A., Gallazzi, A., Fontanot, F., van den Bosch, F. C., De Lucia, G., Mo, H. J., & Yang, X. 2010, MNRAS, 407, 937

Pasquali, A., Gallazzi, A., & van den Bosch, F. C. 2012, MNRAS, 425, 273

Pasquali, A., Smith, R., Gallazzi, A., De Lucia, G., Zibetti, S., Hirschmann, M., & Yi, S. K. 2019, MNRAS, 484, 1702

Peng, Y.-J., & Maiolino, R. 2014, MNRAS, 438, 262

Peng, Y., Maiolino, R., & Cochrane, R. 2015, Nature, 521, 192

Péroux, C., et al. 2019, MNRAS, 485, 1595

Petropoulou, V., Vílchez, J., & Iglesias-Páramo, J. 2012, ApJ, 749, 133

Pety, J., et al. 2013, ApJ, 779, 43

Pillepich, A., et al. 2018, MNRAS, 473, 4077

Planck Collaboration, et al. 2016, A&A, 596, A101

Poggianti, B. M., et al. 2017, ApJ, 844, 48

Poggianti, B. M., et al. 2019, MNRAS, 482, 4466

Putman, M. E., Zheng, Y., Price-Whelan, A. M., Grcevich, J., Johnson, A. C., Tollerud, E., & Peek, J. E. G. 2021, arXiv e-prints, p. arXiv:2101.07809

Quilis, V., Moore, B., & Bower, R. 2000, Sci, 288, 1617

Rafieferantsoa, M., Davé, R., & Naab, T. 2019, MNRAS, 486, 5184
Ramatsoku, M., et al. 2019, MNRAS, 487, 4580
Randall, S., Nulsen, P., Forman, W. R., Jones, C., Machacek, M., Murray, S. S., & Maughan, B. 2008, ApJ, 688, 208
Rasmussen, J., Ponman, T. J., & Mulchaey, J. S. 2006, MNRAS, 370, 453
Rasmussen, J., Ponman, T. J., Verdes-Montenegro, L., Yun, M. S., & Borthakur, S. 2008, MNRAS, 388, 1245
Rasmussen, J., et al. 2012, ApJ, 747, 31
Rees, M. J., & Ostriker, J. P. 1977, MNRAS, 179, 541
Rhee, J., Smith, R., Choi, H., Contini, E., Jung, S. L., Han, S., & Yi, S. K. 2020, ApJS, 247, 45
Rhee, J., Smith, R., Choi, H., Yi, S. K., Jaffé, Y., Candlish, G., & Sánchez-Jánssen, R. 2017, ApJ, 843, 128
Ricarte, A., Tremmel, M., Natarajan, P., & Quinn, T. 2020, ApJ, 895, L8
Rieke, G. H., Lebofsky, M. J., Thompson, R. I., Low, F. J., & Tokunaga, A. T. 1980, ApJ, 238, 24
Roberts, I. D., & Parker, L. C. 2020, MNRAS, 495, 554
Roberts, I. D., Parker, L. C., Brown, T., Joshi, G. D., Hlavacek-Larrondo, J., & Wadsley, J. 2019, ApJ, 873, 42
Roberts, M. S. 1968, ApJ, 151, 117
Robinson, B. J., & Koehler, J. A. 1965, Nature, 208, 993
Roediger, E., & Brüggen, M. 2007, MNRAS, 380, 1399
Roediger, E., Bruggen, M., Owers, M. S., Ebeling, H., & Sun, M. 2014, MNRAS, 443, L114
Roediger, E., & Hensler, G. 2005, A&A, 433, 875
Roediger, E., Lovisari, L., Dupke, R., Ghizzardi, S., Brüggen, M., Kraft, R. P., & Machacek, M. E. 2012, MNRAS, 420, 3632
Roman-Duval, J., Heyer, M., Brunt, C. M., Clark, P., Klessen, R., & Shetty, R. 2016, ApJ, 818, 144
Romeo, A. B., & Mogotsi, K. M. 2018, MNRAS, 480, L23
Rose, J. A., Robertson, P., Miner, J., & Levy, L. 2010, AJ, 139, 765
Rots, A. H., 1975, A&A, 45, 43
Safonova, E. S. 2011, ARep, 55, 1016
Saintonge, A., & Spekkens, K. 2011, ApJ, 726, 77
Saintonge, A., et al. 2011, MNRAS, 415, 32
Saintonge, A., et al. 2017, ApJS, 233, 22
Sánchez Almeida, J. 2020, MNRAS, 495, 78
Sánchez, S. F., et al. 2012, A&A, 538, A8
Schaefer, A. L., et al. 2017, MNRAS, 464, 121
Schaefer, A. L., et al. 2019a, MNRAS, 483, 2851
Schaefer, A. L., et al. 2019b, ApJ, 884, 156
Schaye, J., et al. 2015, MNRAS, 446, 521
Schinnerer, E., et al. 2013, ApJ, 779, 42
Schinnerer, E., et al. 2016, ApJ, 833, 112
Scott, T. C., et al. 2010, MNRAS, 403, 1175
Scott, T. C., Cortese, L., Brinks, E., Bravo-Alfaro, H., Auld, R., & Minchin, R. 2012, MNRAS, 419, L19
Scott, T. C., Usero, A., Brinks, E., Boselli, A., Cortese, L., & Bravo-Alfaro, H. 2013, MNRAS, 429, 221
Scoville, N., et al. 2016, ApJ, 820, 83
Sengupta, C., & Balasubramanyam, R. 2006, MNRAS, 369, 360
Sengupta, C., Balasubramanyam, R., & Dwarakanath, K. S. 2007, MNRAS, 378, 137
Serra, P., et al. 2012, MNRAS, 422, 1835
Serra, P., et al. 2013, MNRAS, 428, 370
Serra, P., et al. 2015, MNRAS, 452, 2680
Shields, G. A., Skillman, E. D., & Kennicutt Robert, C. J. 1991, ApJ, 371, 82
Sivanandam, S., Rieke, M. J., & Rieke, G. H. 2014, ApJ, 796, 89
Skillman, E. D., Kennicutt, R. C., & Hodge, P. W. 1989, ApJ, 347, 875
Smethurst, R. J., Lintott, C. J., Bamford, S. P., Hart, R. E., Kruk, S. J., Masters, K. L., Nichol, R. C., & Simmons, B. D. 2017, MNRAS, 469, 3670
Smith, R., Davies, J. I., & Nelson, A. H. 2010a, MNRAS, 405, 1723
Smith, R. J., et al. 2010b, MNRAS, 408, 1417
Smith, R., Pacifici, C., Pasquali, A., & Calderón-Castillo, P. 2019, ApJ, 876, 145
Solanes, J. M., Giovanelli, R., & Haynes, M. P. 1996, ApJ, 461, 609
Solanes, J. M., Manrique, A., Garca-Gómez, C., González-Casado, G., Giovanelli, R., & Haynes, M. P. 2001, ApJ, 548, 97
Somerville, R. S., & Davé, R. 2015, ARA&A, 53, 51
Sorce, J. G., Blaizot, J., & Dubois, Y. 2019, MNRAS, 486, 3951
Spekkens, K., Urbancic, N., Mason, B. S., Willman, B., & Aguirre J. E. 2014, ApJ, 795, L5
Spindler, A., et al. 2018, MNRAS, 476, 580
Springel, V., White, S. D. M., Tormen, G., & Kauffmann, G. 2001, MNRAS, 328, 726
Stark, A. A., Knapp, G. R., Bally, J., Wilson, R. W., Penzias, A. A., & Rowe, H. E. 1986, ApJ, 310, 660
Stark, D. V., et al. 2016, ApJ, 832, 126
Steinhauser, D., Haider, M., Kapferer, W., & Schindler, S. 2012, A&A, 544, A54
Steinhauser, D., Schindler, S., & Springel, V. 2016, A&A, 591, A51
Stevens, A. R. H., & Brown, T. 2017, MNRAS, 471, 447
Stevens, A. R. H., Diemer, B., Lagos, C. d. P., Nelson, D., Obreschkow, D., Wang, J., & Marinacci, F. 2019b, MNRAS, 490, 96
Stevens, A. R. H., Lagos, C. d. P., Obreschkow, D., & Sinha, M. 2018, MNRAS, 481, 5543
Stevens, A. R. H., et al. 2019a, MNRAS, 483, 5334
Stevens, A. R. H., et al. 2020, arXiv e-prints, p. arXiv:2011.03226
Stevens, J. B., Webster, R. L., Barnes, D. G., Pisano, D. J., & Drinkwater, M. J. 2004, PASA, 21, 318
Steyrleithner, P., Hensler, G., & Boselli, A. R. 2020, arXiv e-prints, p. arXiv:2003.09591
Struck, C., & Smith, B. J. 2003, ApJ, 589, 157
Sullivan, W. T. I., & Johnson, P. E. 1978, ApJ, 225, 751
Sun, M., Donahue, M., & Voit, G. M. 2007, ApJ, 671, 190
Tecce, T. E., Cora, S. A., Tissera, P. B., Abadi, M. G., & Lagos, C. D. P. 2010, MNRAS, 408, 2008
Teimoorinia, H., Ellison, S. L., & Patton, D. R. 2017, MNRAS, 464, 3796
Thilker, D. A., et al. 2010, ApJ, 714, L171
Tonnesen, S., & Bryan, G. L. 2009, ApJ, 694, 789
Tonnesen, S., & Bryan, G. L. 2021, arXiv e-prints, p. arXiv:2102.05061
Tonnesen, S., Bryan, G. L., & Chen, R. 2011, ApJ, 731, 98
Tonnesen, S., & Stone, J. 2014, ApJ, 795, 148
Toribio, M. C., Solanes, J. M., Giovanelli, R., Haynes, M. P., & Martin, A. M. 2011, ApJ, 732, 93
Troncoso-Iribarren, P., Padilla, N., Santander, C., Lagos, C. D. P., García-Lambas, D., Rodríguez, S., & Contreras S. 2020, MNRAS, 497, 4145
Trussler, J., Maiolino, R., Maraston, C., Peng, Y., Thomas, D., Goddard, D., & Lian J. 2020, arXiv e-prints, p. arXiv:2006.01154
Tumlinson, J., Peeples, M. S., & Werk, J. K. 2017, ARA&A, 55, 389
Valluri M., & Jog, C. J. 1990, ApJ, 357, 367
Valluri, M., & Jog, C. J. 1991, ApJ, 374, 103
van den Bosch, F. C., Aquino, D., Yang, X., Mo, H. J., Pasquali, A., McIntosh, D. H., Weinmann, S. M., & Kang, X. 2008, MNRAS, 387, 79
Verdes-Montenegro, L., Sulentic, J., Lisenfeld, U., Leon, S., Espada, D., Garcia, E., Sabater, J., & Verley, S. 2005, A&A, 436, 443
Verdes-Montenegro, L., Yun, M. S., Williams, B. A., Huchtmeier, W. K., Del Olmo, A., & Perea, J. 2001, A&A, 377, 812
Vijayaraghavan, R., & Ricker, P. M. 2013, MNRAS, 435, 2713
Vijayaraghavan, R., & Sarazin, C. 2017, ApJ, 848, 63
Vogelsberger, M., et al. 2014, MNRAS, 444, 1518
Vollmer, B. 2003, A&A, 398, 525
Vollmer, B. 2009, A&A, 502, 427
Vollmer, B., Cayatte, V., Balkowski, C., & Duschl, W. J. 2001, ApJ, 561, 708
Vollmer, B., Balkowski, C., Cayatte, V., van Driel, W., & Huchtmeier, W. 2004, A&A, 419, 35
Vollmer, B., Braine, J., Pappalardo, C., & Hily-Blant, J. H. 2008, A&A, 491, 455
Vollmer, B., Braine, J., Combes, F., & Sofue, Y. 2005, A&A, 441, 473
von der Linden, A., Wild, V., Kauffmann, G., White, S. D. M., & Weinmann, S. 2010, MNRAS, 404, 1231
Vulcani, B., et al. 2018, ApJ, 866, L25
Vulcani, B., et al. 2020, arXiv e-prints, p. arXiv:2007.04996
Wang, J., Koribalski, B. S., Serra, P., van der Hulst, T., Roychowdhury, S., Kamphuis, P., & Chengalur, J. N. 2016, MNRAS, 460, 2143
Warmels, R. H. 1988, A&AS, 72, 427

Weinmann, S. M., Kauffmann, G., van den Bosch, F. C., Pasquali, A., McIntosh, D. H., Mo, H., Yang, X., & Guo, Y. 2009, MNRAS, 394, 1213

Weinmann, S. M., Kauffmann, G., von der Linden, A., & De Lucia, G. 2010, MNRAS, 406, 2249

Weinmann, S. M., van den Bosch, F. C., Yang, X., & Mo, H. J. 2006, MNRAS, 366, 2

Westmeier, T., Braun, R., & Koribalski, B. S. 2011, MNRAS, 410, 2217

Westmeier, T., Staveley-Smith, L., Calabretta, M., Jurek, R., Koribalski, B. S., Meyer, M., Popping, A., & Wong, O. I. 2015, MNRAS, 453, 338

Wetzel, A. R., Tinker, J. L., & Conroy C. 2012, MNRAS, 424, 232

Wetzel, A. R., Tinker, J. L., Conroy, C., & van den Bosch, F. C. 2013, MNRAS, 432, 336

Wetzel, A. R., Tollerud, E. J., & Weisz, D. R. 2015, ApJ, 808, L27

Wheeler, C., Phillips, J. I., Cooper, M. C., Boylan-Kolchin, M., & Bullock, J. S. 2014, MNRAS, 442, 1396

Whitaker, K. E., van Dokkum, P. G., Brammer, G., & Franx, M. 2012, ApJ, 754, L29

White, S. D. M., & Frenk, C. S. 1991, ApJ, 379, 52

Williams, B. A., Yun, M. S., & Verdes-Montenegro, L. 2002, AJ, 123, 2417

Wootten, A., & Thompson, A. R. 2009, IEEE PROC, 97, 1463

Wu, P.-F., Zahid, H. J., Hwang, H. S., & Geller, M. J. 2017, MNRAS, 468, 1881

Wyder, T. K., et al. 2009, ApJ, 696, 1834

Xie, L., De Lucia, G., Hirschmann, M., & Fontanot, F. 2020, arXiv e-prints, p. arXiv:2003.12757

Xie, L., De Lucia, G., Wilman, D. J., Fossati, M., Erwin, P., Gutiérrez, L., & Kulkarni, S. K. 2018, MNRAS, 480, 3812

Yagi, M., et al. 2010, AJ, 140, 1814

Yamagami, T., & Fujita, Y. 2011, PASJ, 63, 1165

Yang, X., Mo, H. J., & van den Bosch, F. C. 2009, ApJ, 695, 900

Yoon, H., Chung, A., Smith, R., & Jaffé, Y. L. 2017, ApJ, 838, 81

Yoon, I., & Rosenberg, J. L. 2015, ApJ, 812, 4

York, D. G., et al. 2000, AJ, 120, 1579

Yoshida, M., et al. 2008, ApJ, 688, 918

Young, L. M., et al. 2011, MNRAS, 414, 940

Yun, K., et al. 2019, MNRAS, 483, 1042

Yun, M. S., Ho, P. T. P., & Lo, K. Y. 1994, Nature, 372, 530

Zabel, N., et al. 2019, MNRAS, 483, 2251

Zabludoff, A. I., & Mulchaey, J. S. 1998, ApJ, 496, 39

Zasov, A. V., & Rubtsova, T. V. 1989, SAL, 15, 51

Zheng, Z., et al. 2017, MNRAS, 465, 4572

Zoldan, A., De Lucia, G., Xie, L., Fontanot, F., & Hirschmann, M. 2017, MNRAS, 465, 2236